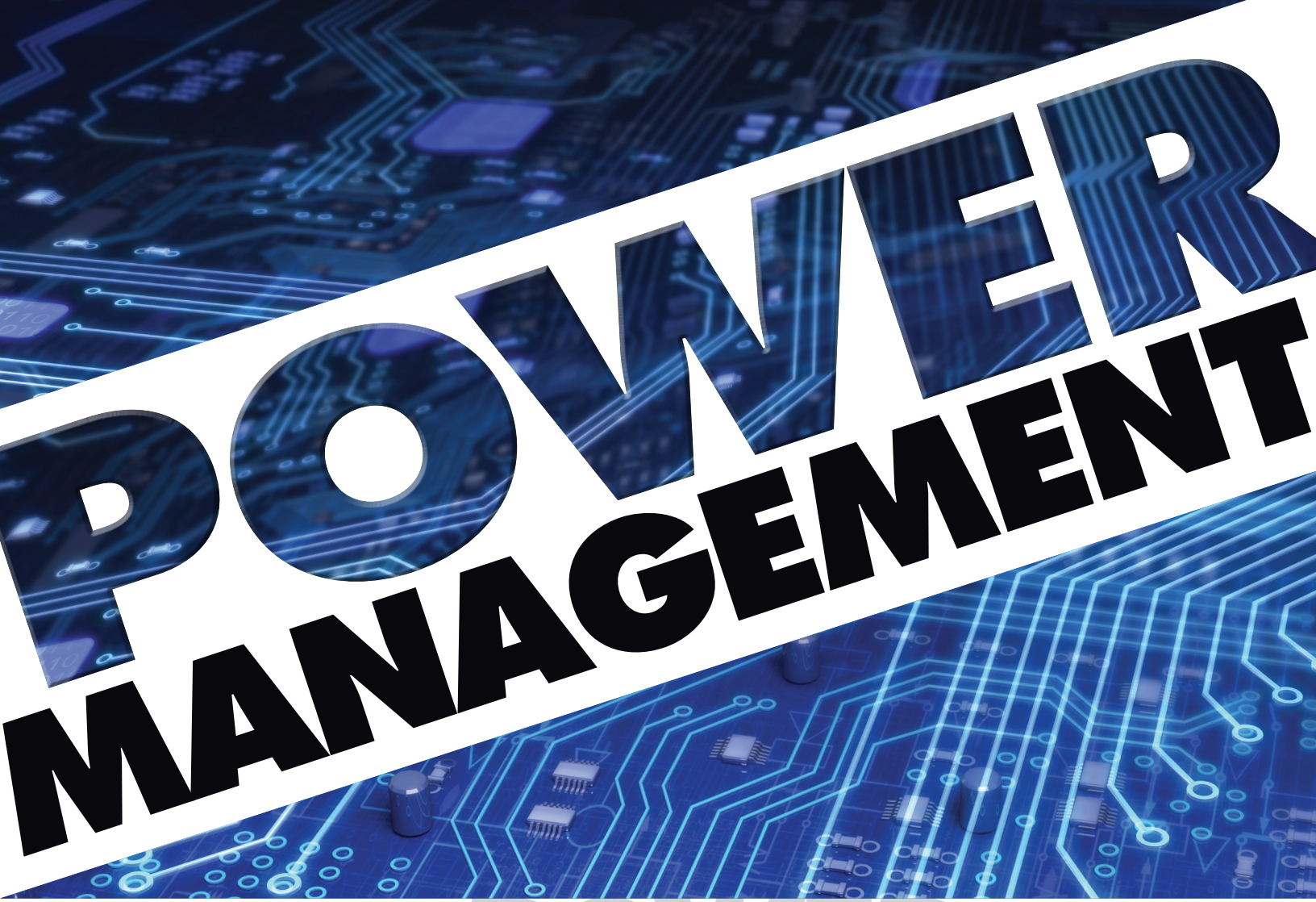

POWER MANAGEMENT

SAM DAVIS

POWER

SUPPLIES

SYSTEMS

APPLICATIONS

COMPONENTS

SEMICONDUCTORS

electronic design

POWER MANAGEMENT

BY **SAM DAVIS**

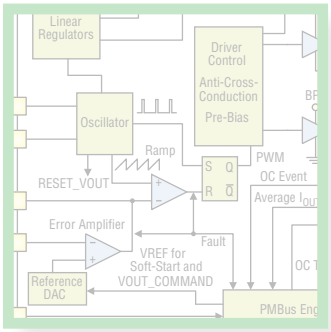

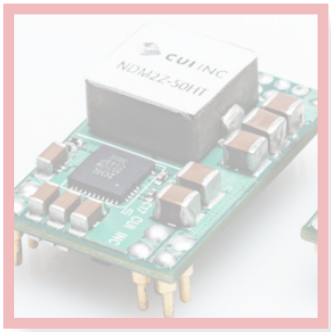

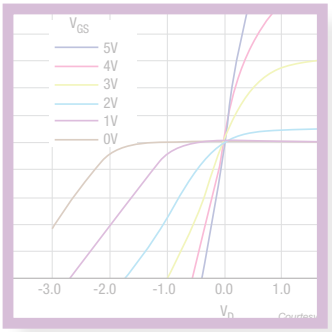

CHAPTER 12:

WIRELESS POWER TRANSFER

You can employ wireless power transfer at different power levels. At the low power level, wireless power transfer is intended for smartphones and other portable battery-powered systems. Higher-power wireless transfer is used to recharge the battery in an electric vehicle. First, we will describe the lower power technology in an FAQ format. Next, we will describe work done at the Oak Ridge National Laboratory for wireless charging batteries in an electric vehicle.

Is there a wireless power transfer standard for portable phones?

Wireless power transfer is based on the Wireless Power Consortium's WPC 1.1 Standard (July 2012) that facilitates cross-compatibility of compliant transmitters and receivers. The Standard defines the physical parameters and the communication protocol used in wireless power transfer.

The Wireless Power Consortium's global standard for compatible wireless charging is called Qi (pronounced "chee"). The Qi standard guarantees that any device carrying the Qi logo will work with any charging surface that carries the Qi logo, regardless of manufacturer or brand. Qi allows design freedom, product differentiation, and guaranteed wireless charging interoperability.

How does wireless power technology work?

Wireless power transfer relies on magnetic induction between planar receiver and transmitter coils. Positioning the receiver coil over the transmitter coil causes magnetic coupling when the transmitter coil is driven. Flux couples into the secondary coil, which induces a voltage and current flows. The secondary voltage is rectified and transferred to the load, wirelessly. Wireless power transfer is usually controlled by two ICs: one transmits and another receives the transferred power, as shown in Fig. 12-1.

How do the receiver and transmitter ICs provide the wireless transfer?

The power-transfer receiver IC provides efficient ac/dc power conversion as required to comply with WPC 1.1 communication protocol. Control algorithms provide an effective and safe Li-Ion and Li-Pol battery charger—eliminating the need for a separate battery charger circuit.

By utilizing near-field inductive power transfer, a secondary coil embedded in the portable device can pick up the power transmitted by the primary coil. The ac signal from the secondary coil is then rectified and conditioned to apply power directly to the battery. Global feedback is established from the secondary to the primary in order to stabilize the power transfer process. This feedback utilizes the WPC 1.1 power communication protocol.

What determines the power transfer?

Power transfer depends on coil coupling, which depends on the distance between coils, alignment,

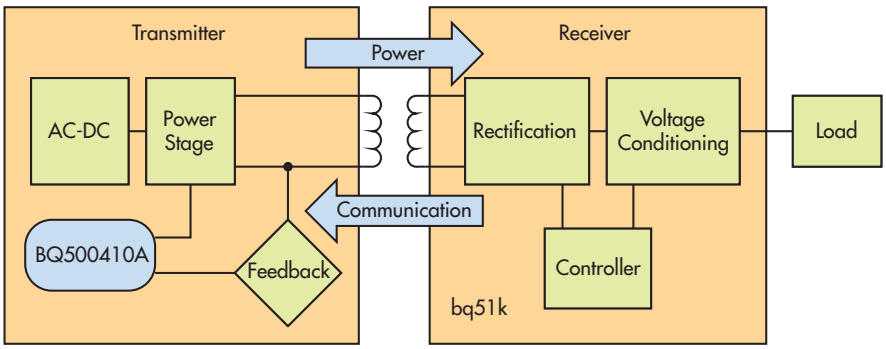

12-1. Qi-compliant wireless power transfer receivers and transmitter circuits. The bq500410a is a Texas Instruments transmitter IC. Companion receiver ICs include the bq51050B, bq51051B, bq51011, bq5013, bq51013A, and bq51013B.

A1 type w/ magnet

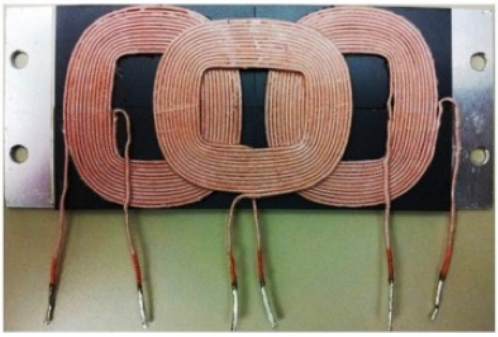

A6 type for rectangular free positioning

12-2. The transmitter IC can employ either of two type of coil configurations. On the left is the A1 single coil and on the right is the A6 three-coil configuration.

coil dimensions, coil materials, number of turns, magnetic shielding, impedance matching, frequency, and duty cycle. Receiver and transmitter coils must be aligned for best coupling and efficient power transfer. The closer the space between the two coils, the better the coupling. However, to account for housing and interface surfaces, the practical distance is set to be less than 5 mm, as defined within the WPC Standard. Shielding is added as a backing to both the transmitter and receiver coils to direct the magnetic field to the coupled zone. Magnetic fields outside the coupled zone do not transfer power. Thus, shielding also serves to contain the wireless fields and avoid coupling to other adjacent system components.

Does the WPC 1.1 Standard set the operating environment for power transfer?

You can control power transfer by varying any one of the coil coupling parameters. However, for WPC compatibility, the transmitter-side coils and capacitance are specified and the resonant frequency point is fixed. Power transfer is regulated by changing the frequency along the resonance curve from 112 kHz to 205 kHz (that is the higher the frequency is, the lower the power). Duty cycle remains constant at 50% throughout the power band and is reduced only once 205 kHz is reached.

What coil configurations are available?

Fig. 12-2 shows the A6 three-coil configuration with a 70 x 20 mm charge surface area as well as the A1 single-coil with 18 mm ×18mm charge space. The 70 mm by 20 mm A6 charge area is 400% larger than 19-mm by 19-mm area used by an A1 coil.

An A6 coil arrangement can achieve greater than 70-percent efficiency. The WPC Standard establishes coil and matching capacitor specification for the A6 transmitter. Although the transmitter is intended to drive an A6 three-coil array, it can also be used to drive a single A1 coil. For single-coil operation, the two outer coils and associated electronics are simply omitted.

The performance of an A6 transmitter can vary based on the design of the A6 coil set. For best performance with small receiver coils under heavy loading, it is best to design the coil set so that it is on the low end of the specified tolerance.

Does the WPC standard set the coil characteristics?

The WPC standard describes the dimensions, materials of the coils, and information regarding the tuning of the coils to resonance. The value of the inductor and resonant capacitor are critical for proper operation and system efficiency.

Why is capacitor selection important?

Capacitor selection is critical to proper system operation. The resonant tank requires a total capacitance value of 68 nF +5.6 nF center coil, which is the WPC system compatibility requirement. Capacitors chosen must be rated for at least 100 V and must be of a high-quality C0G dielectric (sometimes also called NP0). They typically have a 5% tolerance, which is adequate. The designer can combine capacitors to achieve the desired capacitance value. Various combinations can work depending on availability.

Can you monitor power transfer efficiency?

Both parasitic metal detection (PMOD) and foreign object detection (FOD) can continuously monitor the efficiency of the established power transfer. This protects against power lost due to metal objects in the wireless power transfer path. Combining input power, known losses, and the value of power reported by the RX device being charged, the transmitter can estimate how much power is unaccounted for and presumed lost due to misplaced metal objects. Exceeding this unexpected loss indicates a fault and halts power transfer.

PMOD has certain inherent weaknesses as rectified power is not ensured to be accurate per the original WPC1.0 Specification. However, the FOD algorithm uses information from an in-system characterized and WPC1.1 certified receiver and it is therefore more accurate. Where the WPC1.0 specification requires merely the rectified power packet, the WPC1.1 specification additionally uses the received power packet that more accurately tracks power used by the receiver. As default, PMOD and FOD share the same threshold-setting resistor for which the recommended starting point is 400 mW.

How do the receiver and transmitter ICs communicate?

Communication within the WPC standard is from the receiver to the transmitter, where the receiver tells the transmitter to send power and how much. To provide regulation, the receiver must communicate with the transmitter whether to increase or decrease frequency. The receiver monitors the rectifier output and, using Amplitude Modulation (AM), sends packets of information to the transmitter. A packet is comprised of a preamble, header, actual message, and a checksum, as defined in the WPC standard.

The receiver sends a packet by modulating an impedance network. This AM signal reflects back as a change in the voltage amplitude on the transmitter coil. The signal is demodulated and decoded by the transmitter-side electronics and the frequency of its coil-drive output is adjusted to close the regulation loop.

12-3. WPT system installed in an electric Toyota RAV4 equipped with an additional 10kW-hour battery.

Oak Ridge National Laboratory's Demos 20kW, EV Wireless Power Transfer System

A 20 kW wireless charging system for electric vehicles was demonstrated recently at the Department of Energy's Oak Ridge National Laboratory (ORNL). The charging system achieved 90% efficiency at three times the rate of plug-in systems commonly used for electric vehicles.

ORNL's power electronics team achieved the world's first 20 kW wireless charging system for passenger cars by developing a unique architecture that includes an ORNL-built inverter, isolation transformer, vehicle-side electronics, and coupling technologies. For the demonstration, researchers integrated the single-converter system into an electric Toyota RAV4 equipped with an additional 10kW-hour battery (Fig. 12-3).

The researchers are already looking ahead to their next target of a 50kW wireless charger, which would match the power levels of commercially available plug-in quick chargers. Providing the same charging speed with the convenience of wireless charging could increase consumer acceptance of electric vehicles and is considered a key enabler for hands-free autonomous vehicles. As the researchers advance their systems to achieve higher power levels, one of their chief concerns is maintaining safety for the equipment and associated personnel.

Original work on wireless started about three years ago and was described in a paper presented by nine ORNL researchers in a 2013 IEEE Transportation Electrification Initiative (TEI) e-Newsletter. According to David Smith, vehicle systems program manager "wireless power transfer (WPT) represents a paradigm shift in electric-vehicle (EV) charging that offers the consumer an autonomous, safe, and convenient option to conductive charging and its attendant need for cables. Today's technology is a stepping stone toward electrified roadways where vehicles could charge on the go."

The 2013 newsletter said WPT can be fully autonomous due to the vehicle and grid side radio communication systems, and is non-contacting; therefore, issues with leakage currents, ground faults, and touch potentials do not exist. It also eliminates the need for dealing with heavy, bulky, dirty cables and plugs. It eliminates the fear of forgetting to plug-in and running out of charge the following day and eliminates the tripping hazards in public parking lots and in highly populated areas such as malls, recreational areas, etc. Furthermore, the high-frequency magnetic fields employed in power transfer across a large air gap are focused and shielded, so that fringe fields (i.e., magnetic leakage fields) attenuate rapidly over a transition region to levels well below limits set by international standards for the public zone (which starts at the perimeter of the vehicle and includes the passenger cabin).

The ORNL approach to WPT charging places strong emphasis on radio communications in the power regulation feedback channel augmented with software control algorithms. The goal for this WPT is minimization of vehicle onboard complexity by keeping the secondary side content confined to coil tuning, rectification, filtering, and interfacing to the regenerative energy-storage system (RESS). WPT

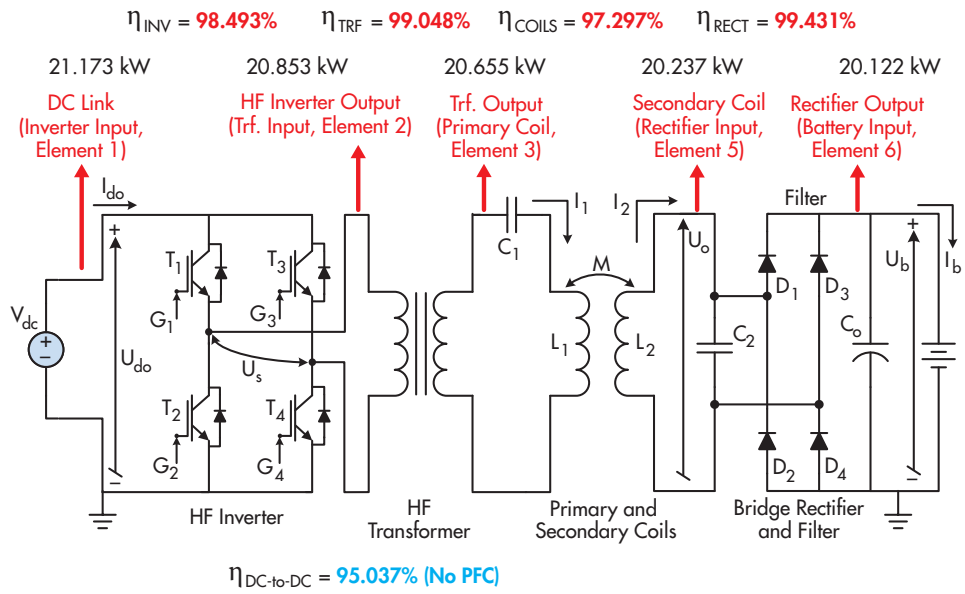

12-4. Block diagram of the ORNL WPT system with five cascaded power conversion stages.

charging represents the end game in the context of the connected vehicle, wireless communications, and eventually, with in-motion deployment of WPT, the ultimate in electric vehicle operation with unlimited range: dynamic wireless charging. Oak Ridge National Laboratory is working toward more efficient coil designs, power electronics converter developments, and communications systems, as well as new control strategies in this field. ORNL WPT programs also define and address concerns related to personal safety and hazards that may arise. ORNL uses electromagnetic resonance inductive coupling system for wireless charging of electric vehicles.

ORNL is the lead organization for this activity and partners with Toyota Motor Corp., Evatran, Clemson University ICAR Center, Cisco, Duke Energy, and International Rectifier. With OEM, commercialization, communications, grid, and device partners, ORNL meets the aggressive power and efficiency goals for future's electric vehicles with stationary and in-motion charging capabilities. At the end of the first phase, ORNL demonstrated 6.6kW and 10kW power transfer over 160mm gap with over ~>90% dc-to-dc efficiency, ~97% coil-to-coil efficiency, and 85% end-to-end (wall outlet to vehicle battery terminals) efficiency. The demonstration used dedicated short range communication (DSRC) systems for vehicle side data monitoring and feedbacks for controlling the grid side units.

Fig. 12-4 is the block diagram of the original ORNL wireless power transfer system. The grid side unit of the WPT system consists of an active front-end rectifier (AFER) with power factor correction (PFC), a high-frequency power inverter, a high-frequency isolation transformer, a tuning capacitor, and the primary coil. On the secondary (vehicle) side, the secondary coil is in parallel with the tuning capacitor, a diode-bridge rectifier, and a filter capacitor.

Active Front-end Rectifier

Fig. 12-5 shows the active front-end rectifier with power factor correction. In the AFER converter, only left leg of the active front-end rectifier is utilized and the right leg acts as a diode phase-leg. The AFER can work as a boost power factor correction circuit and is capable of boosting grid voltage's peak value up to 10 times (normally 2-3 times).

The AFER with PFC can also be interleaved for higher power rating. For high efficiency, low loss, and high switching frequency and reduced current ripple, it uses APT100MC120JCU2 SiC MOSFET phase-leg modules. The converter is operated based on the reference power to be delivered to the vehicle battery. Basically, depending on the battery reference current, a PI (proportional integral) controller is used to determine the reference current magnitude from the grid. A phase-locked-loop (PLL) system determines the grid voltage phase angle and the grid reference current is shaped accordingly. An outer PI controller uses the actual grid current and the internally generated reference ac current and determines the switching states. With the selected architecture, ORNL achieved a power factor of >98% and

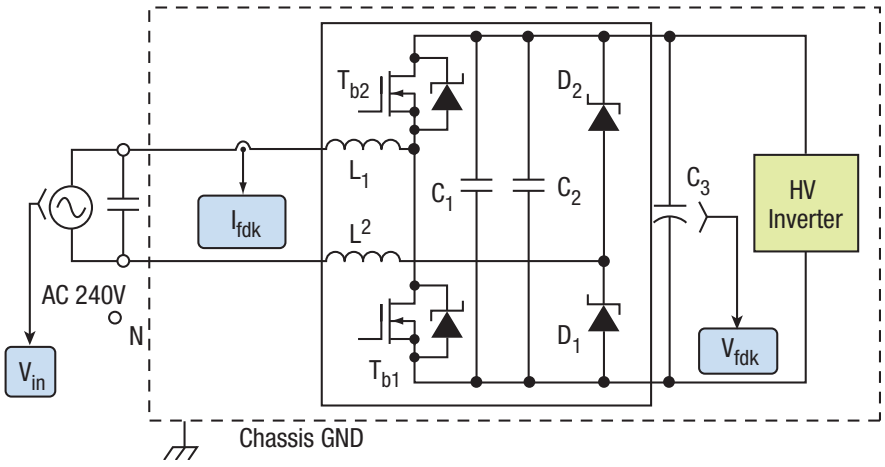

12-5. Active front-end rectifier with power factor correction.

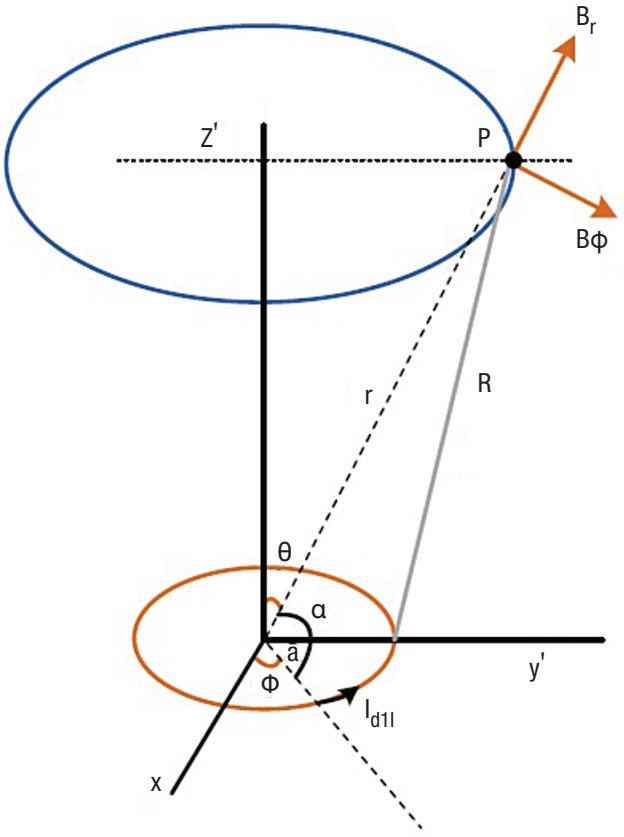

12-6. Vector field analysis diagram (analytical construction) for coupling coil design.

current total harmonic distortions (THDI) of <5%. In addition, because the AFER regulates the primary side DC link voltage, the battery current ripple is reduced to <10 A.

Coupling Coil Design

Electromagnetic design of WPT coupling coils provides the most fundamental investigation into their performance. At ORNL, the WPT team developed couplers based on the magnetic vector potential at a field point due to current flowing in an ideal primary coil conductor. The potential at this field point is defined to lie at the location of the secondary coil. For a coil pair of radius a, assuming infinitesimal conductor radius, and having a coil to coil spacing z, then the radius vector from the primary coil origin to the field point becomes

$$r = \sqrt{a^2 + z^2}$$

(Fig. 12-6). The corresponding vector potential, Aφ, for the case of N1 primary turns and I1 A yield a primary excitation of N1I1 amp-turns.

At the field point P, the magnetic vector potential is strongly dependent on primary coil radius, total current, the co-elevation angle θ, and inverse with the square of the separation distance, r. However, it is the flux density B(r, θ), and total flux Φ at the secondary coil that is most relevant to WPT performance and is given as:

$$B(r,\theta) = \hat{r}\frac{\mu_0 N_1 I_1 a_1^2}{} \cos\theta + \hat{\theta}\frac{\mu_0 N_1 I_1 a_1^2}{} \sin\theta \qquad (1)$$

High Frequency Inverter

Load conditions; i.e., state-of-charge of the battery and coupling coefficient; i.e., vehicle coil to primary pad gap and any misalignment between transmit and receive coils determine the frequency response of the WPT system. The amount of power transferred to the secondary coil is governed by the switching frequency, duty cycle, and the input voltage of the inverter. This relationship can be expressed as:

$$U_1(t) = \frac{4U_{d0}}{\pi} \sin\left(d\frac{\pi}{2}\right)\cos(\omega t) \qquad (2)$$

Where:

U_{d0} = HF power inverter rail voltage

d = pulse duty ratio

ω = angular frequency

Although the primary coil voltage can be controlled by the active front-end converter to vary the dc rail voltage Ud0, the ultimate objective is to dynamically change the switching frequency and the duty cycle in order to achieve the best operating conditions in terms of efficiency and power transfer. In the ORNL laboratory setting, the HF power inverter voltage was adjusted using a power supply. In a commercialized version of this WPT technology, a dedicated short-range communication (DSRC) link as shown in Fig. 12-4 would be needed. The transmitter side of the DSRC collects the measurement data such as battery voltage, battery current, and battery management system (BMS) messages needed for regulation. The grid-side receiver side of the DSRC channel receives this information for control purposes along with supporting primary side measurements. Then, a DSP-based embedded control system determines the switching frequency and the appropriate duty cycle according to the control law being used. The switching signals for the inverter IGBTs are generated by the DSP control algorithm and applied to the HF power inverter gate drives. The control system can also regulate the inverter power based on the reference power commands that can be received through the V2I communications from a smart grid compliant utility.

Portions of this article were prepared by the Oak Ridge National Laboratory, operated by the UT-Battelle for the U.S. Department of Energy under contract DE-AC05-00OR22725. Accordingly, the U.S. Government retains a

non-exclusive, royalty-free, license to publish from the contribution, or allow others to do so, for U.S. Government purposes. The research team included Omer C. Onar, Steven Campbell, Cliff White, Larry Seiber, Chester Coomer, Lixin Tang, Paul Chambon, Madhu Chinthavali, and John M. Miller.

Related Articles

1. Sam Davis, 5W Wireless Power Transmitter IC Boosts Battery-Charging Performance and Efficiency, powerelectronics.com, December 2015.
2. Henri Winand, Is Wireless Charging a $13 Billion Strikeout?, powerelectronics.com, November 2015.
3. Sam Davis, Wireless Power Receiver Supports Contactless Battery Charging, powerelectronics.com, October 2013.
4. Sam Davis, Pair of ICs Improve Wireless Power Transfer, powerelectronics.com, March 2013.
5. Jeff McCutcheon, FFDMs Promise Optimized Wireless Power Charging, electronicdesign.com, February 2012.
6. Tony Antonacci, Take Charge When Creating A Qi-Compliant Wireless-Power Accessory, electronicdesign.com, February 2012.
7. Steve Sandler, Optimize Wireless Power Transfer Link Efficiency Part 1, powerelectronics.com, October 2011.
8. Steve Sandler, Optimize Wireless Power Transfer Link Efficiency Part 2, powerelectronics.com, January 2012.
9. Sam Davis, Wireless Power Receiver IC Complements Existing Transmitter, powerelectronics.com, July 2011.
10. Sam Davis, Sam, Wireless Power Minimizes Interconnection Problems, PET, July, 2011.

BACK TO TABLE OF CONTENTS

CHAPTER 13:

ENERGY HARVESTING

Energy harvesting is the process by which ambient energy is captured and converted into electricity for small autonomous devices, such as satellites, laptops and nodes in sensor networks without the need for battery power. Energy harvesting applications reach from vehicles to the smart grid.

With electronic circuits now capable of operating at microwatt levels, it is feasible to power them from non-traditional sources. This has led to energy harvesting, which provides the power to charge, supplement or replace batteries in systems where battery use is inconvenient, impractical, expensive or dangerous. It can also eliminate the need for wires to carry power or to transmit data. Energy harvesting can power smart wireless sensor networks to monitor and optimize complex industrial processes, remote field installations and building HVAC. In addition, otherwise wasted energy from industrial processes, solar panels, or internal combustion engines, can be harvested for useful purposes. A key component in energy harvesting is a power converter that can operate with ultralow voltage inputs.

Now that we have described why it is feasible and what it can do, how does energy harvesting actually work? Put simply, it is a process that:

- Captures minute amounts of energy
- Accumulates that energy
- Stores the energy
- Maintains the stored energy as a power source

Typical energy harvesting inputs include:

- Solar power
- Thermal energy
- Wind energy
- Salinity gradients
- Kinetic energy

Today, energy harvesters do not usually produce enough energy to perform mechanical work, however they provide small amounts of power to support low-energy electronics. In most cases, the "fuel" " for energy harvesters is naturally present and may be considered free. Using natural sources in remote areas for energy harvesting is an attractive alternative to inconvenient utility and battery power. These natural energy sources may be available maintenance-free for a lifetime. Energy harvesting can also be an alternative energy source that supplements the primary power source and enhances its reliability.

Energy harvesters are intended for applications requiring very low average power, but require periodic pulses of higher load current. For example, in many wireless sensor applications the circuitry is only powered to make measurements and transmit data periodically at a low duty cycle.

Energy harvesting is becoming more feasible today because of the increased efficiency of devices capable of capturing, storing, and producing electrical energy. This can be accomplished with the help of very efficient, very low-voltage input step-up converters. Also, improved low-voltage, high-efficiency microprocessors may allow them to become participants in energy harvesting systems.

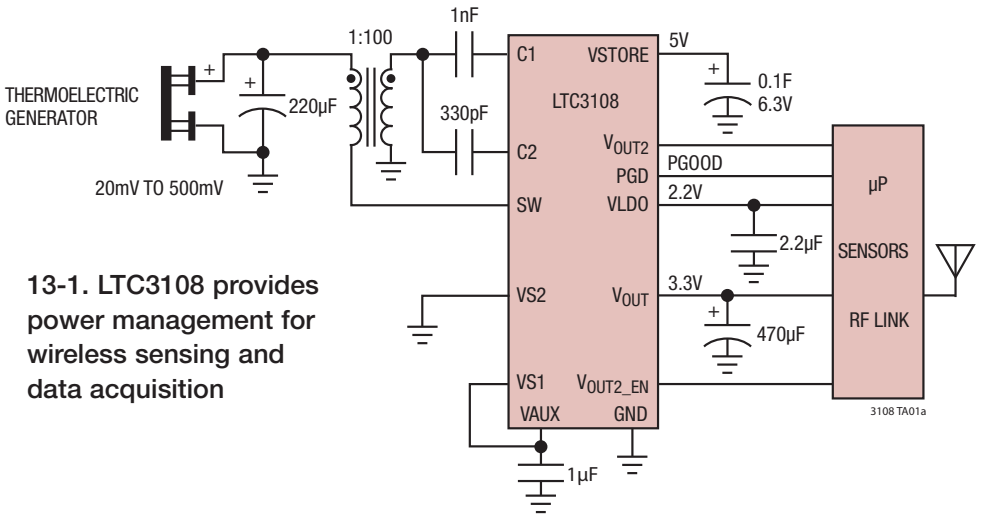

13-1. LTC3108 provides power management for wireless sensing and data acquisition

Energy Harvesting IC

Linear Technology's LTC3108, a highly integrated dc-dc converter is intended for energy harvesting. It can harvest and manage surplus energy from extremely low-input voltage sources such as TEG (thermoelectric generators), thermopiles. and small solar cells.

The circuit in Fig. 13-1 uses a small step-up transformer to boost the input voltage to an LTC3108 that provides a complete power-management solution for wireless sensing and data acquisition. It can harvest small temperature differences and generate system power instead of using traditional battery power. The LTC3108 is available in a small, thermally enhanced12-lead (4mm × 3mm) DFN and a 16-lead SSOP packages.

The LTC3108 utilizes a MOSFET switch to form a resonant step-up oscillator using an external step-up transformer and a small coupling capacitor. This allows it to boost input voltages as low as 20mV, high enough to provide multiple regulated output voltages for powering other circuits. The frequency of oscillation is determined by the inductance of the transformer secondary winding and is typically in the range of 20kHz to 200kHz. For input voltages as low as 20mV, a primary-secondary turns ratio of about 1:100 is recommended. For higher input voltages, this ratio can be lower.

The ac voltage produced on the secondary winding of the transformer is boosted and rectified using an external-charge pump capacitor (from the secondary winding to pin C1) and the rectifiers internal to the LTC3108. The rectifier circuit feeds current into the VAUX pin, providing charge to the external VAUX capacitor and the other outputs.

LDO Output

A 2.2V LDO can support a low-power processor or other low-power ICs. The LDO is powered by the higher value of either VAUX or V_{OUT}. This enables it to become active as soon as VAUX has charged to 2.3V, while the V_{OUT} storage capacitor is still charging. In the event of a step load on the LDO output, current can come from the main VOUT capacitor if VAUX drops below V_{OUT}. The LDO requires a 1µF ceramic capacitor for stability. Larger capacitor values can be used without limitation, but will increase the time it takes for all the outputs to charge up. The LDO output is current limited to 4mA typical.

For pulsed-load applications, size the V_{OUT} capacitor to provide the necessary current for a pulse on load. The capacitor's value will be dictated by the load current, duration of the load pulse, and the voltage droop the circuit can tolerate. The capacitor must be rated for whatever voltage has been selected for V_{OUT} by VS1 and VS2 (Table 13-1).

TABLE 13-1. SETTINGS FOR OUTPUT VOLTAGE

VS2	VS1	V_{OUT}
GND	GND	2.35
GND	VAUX	3.3
VAUX	GND	4.1
VAUX	VAUX	5

There must be enough energy available from the input voltage source for V_{OUT} to recharge the capacitor during the interval between load pulses. Reducing the duty cycle of the load pulse allows operation with less input energy. The VSTORE capacitor may be a very large value (thousands of microfarads or even Farads) to provide holdup at times when the input power may be lost. Note that this capacitor can charge all the way to 5.25V (regardless of the settings for V_{OUT}), so ensure that the holdup capacitor has a working voltage rating of at least 5.5V at the temperature for which it will be used. Fig. 13-2 plots the time for voltage to build up to its final value for a given input voltage and the input transformer turns ratio. The LTC3108's extremely low quiescent current (<6µA) and high-efficiency design ensure the fastest possible charge times for the output reservoir capacitor.

As listed in Table 13-1 above, the main output is pin-selectable via VS1 and VS2 for one of four fixed voltages (2.35V, 3.3V, 4.1V, or 5V) to power a wireless transmitter or sensors. A second switched output can be enabled by the host to power devices that do not have a micropower shutdown capability. The addition of a storage capacitor provides continuous power even when the input energy source is unavailable.

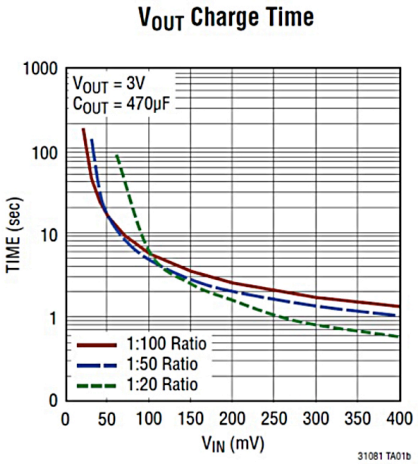

13-2. Plot of time for voltage to build up to its final value using the LTC3108.

A power-good comparator monitors V_{OUT}. The PGD pin is an open-drain output with a weak pull-up (1MΩ) to the LDO voltage. Once V_{OUT} charges to within 7% of its regulated voltage, the PGOOD output goes high. If V_{OUT} drops more than 9% from its regulated voltage, PGD goes low. The PGD output is designed to drive a microprocessor or other chip I/O and is not intended to drive a higher current load such as an LED. Pulling PGOOD up externally to a voltage greater than VLDO will cause a small current to be sourced into VLDO. PGOOD can be pulled low in a wire-OR configuration with other circuitry.

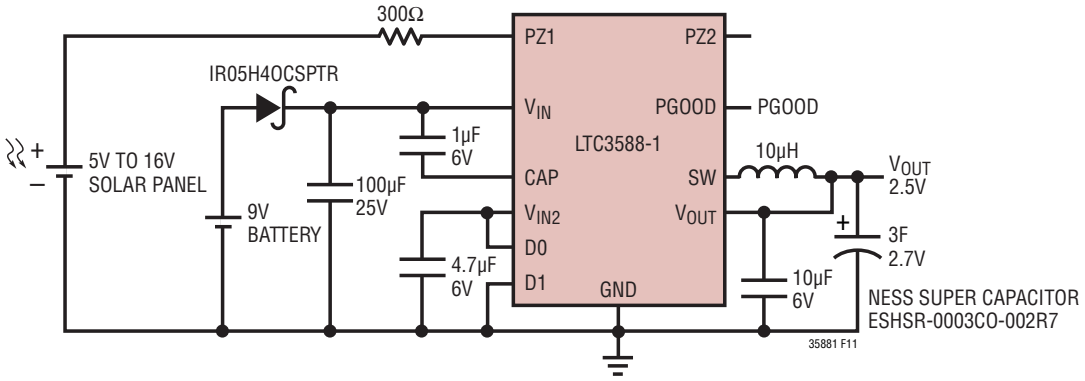

13-3. The LTC3588-1 employs a high efficiency buck converter to harvest solar energy and then convert it to a well-regulated output.

V_{OUT2} is an output that can be turned on and off by the host, using the V_{OUT2}_EN pin. When enabled, V_{OUT2} is connected to VOUT through a 1.3Ω P-channel MOSFET switch. This output, controlled by a host processor, can be used to power external circuits such as sensors and amplifiers, that do not have a low power sleep or shutdown capability. V_{OUT2} can be used to power these circuits only when they are needed.

Piezoelectric Energy Harvesting

Linear Technology's LTC3588-1 is an ultralow quiescent current power supply for energy harvesting and/or low current step-down applications (Fig. 13-3). The IC interfaces directly to a piezoelectric or alternative ac power source, to rectify a voltage waveform and store harvested energy on an external capacitor, bleed off any excess power via an internal shunt regulator, and maintain a regulated output voltage by means of a nanopower high-efficiency synchronous buck regulator.

The LTC3588-1 has an internal full-wave bridge rectifier accessible via the differential PZ1 and PZ2 inputs that rectifies ac inputs such as those from a piezoelectric element. The rectified output is stored on a capacitor at the VIN pin and can be used as an energy reservoir for the buck converter. The low-loss bridge rectifier has a total drop of about 400mV with typical piezo generated currents (~10µA). The bridge is capable of carrying up to 50mA. One side of the bridge can be operated as a single-ended DC input. PZ1 and PZ2 should never be shorted together when the bridge is in use.

When the voltage on VIN rises above the UVLO rising threshold the buck converter is enabled and charge is transferred from the input capacitor to the output capacitor. A wide (~1V) UVLO hysteresis window is employed with a lower threshold approximately 300mV above the selected regulated output voltage to prevent short cycling during buck power-up. When the input capacitor voltage is depleted below the UVLO falling threshold, the buck converter is disabled. Extremely low quiescent current (450nA typical) in UVLO allows energy to accumulate on the input capacitor in situations where energy must be harvested from low power sources.

You can configure the LTC3588-1 for use with dc sources such as a solar panel as shown in Fig. 13-3 by connecting them to one of the PZ1/PZ2 inputs. Connecting the source in this way prevents reverse current from flowing in each element. Current limiting resistors should be used to protect the PZ1 or PZ2 pins. This can be combined with a battery backup connected to VIN with a blocking diode.

Analog Devices' ADP5091/92 is an intelligent integrated energy harvesting nano-powered management solution that converts dc power from PV cells or thermoelectric generators (Fig. 13-4).The IC charges storage elements such as rechargeable Li-Ion batteries, thin film batteries, super capacitors, or conventional capacitors, and powers up small electronic devices and battery-free systems.

The ADP5091/92 provides efficient conversion of the

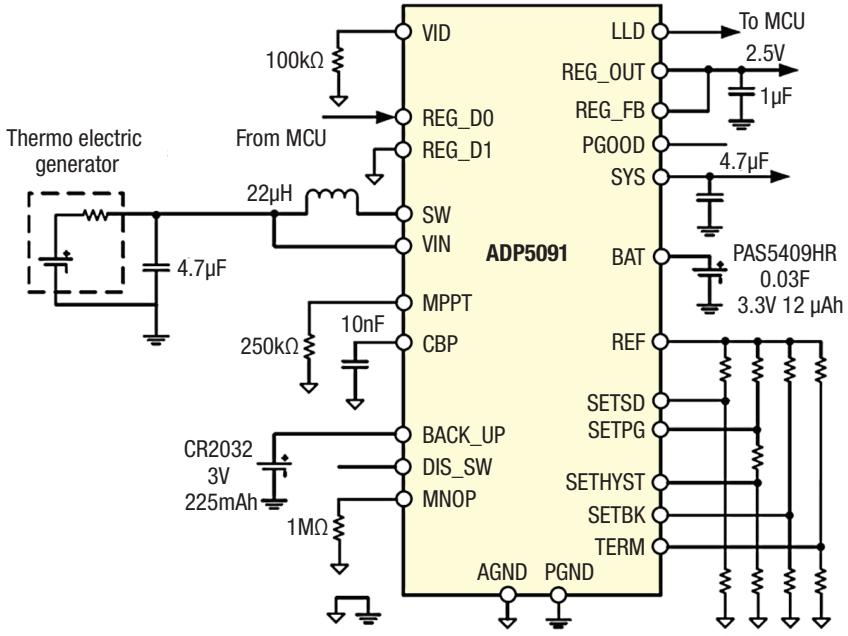

13-4. The ADP5091/92 provides efficient conversion of the harvested limited power from a 16 µW to 600 mW range with sub-µW operation losses.

harvested limited power from a 16 µW to 600 mW range with sub-µW operation losses. With the internal cold-start circuit, the regulator can start operating at an input voltage as low as 380 mV. After a cold startup, the regulator is functional at an input voltage range of 80 mV to 3.3 V. You can program an additional 150mA regulated output with an external resistor divider or VID pin.

By sensing the input voltage, the control loop keeps the input voltage ripple in a fixed range to maintain stable dc-to-dc boost conversion. The OCV dynamic sensing mode and none-sensing mode both programming regulation points of the input voltage allow extraction of the highest possible energy from the harvester. A programmable minimum operation threshold (MINOP) enables boost shutdown during a low light condition. As a low light indicator for microprocessor, the LLD is the MIONP comparator output. In addition, the DIS_SW pin can temporarily shut down the boost regulator and is RF transmission friendly.

The charging control function of ADP5091/92 protects rechargeable energy storage, which is achieved by monitoring the battery voltage with programmable charging termination voltage and shutdown discharging voltage. In addition, a programmable PGOOD flag with programmable hysteresis monitors the SYS voltage.

An optional primary cell battery can be connected and managed by an integrated power path management control block that is programmable to switch the power source from the energy harvester, rechargeable battery, and primary cell battery.

The ADP5091/92 is available in a 24-lead LFCSP and is rated for a –40°C to +125°C junction temperature range.

Related Articles

1. Sam Davis, Energy Harvesting on the Move, powerelectronics.com, March 2015.
2. Sam Davis, Researchers Observe Piezoelectricity and the Piezotronic Effect in Atomically Thin Molybdenum Disulfide (MoS2), powerelectronics.com, November 2014.
3. Sam Davis, Energy Harvesting Poised to Replace Pacemaker Batteries, powerelectronics.com, September 2014.
4. Sam Davis, Thermogalvanic Process Converts Low Temp Waste Heat Into Electricity, powerelectronics.com, June 2014.
5. Frank Schmidt, Power Leap for Energy Harvesting, powerelectronics.com, May 2014.
6. Sam Davis, SolePower: Generate Power When You Walk, powerelectronics.com, June 2013.
7. Sam Davis, Waste Heat-to-Power Update, powerelectronics.com, June 2013.
8. Roger Allan, Energy Harvesting Powers Wireless Sensor Networks In Industrial Apps , electronicdesign.com, September 2012.
9. Roger Allan, Energy Harvesting Efforts Are Picking Up Steam, powerelectronics.com, April 2012.
10. Sam Davis, Effective Energy-Harvesting Requires Appropriate Components, powerelectronics.com, August, 2011.

☞ **BACK TO TABLE OF CONTENTS**

CHAPTER 14:

CIRCUIT PROTECTION DEVICES

Several types of devices are employed in electronic systems to protect against voltage transients, power surges, and excessive voltage or current. Varistors is one of those devices that protect against excessive transient voltages by shunting the current created by the excessive voltage away from sensitive components.

A varistor's resistance varies with the applied voltage. It has a nonlinear, non-ohmic current–voltage characteristic similar to a diode, except that it has the same characteristic for both directions of traversing current. At low voltage it has a high electrical resistance that decreases as the voltage is raised. The most common type of varistor is the metal-oxide varistor (MOV). It is electrically equivalent to a network of back-to-back diode pairs, each pair in parallel with many other pairs.

When a small or moderate voltage is applied across an MOV's electrodes, only a tiny current flows, caused by reverse leakage through the diode junctions. When a large voltage is applied, the diode junction breaks down due to a combination of thermionic emission and electron tunneling, and a large current flows. The result of this behavior is a highly nonlinear current-voltage characteristic, in which the MOV has a high resistance at low voltages and a low resistance at high voltages.

A varistor remains non-conductive as a shunt-mode device during normal operation when the voltage across it remains well below its "clamping voltage", thus varistors are typically used for suppressing line voltage surges.

Varistors will eventually fail from not successfully limiting a very large surge from an event like a lightning strike, where the energy involved is many orders of magnitude greater than the varistor can handle. Follow-through current resulting from a strike may melt, burn, or even vaporize the varistor. This thermal runaway leads to the failure of dominant current paths under thermal stress when the energy in a transient pulse exceeds the manufacture's "Absolute Maximum Ratings". You can reduce the probability of catastrophic failure by increasing the rating, either by using a single varistor of higher rating or by connecting more devices in parallel.

MOV

The most common type of varistor is the metal-oxide varistor (MOV) that contains a ceramic mass of zinc oxide grains, in a matrix of other metal oxides sandwiched between two electrodes). The boundary between each grain and its neighbor forms a diode-like junction, which

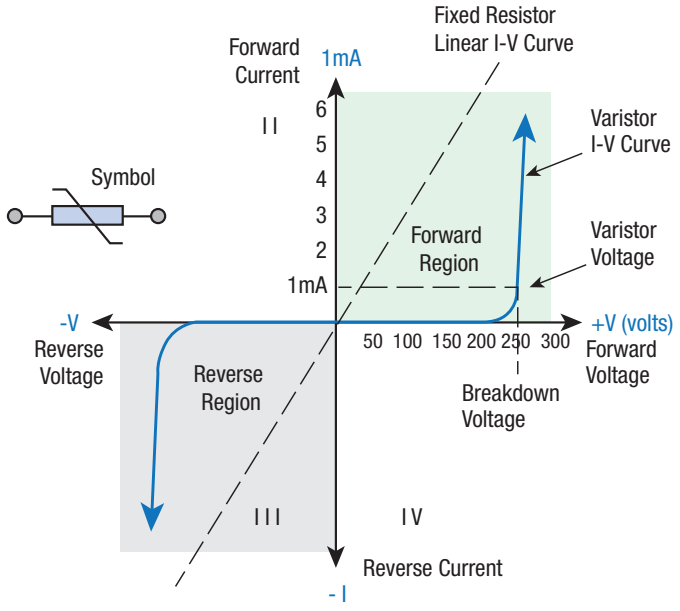

14-1. Voltage vs. current for a typical MOV.

An incorrectly specified MOV may allow frequent lower power swells to degrade its capacity.

allows current to flow in only one direction. When a small or moderate voltage is applied across the electrodes, only a tiny current flows, caused by reverse leakage through the diode junctions. When a large voltage is applied, the diode junction breaks down due to a combination of thermionic emission and electron tunneling, and a large current flows. The result of this behavior is a highly nonlinear current-voltage characteristic, in which the MOV has a high resistance at low voltages and a low resistance at high voltages. Fig. 14-1 shows the current vs. voltage of a typical MOV compared with an SiC diode.

As shown in Fig. 14-1, the varistor has symmetrical bi-directional characteristics. It operates in both directions (quadrant I and III) of a sinusoidal waveform in a manner similar to two zener diodes connected back-to-back. When not conducting, the I-V curve has a linear relationship as the current flowing through the varistor remains constant and low at only a few microamperes of "leakage." This occurs because its high resistance acts as an open circuit and remains constant until the voltage across the varistor (either polarity) reaches its particular rated voltage.

An incorrectly specified MOV may allow frequent lower power swells to degrade its capacity. In this condition the varistor is not visibly damaged and outwardly appears functional, but no longer offers protection. Eventually, it proceeds into a shorted circuit condition as the energy discharges create a conductive channel through the oxides.

The main parameter affecting varistor life expectancy is its energy (Joule) rating. Increasing the energy rating raises the number of (defined maximum size) transient pulses that it can accommodate exponentially as well as the cumulative sum of energy from clamping lesser pulses. As these pulses occur, the "clamping voltage" it provides during each event decreases, and a varistor is typically deemed to be functionally degraded when its "clamping voltage" has changed by 10%. Manufacturer's life-expectancy charts relate current, severity and number of transients to make failure predictions based on the total energy dissipated over the life of the part.

Let-through voltage specifies what spike voltage will cause the protective components inside a surge protector to divert unwanted energy from the protected line. A lower clamping voltage indicates better protection, but can sometimes result in a shorter life expectancy for the overall protective system. The lowest three levels of protection defined in the UL rating are 330 V, 400 V and 500 V. The standard let-through voltage for 120 V AC devices is 330 V.

This number of Joules defines how much energy an MOV-based surge protector can theoretically absorb in a single event, without failure. Counter-intuitively, a lower number may indicate longer life expectancy if the device can divert more energy elsewhere and thus absorb less energy. In other words, a protective device offering a lower clamping voltage while diverting the same surge current will cause more of the surge energy to be dissipated elsewhere in that current's path. Better protectors exceed peak ratings of 1000 joules and 40,000 amperes.

Usually a lower joule rating is undersized protection, since the total energy in harmful spikes can be significantly larger than this. However, if properly installed, for every joule joule absorbed by a protector, another 4 to 30 joules may be dissipated harmlessly into ground. An MOV-based protector with a higher let-through voltage can receive a higher joule rating, even though it lets more surge energy through to the device to be protected.

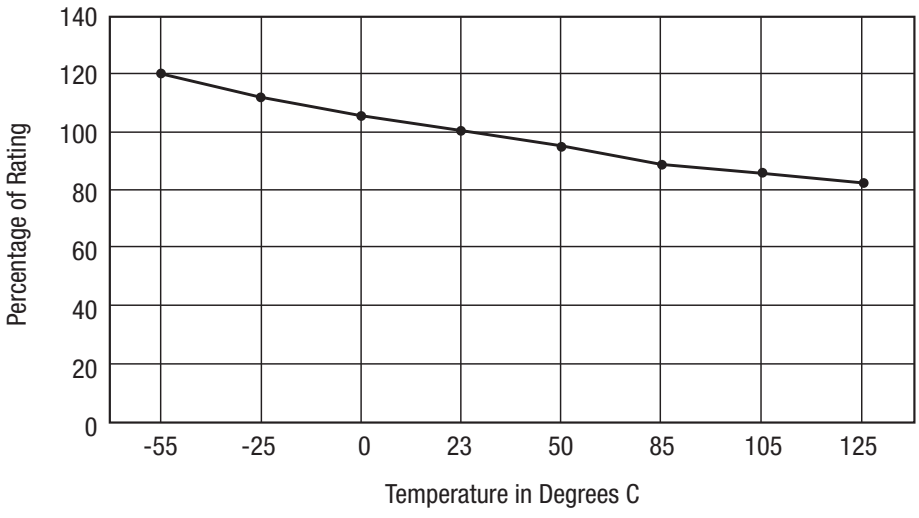

14-2. Fuse derating curves.

The joule rating is a commonly quoted but very misleading parameter for comparing MOV-based surge protectors. A surge of any arbitrary ampere and voltage combination can occur in time, but surges commonly last only for nanoseconds to microseconds, and experimentally modeled surge energy has been far under 100 joules. Well-designed surge protectors should not rely on MOVs to absorb surge energy, but instead to survive the process of harmlessly redirecting it to ground. Generally, more joules means an MOV absorbs

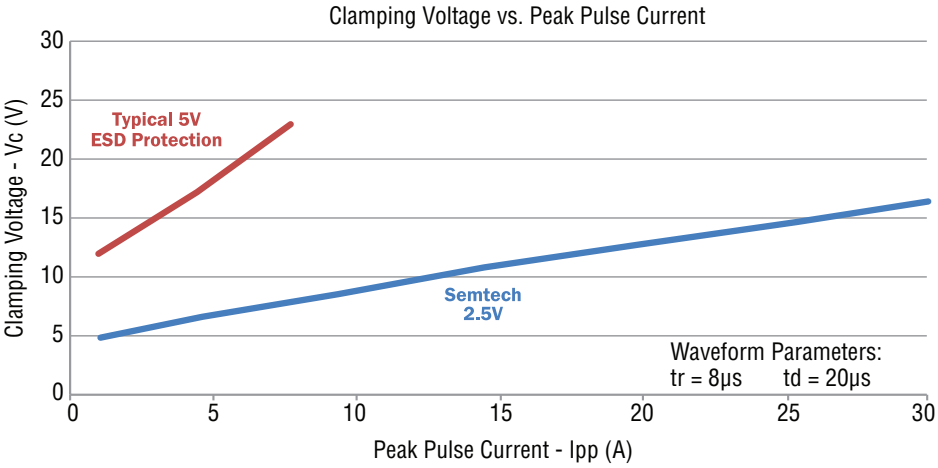

14-3. µClamp3321ZA clamping voltage vs. peak pulse current (tp = 8/20µS).

less energy while diverting even more into ground.

Some manufacturers commonly design higher joule-rated surge protectors by connecting multiple MOVs in parallel. Since individual MOVs have slightly different non-linear responses when exposed to the same overvoltage, any given MOV might be more sensitive than others. This can cause one MOV in a group to conduct more (called "current hogging"), leading to overuse and eventually premature failure of that component. If a single inline fuse is placed in series with the MOVs as a power-off safety feature, it will open and fail the surge protector even if remaining MOVs are intact. Thus, the effective surge energy absorption capacity of the entire system is dependent on the MOV with the lowest clamping voltage, and the additional MOVs do not provide any further benefit. This limitation can be surmounted by using carefully matched sets of MOVs, but this matching must be carefully coordinated with the original manufacturer of the MOV components.

Surge protectors don't operate instantaneously; a slight delay exists. The longer the response time, the longer the connected equipment will be exposed to the surge. However, surges don't happen instantly either. Surges usually take a few microseconds to reach their peak voltage, and a surge protector with a nanosecond response time would kick in fast enough to suppress the most damaging portion of the spike.

Therefore, response time under standard testing is not a useful measure of a surge protector's ability when comparing MOV devices. All MOVs have response times measured in nanoseconds, while test waveforms usually used to design and calibrate surge protectors are all based on modeled waveforms of surges measured in microseconds. As a result, MOV-based protectors have no trouble producing impressive response-time specs.

Each standard defines different protector characteristics, test vectors, or operational purpose.

Frequently listed standards include:

- IEC 61643-1
- EN 61643-11 and 61643-21
- Telcordia Technologies Technical Reference TR-NWT-001011
- ANSI/IEEE C62.xx
- Underwriters Laboratories (UL) 1449

EN 62305 and ANSI/IEEE C62.xx define what spikes a protector might be expected to divert. EN 61643-11 and 61643-21 specify both the product's performance and safety requirements. In contrast, the IEC only writes standards and does not certify any particular product as meeting those standards. IEC Standards are used by members of the CB Scheme of international agreements to test and certify products for safety compliance.

None of those standards guarantee that a protector will provide proper protection in a given application. Each standard defines what a protector should do or might accomplish, based on standardized tests that may or may not correlate to conditions present in a particular real-world situation. A specialized engineering analysis may be needed to provide sufficient protection, especially in situations of high lightning risk.

The UL1449 (3rd Edition) standard for SPDs is a major rewrite of previous editions, and has also been accepted as an ANSI standard for the first time.

Fuses

Selecting the right fuse is critical in electronic system designs. You can prevent catastrophic system failure with the proper fuse on the input of a device. In the event that internal circuits can no longer withstand an overload condition, the fuse will prevent fire or further damage to the board, the device, or neighboring components. Most equipment is protected from short circuits on their outputs by either circuit-sensing current limit and/or thermal overload circuits. Fuses are required to protect against a catastrophic component failure or if a component failure causes a short circuit on the inside of the device. Proper selection of an input fuse involves understanding and consideration of the following factors.

Voltage rating is based on the ac and/or dc circuit voltage into which they can be safely applied. A fuse installed in an ac circuit performs differently than when installed in a dc circuit. With ac circuits, the current is crossing the zero potential at 60 or 50 cycles a second. This helps in breaking the arc forms when the fuse element melts and creates a gap. In dc circuits, the voltage does not go to a

zero potential, making it more difficult to suppress the arc in the melting element's gap. Fuses are insensitive to voltage changes within their ratings so selecting the proper voltage rating is strictly a safety issue. Fuses can operate at any voltage below or equal to their rated voltage.

Current rating is determined by the maximum input current of a device. Typically, the maximum current consumption occurs at the maximum output load and the minimum input voltage. Although some devices are designed for constant current output regulation, most are designed as constant power devices. This means that as the input voltage drops, the input current must increase to uphold the constant output power. The magnitude of the input current can be determined from:

$$I_{input\_max} = \frac{P_{out\_max}}{V_{in\_min} \times E} \quad (1)$$

Where:

P_{out_max} = Maximum output power of the dc-dc converter

V_{in_min} = Minimum input voltage on the input pins of the dc-dc converter

E = Efficiency of the device at P_{out_max} and V_{in_min}

To prevent damage to device components, select a fuse current rating with a large enough current capability so that the fuse will not open under steady state conditions, yet will open during an abnormal (excessive) overload or short-circuit condition. Therefore, select a fuse to be 150% to 200% percent of the maximum steady state input current at maximum load and minimum line input voltage.

Interrupting rating is the maximum current at rated voltage the fuse can safely interrupt. This rating must exceed the maximum fault (short-circuit) current the circuit can produce. Interrupting ratings for ac and DC currents are different and the fuse data sheet should be consulted before selection.

Temperature derating is the ambient temperature exceeding the standard 23°C. The fuse current rating should be derated (a higher current rating with higher temperatures). Conversely, operating at an ambient temperature lower than the 23°C standard allows use of a lower current rating.

Fuse rating is determined by:

$$I_{rated} = \frac{I_{input\_max}}{K_{temp}} \quad (2)$$

Where:

I_{input_max} = the current determined from Equation 1 or the device datasheet

K_{temp} = the temperature derating factor determined from the derating factor (Fig. 14-2)

The lowest suitable fuse rating is obtained by rounding up the calculated value to the next higher current rating shown in the fuse datasheet.

Melting integral, termed melting I^2t, is the thermal energy required to melt a specific fuse element. The fuse element construction, materials and cross sectional area determine this value.

Peak inrush current is usually greater than the steady state current. Also, periodic inrush currents can be sufficiently powerful to warm the fuse element. Though not large enough to melt the element, it can still cause thermal stress to the element. Cyclical expansions and contractions of the fuse element can lead to mechanical fatigue and premature failure.

Calculate the melting I^2t values of the fuse for the condition where the product of the peak current squared and the time when the peak occurs is maximum. For example, the steady state current is maximum at low line so a transient load surge needs to be added to the low line current to establish the maximum peak current for an operating condition. But the inrush current is usually maximum at the highest input voltage. The fuse's melting I^2t must be evaluated at the condition with the highest calculated I^2t to ensure that the fuse will not open during these "normal" operating conditions.

Select a fuse with the minimum I^2t greater than the energy of the inrush current pulse. This ensures that the fuse will not cause a nuisance opening during transient conditions. For reliable system operation for the required number of turn-on cycles, meet the following condition:

$$I^2t\ Fuse \geq I^2t_{\ Pulse} \times F_P \quad (3)$$

Where:

$I^2t_{\ Pulse}$ = Energy of a current pulse

$I^2t_{\ Fuse}$ = Melting integral of a fuse

F_P = Pulse factor (dependent on fuse element construction)

I^2t Fuse can be found in fuse datasheets. Do not use the fuse's maximum melting integral in Equation 3, and use either the minimum or nominal melting integral of the fuse.

Other selection considerations include start-up (inrush) currents and transient load conditions. When a device is initially powered, the input bulk capacitors must be charged. For example, current flowing into the input terminals of a dc-dc converter is approximately I = V/R for typical power supplies with charge times less than 10 mS. When V is the input voltage change, and R is a combination of wiring resistance, your source's resistance under start-up, and the Equivalent Series Resistance (ESR) of the converter's input bulk capacitors.

Larger devices often use a large capacitor with very low ESR inside the converter. This inrush current can have a significant effect on the fuse's life. Size the fuse properly to allow these inrush current pulses to pass without nuisance openings or degrading the fuse element as discussed in melting integral.

14-4. FLAT GDT has a flat package and horizontal circuitry design that meets the need for more sensitive overvoltage protection requirements in high-density and space-restricted applications.

To calculate current pulse energy, first determine the magnitude and duration of the current pulse. The most accurate way to determine parameters of a current pulse is to measure this current in the application under minimum and maximum voltage conditions.

TVS

A transient voltage suppressor (TVS) reacts to sudden or momentary overvoltage conditions. One such common device used for this purpose is known as the transient voltage suppression diode that is simply a Zener diode designed to protect electronics device against overvoltage.

The characteristic of a TVS requires that it respond to overvoltages faster than other common overvoltage protection components such as varistors or gas discharge tubes. This makes TVS devices or components useful for protection against very fast and often damaging voltage spikes. These fast overvoltage spikes are present on all distribution networks and can be caused by either internal or external events, such as lightning or motor arcing.

Applications of transient voltage suppression diodes are used for unidirectional or bidirectional electrostatic discharge protection of transmission or data lines in electronic circuits. The level of energy in a transient overvoltage can be equated to energy measured in joules or related to electric current when devices are rated for various applications. These bursts of overvoltage can be measured with specialized electronic meters that can show power disturbances of thousands of volts amplitude that last for a few microseconds or less.

Semtech's µClamp 3321ZA is a high-performance transient voltage suppression (TVS) for protecting low voltage interfaces (Fig. 14-3). The single-line µClamp3321ZA offers a unique combination of features that protect increasingly sensitive interfaces.

The µClamp3321ZA delivers optimal transient protection for safeguarding devices operating at 3.3V. It features low dynamic resistance, which provides fast response to transients, as well as low-clamping voltage to protect devices from damage. It is housed in an ultra-small, fully encapsulated package, which provides a more robust solution than conventional CSP (Chip Scale Package) solutions. In addition, the µClamp3321ZA extends the battery life of end-user applications by providing low reverse leakage current of <1nA (typical).

These TVS diodes protect sensitive electronics from damage or latch-up due to ESD. They replace 0201 size multilayer varistors (MLVs) in portable applications such as cell phones, notebook computers, and other portable electronics. They feature large cross-sectional area junctions for con¬ducting high transient currents. This device offers desir-able characteristics for board level protection including fast response time, low operating and clamping voltage, and no device degradation.

It features extremely good ESD protec¬tion characteristics highlighted by low typical dynamic resistance of 0.33 Ω, low peak ESD clamping volt¬age, and high ESD withstand voltage (±15kV contact per IEC 61000-4-2). Low maximum capacitance (5pF at VR=0V) minimizes loading on sensitive circuits. Each device will protect one data line operating at 3.3 V.

µClamp3321ZA is in a 2-pin SLP0603P2X3F package. It measures 0.6 × 0.3 mm with a nominal height of only 0.25mm. Leads are finished with NiAu. The small pack¬age provides flexibility to protect single lines in applications where arrays are not practical. The combination of small size and high ESD surge capability makes them ideal for use in portable applications such as cellular phones, digital cameras, and tablet PCs. Fig. 14-3 shows clamping voltage vs. peak pulse current (tp = 8/20µS).

Among its features:

- Transient protection for high-speed signal lines: IEC 61000-4-2 (ESD) ±17kV (air), ±15kV (contact)
- 3.3V working-voltage protection for low-voltage interfaces
- Low ESD clamping voltage of 10.5V at 8kV
- Ultra-small package size: 0.6mm × 0.3mm with nominal height of only 0.25mm
- Low typical dynamic resistance: 0.33 W
- Pb Free and RoHS/WEEE compliant

GDT

A new gas discharge tube (GDT) from Bourns provides a breakthrough flat package design with a volume and

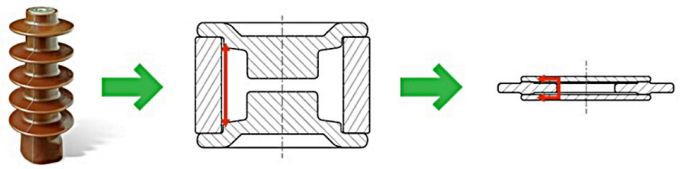

14-5. FLAT GDT design is patterned after a high-voltage insulator, employing "wrinkled" insulating pathways.

space-saving circuit protection design. The two-electrode Model 2017 Series FLAT GDT has a flat package and horizontal circuitry design that meets the need for more sensitive overvoltage protection requirements in high density and space-restricted applications (Fig. 14-4). This new series delivers a 75% savings in volume compared to a standard 8 mm Bourns GDT. Typical applications for the new GDT include:

- Telecom CPE
- Industrial communications
- Surge protective devices
- High-density PCB assemblies

The FLAT GDT is consistent with electronic systems that continue to require higher density and performance in smaller packages. However, as designs become increasing smaller, they are more susceptible to damage from transients such as lightning and high voltage surges. Therefore, circuit-protection technology must follow with smaller, more robust devices. GDTs are a popular circuit-protection solution because of their low capacitance, low leakage characteristics, and high surge-current handling capability.

Traditional high current GDTs are cylindrically shaped devices in an 8 × 6 mm size. These dimensions are critical to effectively handling surge energy and maintain electrical isolation. Their diameter and thermal mass provide much of the current handling capabilities for the GDT. Unfortunately, the larger conventional GDTs offer reliable overvoltage protection, at the cost of valuable PCB space.

Besides reducing height and overall volume, Bourns' new FLAT GDT technology is able to maintain the device's robust isolation and current-handling overvoltage protection capabilities. This new compact GDT offers superior surge current ratings, low leakage, and insertion loss with constant capacitance regardless of voltage. These devices also do not impact signal or system operation due to their voltage limiting capabilities optimized for long-term reliability and performance to satisfy the needs of today's more complex electronics equipment.

The FLAT GDT design is patterned after a high voltage insulator, as shown in Fig. 14-5. Similarly, the new GDT design employs "wrinkled" insulating pathways while maintaining the internal gap of the GDT. This allows the GDT to be compressed in the axial direction, reducing its overall volume/size.

The Model 2017 Series is an ITU K.12 Class III GDT device rated at 10 kA on an 8/2μs waveform. The series features DC breakdown voltages ranging from 90 to 500 V. Maximizing its design flexibility, the FLAT GDT offers multiple mounting options including bottom-side PCB, and is available in horizontal and vertical surface mount versions as well as a leadless design for cartridge or clamp fit applications. The Model 2017 FLAT GDT is RoHS compliant.

Fig. 14-6 shows the voltage vs. time plot for the GDT.

14-6. Voltage vs. time plot for the FLAT GDT.

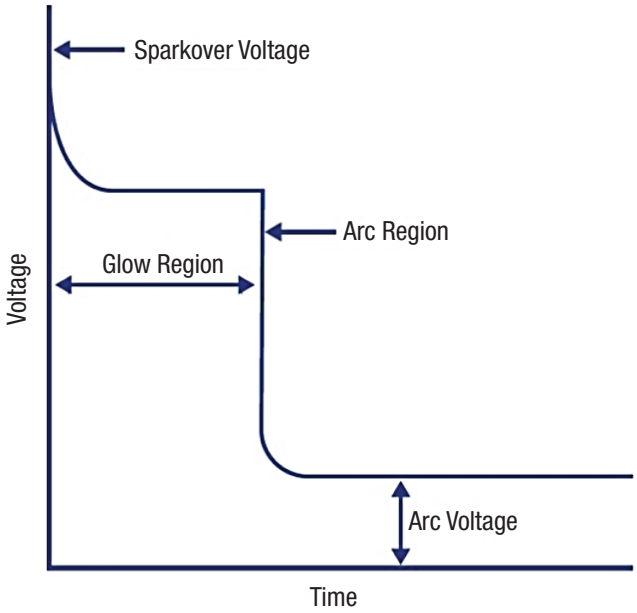

Related Articles

1. Nabil Sadiq, Selecting Fuses: Simple Procedures to Get the Right Overcurrent Protection for DC-DC Converters, powerelectronics.com, August 2010.

2. Brian Ahearne, Next-Generation Resettable Fuses Target Complex Protection Needs, powerelectronics.com, July 2009.

3. Andy Morrish, Limitations of Traditional Circuit Protection for High Energy Surge Threats, powerelectronics.com, January 2013.

4. Mike Smith, Advanced Circuit Protection for RS-485 Ports, powerelectronics.com, May 2012.

5. Sam Davis, Surge Stopper IC Protects Loads From >500V Power Supply Input, powerelectronics.com, March 2012.

6. Deepak Divan, Filling the Gaps in Surge Protection, powerelectronics.com, May 2006.

7. Bruno van Beneden, Varistors: Ideal Solution to Surge Protection, powerelectronics.com, May 2003.

8. Thomas Kugelstadt, How Much On-Chip Transient Protection Is Enough?, Electronic Design, July, 2012.
9. Timothy Hegarty, TVS Clamping in Hot-Swap Circuits, powerelectronics.com, October 2011.
10. Steven J. Goldman, Selecting Protection Devices: TVS Diodes vs. Metal-Oxide Varistors, powerelectronics.com, June 2010.

☞ **BACK TO TABLE OF CONTENTS**

CHAPTER 15:

PHOTOVOLTAIC SYSTEMS

A photovoltaic cell converts light energy directly into electricity by the photovoltaic effect, which is a physical and chemical phenomenon. It is defined as a device whose electrical characteristics, such as current, voltage, or resistance, vary when exposed to light. Solar cells are the building blocks of photovoltaic modules, known as solar panels.

Multiple solar cells in an integrated group, all oriented in one plane, constitute a solar photovoltaic panel or solar photovoltaic module. Photovoltaic modules often have a sheet of glass on the sun-facing side, allowing light to pass while protecting the semiconductor wafers. Solar cells are usually connected in series in modules, creating an additive voltage. Connecting cells in parallel yields a higher current; however, problems such as shadow effects can shut down the weaker (less illuminated) parallel string (a number of series-connected cells) causing substantial power loss and possible damage because of the reverse bias applied to the shadowed cells by their illuminated partners. Strings of series cells are usually handled independently and not connected in parallel, though (as of 2014) individual power boxes are often supplied for each module, and are connected in parallel. Although modules can be interconnected to create an array with the desired peak dc voltage and loading current capacity, using independent MPPTs (maximum power point trackers) is preferable. Otherwise, shunt diodes can reduce shadowing power loss in arrays with series/parallel connected cells.

Adjusting for inflation, it cost $96 per watt for a solar module in the mid-1970s. Process improvements and a very large boost in production have brought that figure down 99%, to 68 cents per watt in 2016, according to data from Bloomberg New Energy Finance. Swanson's Law is an observation similar to Moore's Law that states that solar cell prices fall 20% for every doubling of industry capacity.

During the 1990s, polysilicon ("poly") cells became increasingly popular. These cells offer less efficiency than their mono-silicon ("mono") counterparts, but they are grown in large vats that reduce cost. By the mid-2000s, poly was dominant in the low-cost panel market, but more recently the mono returned to widespread use.

Manufacturers of wafer-based cells responded to high silicon prices in 2004-08 with rapid reductions in silicon consumption. Current cells use 8-9 grams (0.28-0.32 oz) of silicon per watt of power generation, with wafer thicknesses in the neighborhood of 200 microns.

The overall efficiency is the product of these individual metrics, which are:

- Charge carrier separation efficiency
- Reflectance efficiency
- Thermodynamic efficiency
- Conductive efficiency

A solar cell has a voltage-dependent efficiency curve, temperature coefficients, and allowable shadow angles.

Due to the difficulty in measuring these parameters directly, other parameters are substituted:

- Thermodynamic efficiency
- Quantum efficiency
- Integrated quantum efficiency
- V_{OC} ratio
- Fill factor

Reflectance losses are a portion of quantum efficiency under "external quantum efficiency." Recombination losses make up another portion of quantum efficiency, V_{OC} ratio, and fill factor. Resistive losses are predominantly categorized under fill factor, but also make up minor portions of quantum efficiency, V_{OC} ratio, "OC" is open circuit.

The Fill Factor is the ratio of the actual maximum obtainable power to the product of the open circuit voltage and short circuit current. This is a key parameter in evaluating performance. In 2009, typical commercial solar cells had a Fill Factor > 0.70. Grade B cells were usually between 0.4 to 0.7. Cells with a high Fill Factor have a low equivalent

series resistance and a high equivalent shunt resistance, so less of the current produced by the cell is dissipated in internal losses.

Single p–n junction crystalline silicon devices are now approaching the theoretical limiting power efficiency of 33.7%, noted as the Shockley–Queisser limit in 1961. In the extreme, with an infinite number of layers, the corresponding limit is 86% using concentrated sunlight.

For triple-junction thin-film solar cells, the world record is 13.6%, set in June 2015.

Solar cells can be classified into first-, second-, and third-generation cells.

- First-generation cells—also called conventional, traditional, or wafer-based cells—are made of crystalline silicon, the commercially predominant PV technology that includes materials such as polysilicon and monocrystalline silicon.
- Second-generation cells are thin-film solar cells that include amorphous silicon, CdTe, and CIGS cells and are commercially significant in utility-scale photovoltaic power stations, building integrated photovoltaics or in small stand-alone power system.
- Third-generation solar cells include a number of thin-film technologies often described as emerging photovoltaics—most of them have not yet been commercially applied and are still in the research or development phase. Many use organic materials, often organometallic compounds as well as inorganic substances. Despite the fact that their efficiencies had been low and the stability of the absorber material was often too short for commercial applications, there is a lot of research invested into these technologies as they promise to achieve the goal of producing low-cost, high-efficiency solar cells.

By far, the most prevalent bulk material for solar cells is crystalline silicon (c-Si), also known as "solar grade silicon." Bulk silicon is separated into multiple categories according to crystallinity and crystal size in the resulting ingot, ribbon, or wafer. These cells are entirely based around the concept of a p-n junction. Solar cells made of c-Si are made from wafers between 160 to 240 micrometers thick.

Monocrystalline silicon (mono-Si) solar cells are more efficient and more expensive than most other types of cells. The corners of the cells look clipped, like an octagon, because the wafer material is cut from cylindrical ingots that are typically grown by the Czochralski process. Solar panels using mono-Si cells display a distinctive pattern of small white diamonds.

Epitaxial wafers can be grown on a monocrystalline silicon "seed" wafer by atmospheric-pressure CVD in a high-throughput inline process, and then detached as self-supporting wafers of some standard thickness (e.g., 250 µm) that can be manipulated by hand, and directly substituted for wafer cells cut from monocrystalline silicon ingots. Solar cells made with this technique can have efficiencies approaching those of wafer-cut cells, but at appreciably lower cost.

Polycrystalline silicon, or multi-crystalline silicon (multi-Si) cells are made from cast square ingots—large blocks of molten silicon carefully cooled and solidified. They consist of small crystals giving the material its typical metal flake effect. Polysilicon cells are the most common type used in photovoltaics and are less expensive, but also less efficient, than those made from monocrystalline silicon.

Ribbon silicon is a type of polycrystalline silicon—it is formed by drawing flat thin films from molten silicon and results in a polycrystalline structure. These cells are cheaper to make than multi-Si, due to a great reduction in silicon waste, as this approach does not require sawing from ingots. However, they are also less efficient.

Thin-film solar-cell technologies reduce the amount of active material in a cell. Most designs sandwich active material between two panes of glass. Since silicon solar panels only use one pane of glass, thin film panels are approximately twice as heavy as crystalline silicon panels, although they have a smaller ecological impact (determined from life-cycle analysis). The majority of film panels have 2-3 percentage points lower conversion efficiencies than crystalline silicon. Cadmium telluride (CdTe), copper indium gallium selenide (CIGS), and amorphous silicon (a-Si) are three thin-film technologies often used for outdoor applications. Thin-film solar cells are increasing due to it being silent, renewable, and solar energy being the most abundant energy source on Earth.

Cadmium telluride is the only thin-film material so far to rival crystalline silicon in cost/watt. However, cadmium is highly toxic and tellurium (anion: "telluride") supplies are limited. The cadmium present in the cells would be toxic if released. However, release is impossible during normal operation of the cells and is unlikely during fires in residential roofs. A square meter of CdTe contains approximately the same amount of Cd as a single C cell nickel-cadmium battery, in a more stable and less soluble form.

Copper indium gallium selenide (CIGS) is a direct band gap material. It has the highest efficiency (~20%) among all commercially significant thin film materials. Traditional methods of fabrication involve vacuum processes including co-evaporation and sputtering. Recent developments attempt to lower the cost by using non-vacuum solution processes.

Silicon thin-film cells are mainly deposited by chemical vapor deposition (typically plasma-enhanced, PE-CVD) from silane gas and hydrogen gas. Depending on the deposition parameters, this can yield amorphous silicon (a-Si or a-Si:H), protocrystalline silicon, or nanocrystalline sili-

con (nc-Si or nc-Si:H), also called microcrystalline silicon.

Amorphous silicon is the most well-developed thin film technology to-date. An amorphous silicon (a-Si) solar cell is made of non-crystalline or microcrystalline silicon. Amorphous silicon has a higher bandgap (1.7 eV) than crystalline silicon (c-Si) (1.1 eV), which means it absorbs the visible part of the solar spectrum more strongly than the higher-power density infrared portion of the spectrum. The production of a-Si thin-film solar cells uses glass as a substrate and deposits a very thin layer of silicon by plasma-enhanced chemical vapor deposition (PECVD).

Protocrystalline silicon with a low-volume fraction of nanocrystalline silicon is optimal for high open-circuit voltage. Nc-Si has about the same bandgap as c-Si and nc-Si and a-Si can advantageously be combined in thin layers, creating a layered cell called a tandem cell. The top cell in a-Si absorbs the visible light and leaves the infrared part of the spectrum for the bottom cell in nc-Si.

Gallium arsenide (GaAs) is also used for single-crystalline thin film solar cells. Although GaAs cells are very expensive, they hold the world's record in efficiency for a single-junction solar cell at 28.8%. GaAs is more commonly used in multi-junction photovoltaic cells for concentrated photovoltaics (CPV, HCPV) and for solar panels on spacecrafts, as the industry favors efficiency over cost for space-based solar power.

PV cells come in many sizes and shapes, from smaller than a postage stamp to several inches across. They are often connected together to form PV modules that may be up to several feet long and a few feet wide.

Modules, in turn, can be combined and connected to form PV arrays of different sizes and power output. The modules of the array make up the major part of a PV system, which can also include electrical connections, mounting hardware, power-conditioning equipment, and batteries that store solar energy for use when the sun is not shining.

PV Arrays are made up of PV modules, which are environmentally sealed collections of PV Cells. The most common PV module is 5 to 25 square feet in size and weighing about 3 to 4 lb/sq. ft. Often sets of four or more smaller modules are framed or attached together by struts in what is called a panel. This panel is typically around 19 to 35 square feet in area for ease of handling on a roof. This allows some assembly and wiring functions to be done on the ground if called for by the installation instructions.

When light shines on a PV cell, it may be reflected, absorbed, or pass right through. But only the absorbed light generates electricity. The energy of the absorbed light is transferred to electrons in the atoms of the PV cell semiconductor material. With their newfound energy, these electrons escape from their normal positions in the atoms and become part of the electrical flow, or current, in an electrical circuit. A special electrical property of the PV cell—what is called a "built-in electric field"—provides the force, or voltage, needed to drive the current through an external load, such as a light bulb.

Solar Modules

The heart of a photovoltaic system is the solar module. Many photovoltaic cells are wired together by the manufacturer to produce a solar module. When installed at a site, solar modules are wired together in series to form strings. Strings of modules are connected in parallel to form an array.

Module Types–Rigid flat-framed modules are currently most common and most of these are composed of silicon. Silicon cells have atomic structures that are single-crystalline (mono-crystalline), poly-crystalline (multi-crystalline), or amorphous (thin film silicon). Other cell materials used in solar modules are cadmium telluride (CdTe, commonly pronounced "CadTel") and copper indium diselenide (CIS). Some modules are manufactured using combinations of these materials. An example is a thin film of amorphous silicon deposited onto a substrate of single-crystalline silicon.

In 2005, approximately 90% of modules sold in the United States were composed of crystalline silicon, either single-crystalline or poly-crystalline. The market share of crystalline silicon is down from previous years, however, and continues to drop as sales of amorphous silicon, CdTe and CIS modules are growing.

Rated Power–Grid-connected residential PV systems use modules with rated power output ranging from 100 to 300 watts. Modules as small as 10 watts are used for other applications. Rated power is the maximum power the panel can produce with 1,000 watts of sunlight per square meter at a module temperature of 25°C or 77°F in still air. Actual conditions will rarely match rated conditions and so actual power output will almost always be less.

PV System Voltage–Modern systems without batteries are typically wired to provide from 235V to 600V. In battery-based systems, the trend is also toward use of higher array voltages, although many charge controllers still require lower voltages of 12V, 24V, or 48V to match the voltage of the battery string.

Using Manufacturer's Product Information to Compare Modules–Since module costs and efficiencies continue to change as technology and manufacturing methods improve, it is difficult to provide general recommendations that will be true into the future regarding, for example, which type of module is cheapest or the best overall choice. It is best to make comparisons based on current information provided by manufacturers, combined with the specific requirements of your application.

Two figures that are useful in comparing modules are:

• Price per watt
• Rated power output per area (or efficiency)

When looking through a manufacturer's catalog of solar modules, you will often find the rated power, the overall dimensions of the module, and its price. Find the cost per watt by dividing the module's price by its rated output in watts. Find the watts per area, by dividing its rated output by its area.

Module Cost per Watt–As a general rule, thin film modules have lower costs than crystalline silicon modules for modules of similar powers.

Module Efficiency (Watts per Area)–Modules with higher efficiency will have a higher ratio of watts to area. The higher the efficiency, the smaller the area (i.e., fewer modules) will be required to achieve the same power output of an array. Installation and racking costs will be less with more efficient modules, but this must be weighed against the higher cost of the modules. Amorphous silicon, thin-film CdTe, and CIS modules have rated efficiencies that are lower than crystalline silicon modules, but improvements in efficiency continue.

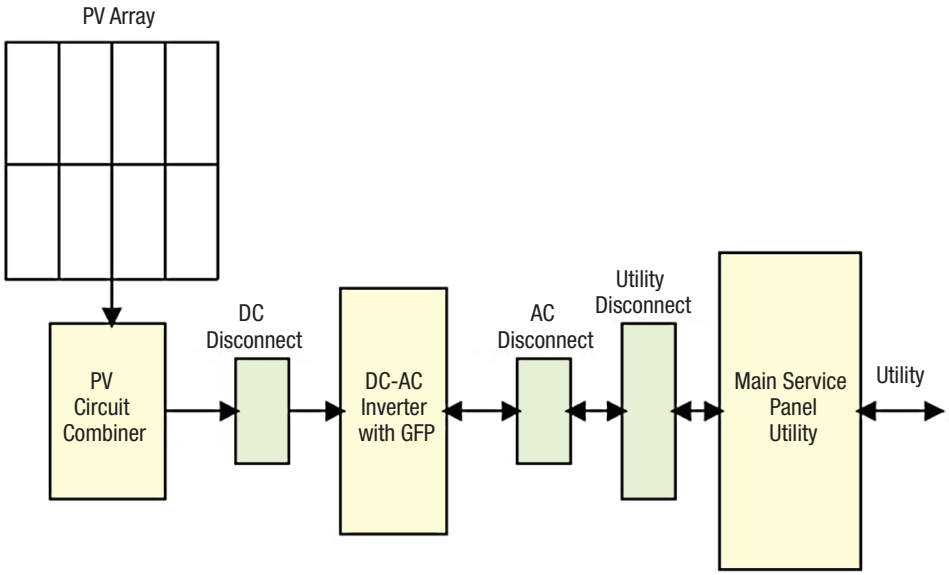

15-1. Grid-interactive with no battery backup only operates when the utility is available.

Arrays are most commonly mounted on roofs or on steel poles set in concrete. In certain applications, they may be mounted at ground level or on building walls. Solar modules can also be mounted to serve as part or all of a shade structure such as a patio cover. On roof-mounted systems, the PV array is typically mounted on fixed racks, parallel to the roof for aesthetic reasons and stood off several inches above the roof surface to allow airflow that will keep them as cool as practical.

Adjustability–The tilt of sloped rooftop arrays is usually not changed, since this is inconvenient in many cases and sometimes dangerous. However, many mounting racks are adjustable, allowing resetting of the angle of the PV modules seasonally.

Tracking–Pole-mounted PV arrays can incorporate tracking devices that allow the array to automatically follow the sun. Tracked PV arrays can increase the system's daily energy output by 25% to 40%. Despite the increased power output, tracking systems usually are not justified by the increased cost and complexity of the system.

Photovoltaic system types can be broadly classified by answers to the following questions:
• Will it be connected to the utility's transmission grid?
• Will it produce alternating current (ac) or direct current (dc) electricity, or both?
• Will it have battery backup?
• Will it have backup by a diesel, gasoline, or propane generator set?

Grid-connected, or grid-intertied systems, generate approximately the same quality of alternating current (ac) electricity as is provided by your utility. The energy generated by a grid-connected system is used first to power the ac electrical needs of the home or business. Any surplus power that is generated is fed or "pushed" onto the electric utility's transmission grid. Any of the building's power requirements that are not met by the PV system are powered by the transmission grid. In this way, the grid can be thought of as a virtual battery bank for the building.

Common System Types–Most new PV systems being installed in the United States are grid-connected residential systems without battery backup. Many grid-connected ac systems are also being installed in commercial or public facilities.

There are two main types of grid-connected systems, although others exist:
• Grid-connected ac system with no battery or generator backup
• Grid-connected ac system with battery backup

Example configurations of systems with and without batteries are shown in Fig. 15-1 and Fig. 15-2. Note there are common variations on the configurations shown, although the essential functions and general arrangement are similar.

Is a Battery Bank Really Needed?–The simplest, most reliable, and least expensive configuration does not have battery backup. Without batteries, a grid-connected PV system will shut down when a utility power outage occurs. Battery backup maintains power to some or all of the electric equipment, such as lighting, refrigeration, or fans, even

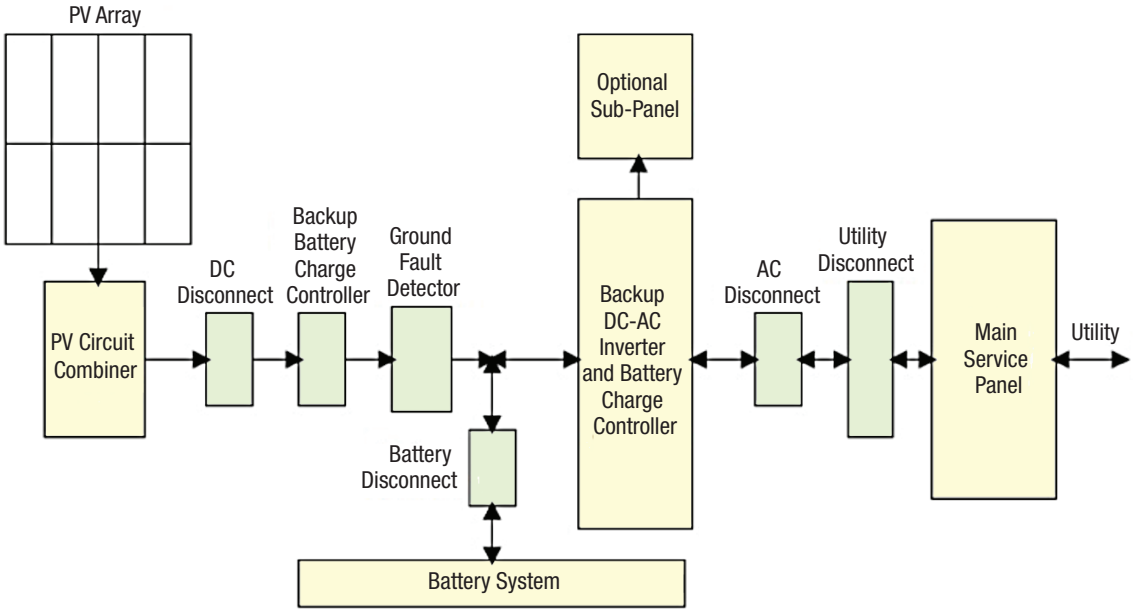

15-2. PV system includes battery backup to continue operation if the utility goes out.

when a utility power outage occurs. A grid-connected system may also have generator backup if the facility cannot tolerate power outages.

As an example of a variation on the configuration shown in Fig. 15-1, the inverter has been shown in an interior location, while very often it is installed outside. If located outside, there may not be a need for a separate array disconnect and inverter dc disconnect, as a single dc disconnect can serve both functions. In Fig. 15-2, system meter functions are often included in charge controllers and so a separate system meter may not be required.

With battery backup, power outages may not even be noticed. However, adding batteries to a system comes with several disadvantages that must be weighed against the advantage of power backup. These disadvantages are:

- Batteries consume energy during charging and discharging, reducing the efficiency and output of the PV system by about 10% for lead-acid batteries.
- Batteries increase the complexity of the system. Both first cost and installation costs are increased.
- Most lower-cost batteries require maintenance.
- Batteries will usually need to be replaced before other parts of the system and at considerable expense

The ac energy output of a solar array is the electrical ac energy delivered to the grid at the point of connection of the grid-connect inverter to the grid. The output of the solar array is affected by:

- Average solar radiation data for selected tilt angle and orientation
- Manufacturing tolerance of modules
- Temperature effects on the modules
- Effects of dirt on the modules
- System losses (e.g., power loss in cable)
- Inverter efficiency

Several parameters must be derated:

1. Derating due to manufacturer's output tolerance
2. Derating due to dirt
3. Derating due to temperature

The output of a PV module is specified in watts and with a manufacturing tolerance based on a cell temperature of 25°C. Historically the manufacturing tolerance has been ±5%, but in recent years the tolerance dropped to about ±3%. A buildup of dirt on the surface of the PV module can reduce its output. So an acceptable derating might be 5% for dirt and the manufacturers' tolerances.

Solar-module output power decreases above 25°C and increases below 25°C minimum. Temperature derating is based on an ambient temperature of 25°C. Monocrystalline modules typically have a temperature coefficient of –0.45%/°C. Polycrystalline modules typically have a temperature coefficient of–0.5%/°C. Thin-film modules have a temperature coefficient, typically around to -0.25%/°C.

The dc energy output of the solar array will be further reduced by the power loss (voltage drop) in the dc cable connecting the solar array to the grid connect inverter. The dc energy delivered to the input of the inverter will be further reduced by the power/energy loss in the inverter. The ac energy output of the inverter will be further reduced by the power loss in the ac cable connecting the inverter to the grid, say switchboard where it is connected.

NEC

In the United States, the relevant codes and standards include:

- Electrical Codes-National Electrical Code (NEC) Article 690: Solar
- Photovoltaic Systems and NFPA 70
- Uniform Solar Energy Code
- Building Codes- ICC, ASCE 7
- UL Standard 1701; Flat Plat Photovoltaic Modules and Panels
- IEEE 1547, Standards for Interconnecting distributed

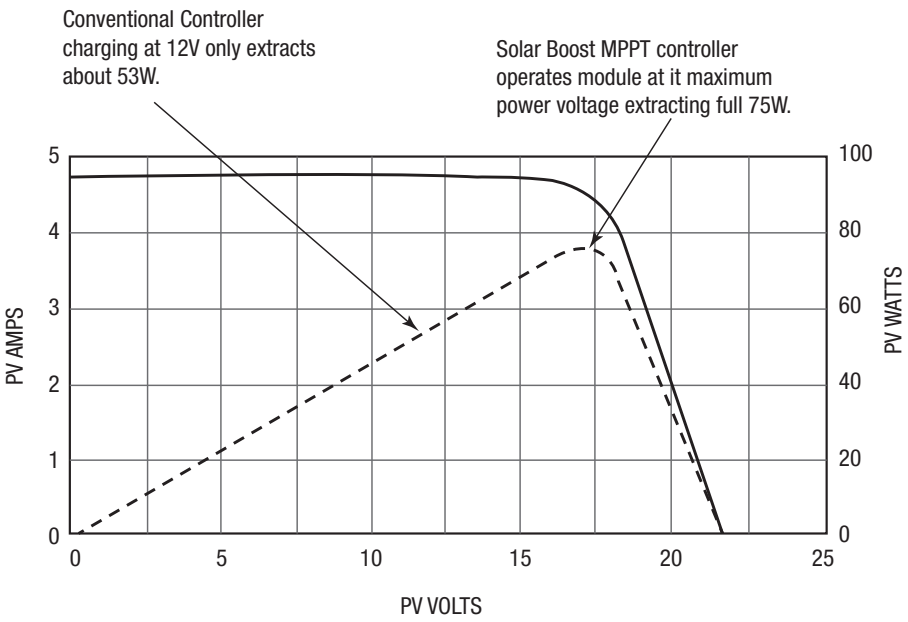

15-3. Solar inverters use maximum power point tracking (MPPT) to get the maximum possible power from the PV array.

Resources with Electric Power Systems

- UL Standard 1741, Standard for Inverter, converters, Controllers and Interconnection System Equipment for use with Distributed Energy Resources

PV inverters

PV inverters convert the PV panel's dc output into a utility-frequency ac that can be fed into a commercial electrical grid or used by a local, off-grid electrical network. It, allows use of ordinary ac-powered equipment. Solar inverters have special functions adapted for use with photovoltaic arrays, including maximum power-point tracking and anti-islanding protection.

Solar inverters use maximum power-point tracking (MPPT) to get the maximum possible power from the PV array (Fig. 15-3). Solar cells have a complex relationship between solar irradiation, temperature, and total resistance that produces a nonlinear output efficiency. The MPPT system samples the output of the cells and determines a resistance (load) that obtains maximum power for any given environmental conditions.

The fill factor (FF) is a parameter which, in conjunction with the open-circuit voltage (V_{OC}) and short circuit current(I_{SC}) of the panel, determines the maximum power from a solar cell. Fill factor is defined as the ratio of the maximum power from the solar cell to the product of V_{OC} and I_{SC}.

ADSP-CM41x

Analog Devices' ADSP-CM41x power-conversion platform employs a series of mixed-signal control processors intended to simplify system design, lower cost, and improve efficiency and safety in solar, energy storage, and electric vehicle infrastructure (Fig. 15-4). Solar panels and battery systems have a need for inverter technologies to drive the next wave of efficiencies in solar energy. Although disruptive new inverter designs are making improvements in size, weight, and cost reductions, they require further advances in digital processing to unlock their full potential. The ADSP-CM41x control processors represent a breakthrough in power conversion design, with an unmatched level of hardware integration specifically tailored to solar and other emerging energy applications. By alleviating the need for complex external circuitry, the ADSP-CM41x control processors deliver design time and cost reductions, safety improvements, and the precision gains intended to maximize the impact of new inverter designs.

Central to the ADSP-CM41x design is its breakthrough "dual independent core" safety concept, which enables the integration of safety redundancy and functions into a single chip. This first-ever architecture saves considerable development time and system cost by eliminating the need for an external supervisory element, which is the current standard. Equally important is the on-board integration of optimized hardware accelerators, designed to offload work from the processor core and boost the processing power available for core functions. Additionally, the device's on-board arc fault detection simplifies design, and enhances safety by using intelligent decision making to improve reliability and accuracy.

Building upon an already state-of-the-art power-conversion platform, the ADSP-CM41x establishes a new benchmark in ARM core processing and analog precision, adding to the industry performance established by the ADSP-CM40x power conversion series. The ADSP-CM41x series seamlessly integrates with other critical signal-chain components, including the AD740x sigma delta-based A/D converter, which replaces larger, more expensive sensor modules to reduce system cost and improve isolated current measurement. Also included in the platform is the ADuM413x series of isolated gate drivers featuring iCoupler isolation technology that enables faster switching to further increase system efficiency.

The ADSP-CM41xF family of mixed-signal control processors is based on the ARM Cortex-M4TM processor core with floating point unit operating at frequencies up to 240 MHz, and the ARM Cortex-M0TM processor core operating

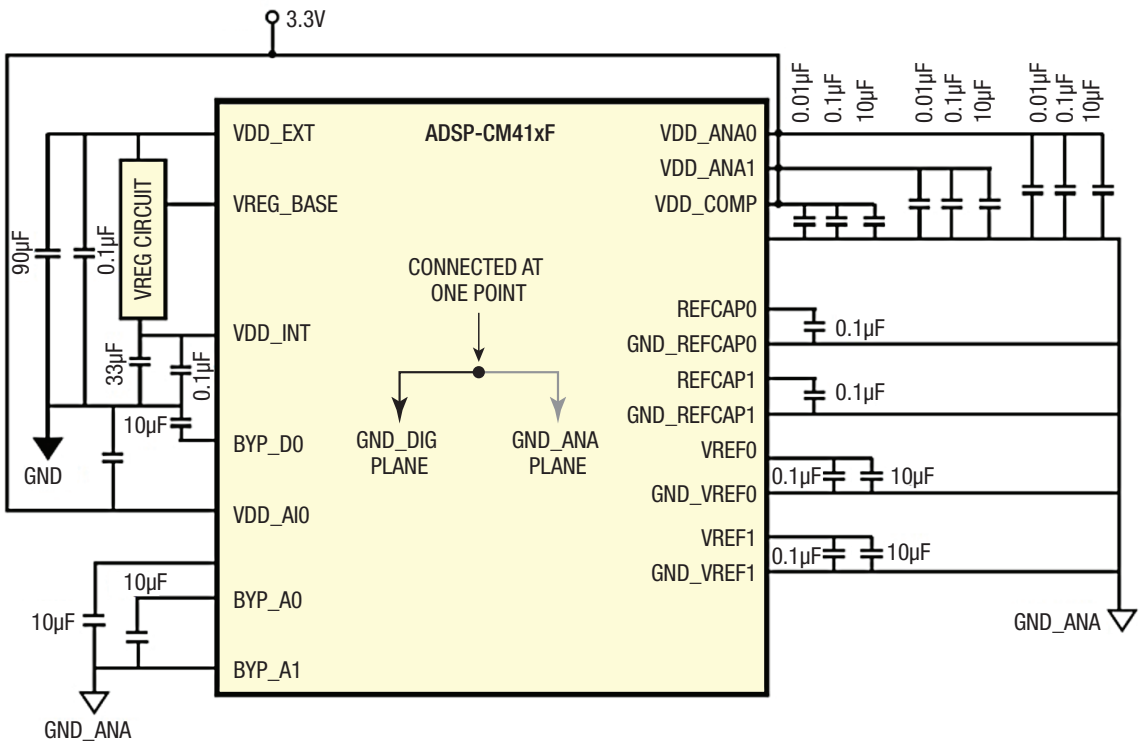

15-4. ADSP-CM41x (Analog Devices) power conversion platform employs a series of mixed-signal control processors intended to simplify system design, lower cost, and improve efficiency and safety in solar, energy storage, and electric vehicle infrastructure.

at frequencies up to 100 MHz. The processors integrate up to 160K Bytes of SRAM memory with ECC, up to 1M Byte of flash memory with ECC, accelerators and peripherals optimized for motor control and photovoltaic inverter control, and an analog module consisting of up to two 16-bit SAR-type ADCs, one 14-bit ADC and one 12-bit DAC. The ADSP-CM41xF family operates from a single voltage supply, generating its own internal voltage supplies using internal voltage regulators and an external pass transistor.

By integrating a rich set of industry-leading system peripherals and memory, the ADSP-CM41xF mixed-signal control processors are the platform of choice for next-generation applications that require RISC programmability and leading-edge signal processing in one integrated package.

Micro-Inverter

A micro-inverter converts dc from a single solar module to ac. The output from several micro-inverters is combined and often fed to the electrical grid. Micro-inverters contrast with conventional string and central solar inverters, which are connected to multiple solar modules or panels of the PV system.

Micro-inverters' main advantage is that small amounts of shading, debris, or snow lines on any one solar module, or even a complete module failure, do not disproportionately reduce the output of the entire array. Each micro-inverter harvests optimum power by performing maximum power-point tracking for its connected module. Simplicity in system design, simplified stock management, and added safety are other factors introduced with the micro-inverter solution.

The primary disadvantages of a micro-inverter include a higher initial equipment cost per peak watt than the equivalent power of a central inverter, and increased installation time since each inverter needs to be installed adjacent to a panel (usually on a roof). This also makes them harder to maintain and more costly to remove and replace (O&M). Some manufacturers have addressed these issues with panels with built-in micro-inverters.

The main problem with the "string inverter" approach is the string of panels acts as if it were a single larger panel with a max current rating equivalent to the poorest performer in the string. For example, if one panel in a string has 5% higher resistance due to a minor manufacturing defect, the entire string suffers a 5% performance loss. This situation is dynamic. If a panel is shaded its output drops dramatically, affecting the output of the string, even if the other panels are not shaded. Even slight changes in orientation can cause output loss in this fashion. However, this effect is not entirely accurate and ignores the complex interaction between modern string inverter maximum power point tracking and even module bypass diodes.

Efficiency of a panel's output is strongly affected by the load the inverter places on it. To maximize production, inverters use a technique called maximum power point tracking (MPPT) to ensure optimal energy harvest by adjusting the applied load. However, the same issues that cause output to vary from panel to panel affect the proper load that the MPPT system should apply. If a single panel operates at a different point, a string inverter can only see the overall change, and moves the MPPT point to match. This results

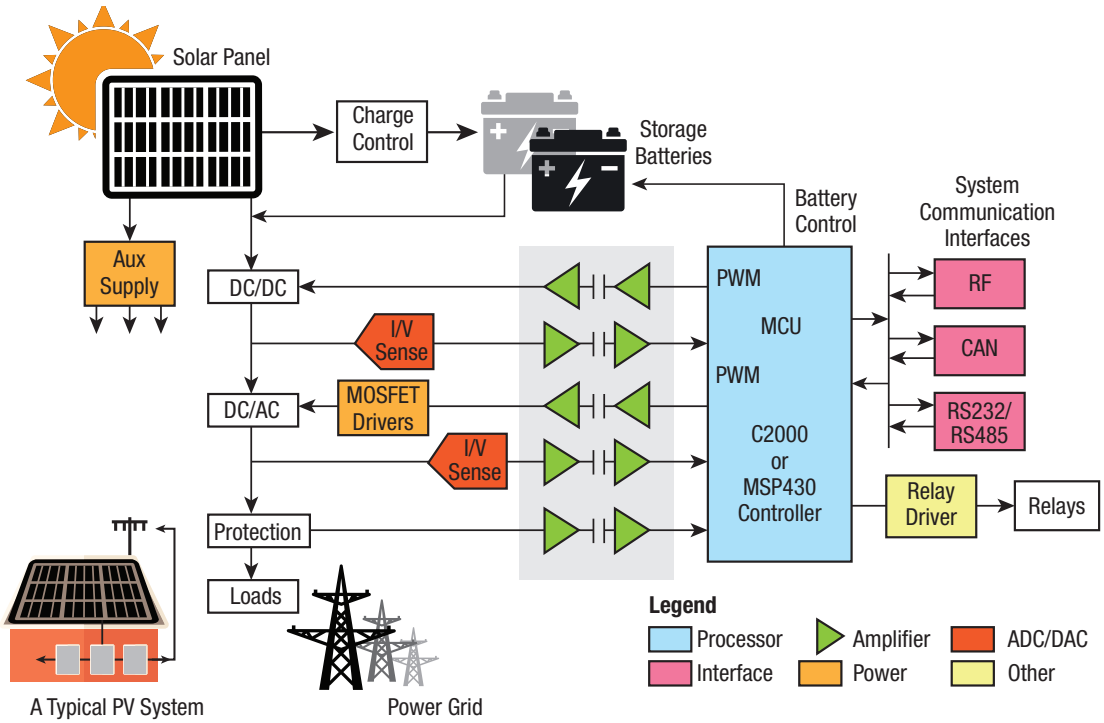

15-5. Conventional power converter architecture includes a solar inverter, which accepts the low dc output voltage from a photovoltaic array and produces an ac line voltage.

in not just losses from the shadowed panel, but the other panels, too. Shading of as little as 9% of the surface of an array can, in some circumstances, reduce systemwide power as much as 54%. However, as stated above, these yearly yield losses are relatively small and newer technologies allow some string inverters to significantly reduce the effects of partial shading.

Other challenges associated with centralized inverters include the space required to locate the device, as well as heat dissipation requirements. Large central inverters are typically actively cooled. Cooling fans make noise, so location of the inverter relative to offices and occupied areas must be considered. And because cooling fans have moving parts, dirt, dust, and moisture can negatively affect their performance over time. String inverters are quieter but might produce a humming noise in late afternoon when inverter power is low.

Grid-Tie Inverter

A grid-tie inverter is a power inverter that converts dc into ac with an ability to synchronize its interface with a utility line. Its applications are converting dc sources such as solar panels or small wind turbines into ac for tying with the grid. Fig. 15-5 shows a diagram of a grid-tie inverter installation.

The grid-tie inverter (GTI) must synchronize its frequency with that of the grid (50 or 60 Hz) using a local oscillator and limit the voltage to no higher than the grid voltage. A high-quality modern GTI has a fixed-unity power factor, which means its output voltage and current are perfectly lined up, and its phase angle is within 1 deg. of the ac power grid. The inverter has an on-board computer that senses the current AC grid waveform, and outputs a voltage to correspond with the grid. However, supplying reactive power to the grid might be necessary to keep the voltage in the local grid inside allowed limitations. Otherwise, in a grid segment with considerable power from renewable sources, voltage levels might rise too much at times of high production.

Grid-tie inverters must quickly disconnect from the grid if the utility grid goes down. This is an NEC requirement that ensures that in the event of a blackout, the grid tie inverter will shut down to prevent the energy it transfers from harming any line workers who are sent to fix the power grid.

Technologies available to grid-tie inverters include newer high-frequency transformers, conventional low-frequency transformers, or they may operate without transformers altogether. Instead of converting direct current directly to 120 or 240 volts ac, high-frequency transformers employ a computerized multi-step process that involves converting the power to high-frequency ac and then back to dc and then to the final ac output voltage.

Most grid-tie inverters include a maximum power point tracker on the input side that enables the inverter to extract a maximum amount of power from its intended power source. Since MPPT algorithms differ for solar panels and wind turbines, specially made inverters for each of these power sources are available.

A charge controller may be used to power dc equipment with solar panels. The charge controller provides a regulated dc output and stores excess energy in a battery as well as monitoring the battery voltage to prevent under/overcharging. More expensive units also perform maximum power point tracking.

Inverter manufacturer datasheets generally include the following information:

- Rated output power in watts or kilowatts: some inverters may provide an output rating for different output voltages.
- Output voltage(s): indicates to which utility voltages the inverter can connect and may also produce three phase power.
- Peak efficiency: represents the highest efficiency that the inverter can achieve.
- CEC weighted efficiency: this efficiency is published by the California Energy Commission on its GoSolar website. This is an average efficiency and is a better representation of the inverter's operating profile.
- Maximum input current: maximum dc the inverter can use.
- Maximum output current: The maximum continuous ac that the inverter will supply.
- Peak power tracking voltage: dc voltage range in which the inverter's maximum point power tracker will operate.
- Start voltage: indicates the minimum dc voltage that is required in order for the inverter to turn on and begin operation.
- IPxx rating: the Ingress Protection rating or IP Code classifies and rates the level of protection provided against the ingress of solid foreign objects (first digit) or water (second digit), a higher digit means greater protection. In the United States, the NEMA enclosure type is used similarly to the international rating.

Balance of system equipment (BOS) includes mounting systems and wiring systems used to integrate the solar modules into the structural and electrical systems of the home. The wiring systems include disconnects for the dc and ac sides of the inverter, ground-fault protection, and overcurrent protection for the solar modules. Most systems include a combiner board of some kind since most modules require fusing for each module source circuit. Some inverters include this fusing and combining function within the inverter enclosure.

Related Articles

1. Sam Davis, World Energy Resources, powerelectronics.com, January 2016.
2. Sam Davis, Solar System Efficiency: Maximum Power Point Tracking Is Key, powerelectronics.com, December 2015.
3. Sam Davis, IBM Research Solar Camera Watches for and Predicts Solar Energy, powerelectronics.com, November 2015.
4. Sam Davis, CWRU Researchers Efficiently Charge a Lithium-Ion Battery with Solar Cell, powerelectronics.com, October 2015.
5. Spencer Chin, Solar Fuel a Step Closer To Reality, powerelectronics.com, March 2015.
6. Spencer Chin, Solar Energy System Generates Electricity On Demand, powerelectronics.com, January 2015.
7. Sam Davis, Revolutionary Solar-friendly Form of Silicon Shines, powerelectronics.com, December 2014.
8. Arpita Agarwal, Direct Duty Cycle Control for MPPT Digital Implementation, powerelectronics.com, August 2014.
9. Richard J. Bravo, Solar Inverters Can Improve Power Quality, powerelectronics.com, April 2014.
10. Guerra, Alberto, Inverter/Modules Aid Energy, Appliance, PV and Motor Sectors, powerelectronics.com, April 2011.

BACK TO TABLE OF CONTENTS

CHAPTER 16:

WIND POWER

Wind power, as an alternative to burning fossil fuels, is plentiful, renewable, widely distributed, clean, produces no greenhouse gas emissions during operation, and uses little land. The net effects on the environment are far less problematic than those of nonrenewable power sources.

Wind power is very consistent from year to year, but has significant variation over shorter time scales. It is therefore used in conjunction with other electric power sources to give a reliable supply. As the proportion of wind power in a region increases, a need to upgrade the grid, and a lowered ability to supplant conventional production can occur.

Wind farms consist of many individual wind turbines connected to the electric power transmission network (Fig. 16-1). Onshore wind is an inexpensive source of electricity, competitive with or in many places cheaper than coal or gas plants. Offshore wind is steadier and stronger than on land, and offshore farms have less visual impact, but construction and maintenance costs are considerably higher. Small onshore wind farms can feed some energy into the grid or provide electricity to isolated off-grid locations.

Wind turbines (Fig. 16-2) operate on a simple principle. The energy in the wind turns two or three propeller-like blades around a rotor. The rotor is connected to the main shaft, which spins a generator to create electricity. The wind turns the blades, which spin a shaft, which connects to a generator and makes electricity.

A typical electrical circuit for a wind-turbine installation includes generator, storage batteries, and charge controller. The ac output normally goes to a local transformer station (that collects all the turbines' outputs), it is then transformed to a higher voltage and transmitted via a cable or overhead line to an infeed point (another transformer station), where the connection to the normal power grid is made. When being connected to the grid, this voltage must be synchronized with the utility grid.

16-1. Typical wind farm.

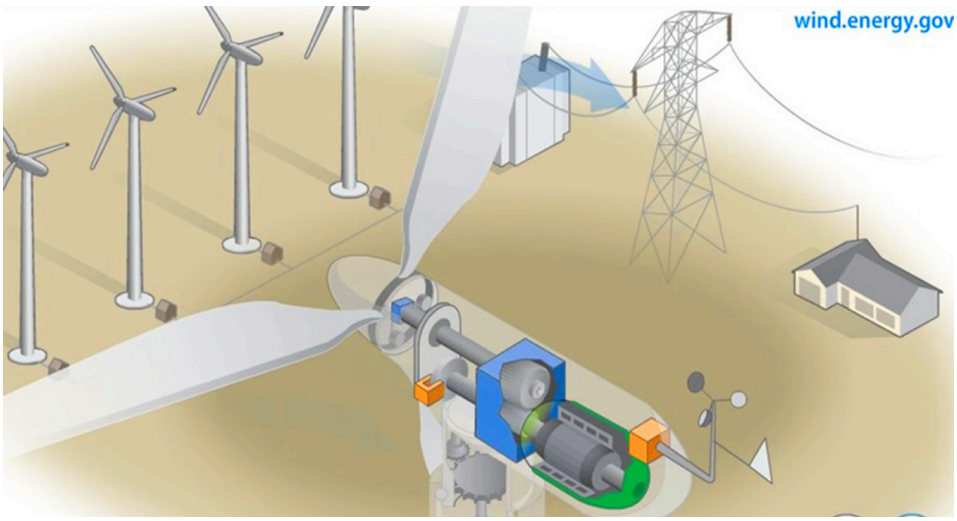

16-2. Typical wind turbine.

Wind is actually a form of solar energy and is a result of the uneven heating of the atmosphere by the sun, the irregularities of the earth's surface, and the rotation of the earth. Wind flow patterns and speeds vary greatly across the United States and are modified by bodies of water, vegetation, and differences in terrain. Humans use this wind flow, or motion energy, for many purposes: sailing, flying a kite, and even generating electricity.

Horizontal-axis wind turbines typically either have two or three blades. These three-bladed wind turbines are operated "upwind," with the blades facing into the wind.

Utility-scale turbines range in size from 100 kilowatts to as large as several megawatts. Larger wind turbines are more cost-effective and are grouped together into wind farms, which provide bulk power to the electrical grid. In recent years, there has been an increase in large offshore wind installations in order to harness the huge potential that wind energy offers off the coasts of the U.S.

Single small turbines, below 100 kilowatts, are used for homes, telecommunications dishes, or water pumping. Small turbines are sometimes used in connection with diesel generators, batteries, and photovoltaic systems. These systems are called hybrid wind systems and are typically used in remote, off-grid locations, where a connection to the utility grid is not available.

Today, most turbines use variable speed generators combined with partial- or full-scale power converter between the turbine generator and the collector system, which generally have more desirable properties for grid interconnection and have low-voltage ride-through capabilities. Modern concepts use either doubly fed machines with partial-scale converters or squirrel-cage induction generators or synchronous generators (both permanently and electrically excited) with full-scale converters.

Power-management techniques such as having excess capacity, geographically distributed turbines, dispatchable backing sources, sufficient hydroelectric power, exporting and importing power to neighboring areas, using vehicle-to-grid strategies or reducing demand when wind production is low, can in many cases overcome these problems. In addition, weather forecasting permits the electricity network to be readied for the predictable variations in production that occur.

In a wind farm, individual turbines are interconnected with a medium voltage (often 34.5 kV), power-collection system, and communications network. At a substation, this medium-voltage electric current is increased in voltage with a transformer for connection to the high-voltage electric power transmission system.

One of the biggest current challenges to wind-power-grid integration in the United States is the necessity of developing new transmission lines to carry power from wind farms, usually in remote, lowly populated states in the middle of the country due to availability of wind, to high-load locations, usually on the coasts where population density is higher. The current transmission lines in remote locations were not designed for the transport of large amounts of energy. As transmission lines become longer, the losses associated with power transmission increase, as modes of losses at lower lengths are exacerbated and new modes of losses are no longer negligible as the length is increased, making it harder to transport large loads over large distances.

However, resistance from state and local governments makes it difficult to construct new transmission lines. Multi-state power-transmission projects are discouraged by states with cheap electricity rates for fear that exporting their cheap power will lead to increased rates. A 2005 energy law gave the Energy Department authority to approve transmission projects states refused to act on, but after an attempt to use this authority, the Senate declared the department was being overly aggressive in doing so. Another problem is that wind companies find out after the fact that the transmission capacity of a new farm is below the generation capacity, largely because federal utility rules to encourage renewable energy installation allow feeder lines to meet only minimum standards. These are important issues that need to be solved, as when the transmission capacity does not meet the generation capacity, wind farms are forced to produce below their full potential or stop run-

16-3. Offshore wind farm.

ning all together, in a process known as curtailment. While this leads to potential renewable generation left untapped, it prevents possible grid overload or risk to reliable service.

Offshore Wind Power

The near-term technology is still immature, which is an obstacle to offshore wind development (Fig. 16-3). High cost of wind energy can, in part, be addressed directly with technology innovations that increase reliability and energy output and lower system capital expenses. The current technology limits the domain for offshore machines to shallow-water sites at a cost premium that is reflective of the industry's early state. New technology is needed to lower costs, increase reliability and energy production, solve regional deployment issues, expand the resource area, develop infrastructure and manufacturing facilities, and mitigate known environmental impacts. Because of the high up-front investment costs required to explore new technology innovation and the long timeline that is usually required to reap the full benefits of high-risk game-changing innovations, many companies may not be motivated to invest in R&D for offshore wind.

Shallow water is defined in this study as between 0 m and 30 m. This definition captures the water depth of most of the projects installed today, as well as the bulk of industry experience. Transitional depths range between 30 m and 60 m. Beyond 60 m in depth, several floating concepts derived from the oil and gas industry have been developed.

As a caution, note that the above-water depth bands for shallow, transitional, and deep water are specific to offshore wind turbines and are not derived from the oil and gas vocabulary, where deep water can mean 2,000 m or more. In addition, these depth bands only approximate the break points for the three technologies, but not enough experience exists to know if they are chosen accurately. They serve as good guides, though, for estimating the resource and the need to develop new solutions.

As water depth increases, the cost of offshore substructures is likely to increase because of the added complexity of design, fabrication, and installation, as well as the additional materials needed below the waterline. Rising costs resulting from water depth may appear in stages as technology limits are reached. Industry trends indicate that technology solutions might be able to mitigate these jumps for the specific site characteristics as the industry gains experience.

A transmission line is required to bring the generated power to (often remote) markets. For an off-shore plant, this may require a submarine cable. Construction of a new high-voltage line may be too costly for the wind resource alone, but wind sites may take advantage of lines installed for conventionally fueled generation.

Capacity Factor

Since wind speed is not constant, a wind farm's annual energy production is never as much as the sum of the generator nameplate ratings multiplied by the total hours in a year. The ratio of actual productivity in a year to this theoretical maximum is called the capacity factor. Typical capacity factors are 15% to 50%; values at the upper end of the range are achieved in favorable sites and are due to wind turbine design improvements.

Unlike fueled generating plants, the capacity factor is affected by several parameters, including the variability of the wind at the site and the size of the generator relative to the turbine's swept area. A small generator would be

cheaper and achieve a higher capacity factor but would produce less electricity (and thus less profit) in high winds. Conversely, a large generator would cost more but generate little extra power and, depending on the type, may stall out at low wind speed. Thus an optimum capacity factor of around 40% to 50% would be aimed for.

Penetration

Wind energy penetration refers to the fraction of energy produced by wind compared with the total generation. There is no generally accepted maximum level of wind penetration. The limit for a particular grid will depend on the existing generating plants, pricing mechanisms, capacity for energy storage, demand management, and other factors. An interconnected electricity grid will already include reserve generating and transmission capacity to allow for equipment failures. This reserve capacity can also serve to compensate for the varying power generation produced by wind stations. Studies have indicated that 20% of the total annual electrical energy consumption may be incorporated with minimal difficulty. These studies have been for locations with geographically dispersed wind farms, some degree of dispatchable energy or hydropower with storage capacity, demand management, and interconnected to a large grid area enabling the export of electricity when needed. Beyond the 20% level, there are few technical limits, but the economic implications become more significant. Electrical utilities continue to study the effects of large scale penetration of wind generation on system stability and economics.

A wind energy penetration figure can be specified for different durations of time, but is often quoted annually. To obtain 100% from wind annually requires substantial long-term storage or substantial interconnection to other systems which may already have substantial storage. On a monthly, weekly, daily, or hourly basis—or less—wind might supply as much as or more than 100% of current use, with the rest stored or exported. Seasonal industry might then take advantage of high wind and low usage times such as at night when wind output can exceed normal demand. Such industry might include production of silicon, aluminum, steel, or of natural gas, and hydrogen, and using future long term storage to facilitate 100% energy from variable renewable energy.

Variability

Electricity generated from wind power can be highly variable at several different timescales: hourly, daily, or seasonally. Annual variation also exists, but is not as significant. Because instantaneous electrical generation and consumption must remain in balance to maintain grid stability, this variability can present substantial challenges to incorporating large amounts of wind power into a grid system. Intermittency and the non-dispatchable nature of wind energy production can raise costs for regulation, incremental operating reserve, and (at high penetration levels) could require an increase in the already existing energy demand management, load shedding, storage solutions or system interconnection with HVDC cables.

Wind power is variable, and during low wind periods it must be replaced by other power sources. Transmission networks presently cope with outages of other generation plants and daily changes in electrical demand, but the variability of intermittent power sources such as wind power, are unlike those of conventional power generation plants, which, when scheduled to be operating, may be able to deliver their nameplate capacity around 95% of the time.

Presently, grid systems with large wind penetration require a small increase in the frequency of usage of natural gas spinning reserve power plants to prevent a loss of electricity in the event that conditions are not favorable for power production from the wind. At lower wind-power-grid penetration, this is less of an issue. Conversely, on particularly windy days, even with penetration levels of 16%, wind-power generation can surpass all other electricity sources in a country.

The combination of diversifying variable renewables by type and location, forecasting their variation, and integrating them with dispatchable renewables, flexible fueled generators, and demand response can create a power system that has the potential to meet power supply needs reliably. Integrating ever-higher levels of renewables is being successfully demonstrated in the real world.

High-Altitude Wind Power

Considering all costs, airborne wind energy could be the world's cheapest energy source. (Possible exceptions are limited hydro sources and limited situations where surface-based wind turbines may be the most economic for supplying relatively local needs.)

High-energy winds are at altitudes high above us, not just at a few hundred feet where they can be tapped by tower-based turbine rotors. Airborne Wind Energy technologies will employ tethered wind energy capture devices that "fly" to these altitudes where wind power is much greater than it is at ground level.

There are several groups developing Airborne Wind Energy (AWE) technologies intended for use up to 2,000 ft. above ground level (AGL) and others intended for use at altitudes greater than 2,000 ft. AGL. Some technologies might be able to bridge this segmentation, but not always in the exact incarnations for above and below that altitude. The 2,000 ft. was chosen because that is the altitude above which the FAA is not currently interested in approving what

it considers to be "obstructions." AWE technologies can be flown higher outside the 12 nautical mile limit off the coast into international airspace, but still in the U.S. "economic zone."

Still to be demonstrated is an efficient approach for transmitting power from a high-altitude wind source to the ground where it can be used. The voltage across the connecting cable would be too high using conventional methods.

Related Articles

1. Sam Davis, World Energy Resources, powerelectronics.com, January 2016.
2. Sam Davis, A Wind Turbine Without Blades, powerelectronics.com, June 2015.
3. Sam Davis, American Wind Energy Association Touts Wind Energy Advantages, powerelectronics.com, March 2015.
4. Sam Davis, Efficiency, Reliability Issues Dictate Wind Farm Performance and Profit, powerelectronics.com, November 2014.
5. Sam Davis, Hybrid Solar-Wind Energy Technology Produces 435 to 1250 Megawatt-Hours/Hour, powerelectronics.com, June 2014.
6. Davis, Sam, The Sky's the Limit for Airborne Wind Energy Power Conversion, powerelectronics.com, August 2011.
7. Paul Schimel, Wind Turbine of the Future, electronicdesign.com, September 2013.
8. Sam Davis, Technology Solutions Key to Achieving Offshore Wind Power Benefits, powerelectronics.com, April 2011.
9. Lou Pechi, Answers to Energy Crisis Are Blowin' in the Wind, powerelectronics.com, September 2007.
10. PET, Wind Will Power Component Development Too, powerelectronics.com, July 2006.

BACK TO TABLE OF CONTENTS

CHAPTER 17: ENERGY STORAGE

The book *Solar Energy Storage* by Brent Sorensen notes that "electricity generated from intermittent sources requires efficient advanced electricity storage systems (ESSs). Electrical energy storage refers to the process of converting electrical energy from a power network into a form that can be stored and then converted to electrical energy when needed. Such a process enables electricity to be produced at times of either low demand or low generation cost, or from intermittent renewable energy sources, and to be used at times of high demand, high generation cost, or when no other generation means is available."

Sorensen notes that energy storage is crucial for increasing the share of energy from renewable energy source (RES) generators. This especially applies to energy from the sun and wind, which is characterized by intermittence. However, the problem with some of the present energy storage technologies is that they can be stored for a relatively small amount of energy, and in that sense a relatively short period of time to balance intermittent energy from RES generators (i.e., hourly, daily up to a maximum weekly value).

Energy storage materially improves the stability and predictability of renewable energy. It allows higher penetration of renewables for distributed (commercial and industrial), micro-grid, and utility-scale applications where higher electricity prices, unstable grids, and lower regulatory hurdles provide a needed storage environment. Combining batteries with renewable energy can reduce diesel consumption by 75% and reduces the cost of electricity by 40% to 50% over diesel generation alone.

Flow-Battery Energy-Storage System

ViZn Energy Systems Inc. (ViZn) has bolstered its proprietary flow-battery technology to enhance the capabilities, reliability, and lifetime of all next-generation flow-battery systems for multi-megawatt energy storage applications. Designated Vanguard II, the battery stack further expands the operating range of ViZn's systems by enhancing the fast switching and high power cycling capabilities required for many applications, further maximizing ROI and providing industry-leading payback periods.

The Vanguard II battery stack has demonstrated 20% greater capacity and is immune to cycle-life degradation, providing more headroom to handle spikes in power requirements for demanding and unpredictable applications on both sides of the meter. All ViZn flow batteries incorporate the new Vanguard II stack control technology, which eliminates life-limiting issues such as dendrite growth, simplifies cell balancing, and removes thermal and electrolyte

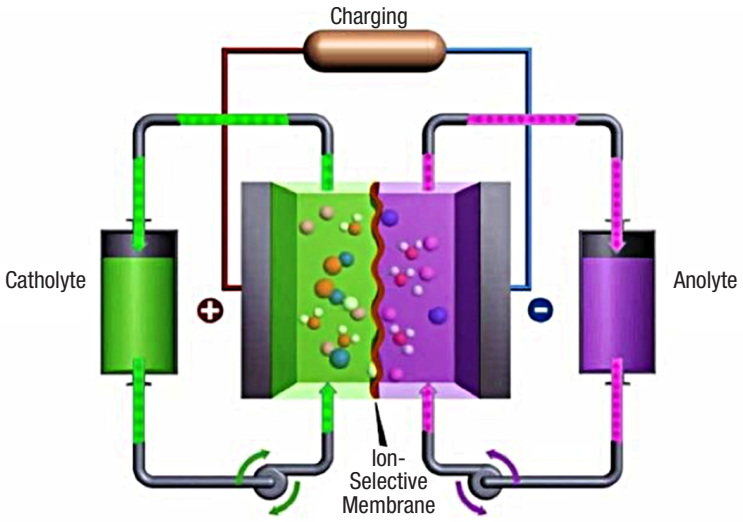

17-1. Simplified flow-battery system employed by ViZn. Pumps on the right and left bottom keep the zinc-iron electrolyte flowing.

17-2. ViZn flow battery in 20'L x 8'W x 9'6"H enclosure

breakdown issues associated with high frequency power switching. This unique multi-use capability is necessary for frequency regulation and other high power applications while adding value to longer duration storage. All of ViZn's systems are scalable, adding value for even the largest utility requirements. By interconnecting multiple units, both power and energy capabilities can be increased to offer utilities, as well as commercial and industrial customers the optimal fit for any size project.

All of ViZn's systems utilize the inherently safe, non-toxic, non-explosive zinc-iron electrolyte as shown in the simplified system in Fig. 17-1.The ViZn battery is a redox type, which is a contraction of the terms reduction and oxidation. Redox flow batteries usually employ two electrolytes, acting as liquid energy carriers that are pumped simultaneously through the two half-cells of the reaction cell separated by a membrane. On charging, the electrical energy supplied causes a chemical reduction reaction in one electrolyte and an oxidation reaction in the other. The ion-selective membrane between the half-cells prevents the electrolytes from mixing but allows selected ions to pass through to complete the redox reaction. On discharge, the chemical energy contained in the electrolyte is released in the reverse reaction and electrical energy can be drawn from the electrodes. When in use, the electrolytes are continuously pumped in a circuit between reactor and storage tanks.

High-power flow batteries use multiple stacks of cells. The size and number of electrodes in the cell stacks is fixed and determines the system's power rating. An advantage of this system is that it provides electrical storage capacity, limited by the capacity of the electrolyte storage reservoirs. Facilitating thermal management is use of the electrolytes as the thermal working fluids as they are pumped through the cells.

Flow batteries are typically sized for power by the physical dimensions of the electrodes. The next-generation flow batteries have greatly increased the ability to deliver power while maintaining the long duration energy capacity.

ViZn's zinc-iron redox storage technology provides large-scale energy storage. A modular unit is a 20- or 40-foot shipping container that can be combined and scaled to provide storage solutions for projects ranging from 100 kW to 100 MW. This technology provides safety, simplicity, and the use of abundant core non-toxic raw materials to achieve a 20-year expected life. Fig. 17-2 shows a typical ViZn flow battery package and Fig. 17-3 shows the internal construction. Table 17-1 lists the characteristics of a five-stack, Z20-5 battery.

Battery Stores Wind or Solar Power

Renewable energy power systems can take advantage of Axion's proprietary PbC battery technology for short-term power storage. In a solar installation, the solar panels charge the batteries whose output powers a dc-to-ac inverter that provides a tightly controlled frequency and

TABLE 17-1. Z20-5 ENERGY STORAGE UNIT (ESU) SPECIFICATIONS (5 STACKS)

Parameter	Description
Exterior dimensions	20'L x 8'W x 9'6"H
ESU weight dry/wet	18,000/50,000 lbs.
Nominal power	28kW
Energy at nominal power	160kWh
Duration at nominal power	5.65 hrs
Maximum power	80kW
Energy at max. power (continuous charge/discharge)	125 kWh (160kWh at nominal power)
Duration of max. power	1.5 hrs
Duty cycle up to 2x power = continuous	Duty cycle at 2.8x power = 25%
Nominal dc voltage range (min/max)	40/60 VDC
Nominal dc current range	470 – 700A
Max. dc current range	1,320 – 2,000A
ESU efficiency	74% at nominal power
Stack efficiency	90% at nominal power, 80% at max. power
Auxiliary power required	208 VAC, 60Hz, 3-phase
Communication	USB, 485, Modbus Ethernet
Humidity	5 – 95% (non-condensing)
Safety/regulatory	Designed using industry-standard guidelines

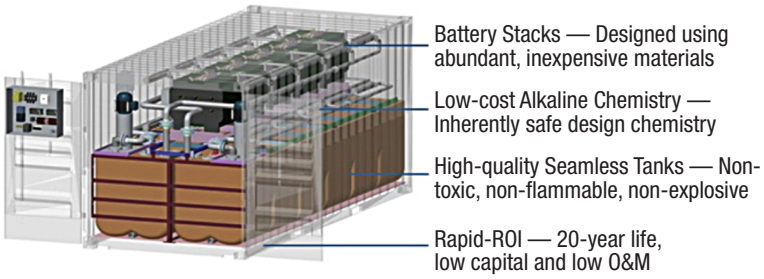

17-3. Internal construction of a ViZn flow battery.

amplitude output to the utility grid. Compared with conventional lead-acid batteries, PbC batteries used with a solar or wind power system offer:

- Faster recharge rates
- Greater charge acceptance
- Longer cycle lives in deep discharge applications
- Minimal maintenance

Shown in Fig. 17-4, the Axion battery is a multi-celled asymmetrically supercapacitive lead-acid-carbon hybrid battery. Like the conventional lead-acid battery, the Axion battery consists of a series of cells. Within its individual cells, however, construction is more complex. Negative electrodes in conventional lead-acid batteries have simple sponge lead plates. In contrast, the Axion's negative electrodes are five-layer structures consisting of a carbon electrode, corrosion barrier, current collector, second corrosion barrier, and second carbon electrode. These electrode structures are sandwiched together with conventional separators and positive electrodes and its cells are connected in series. The battery is filled with an acid electrolyte and is completely sealed.

Since 2004, laboratory prototypes of Axion's PbC batteries have undergone extensive testing. The test protocol involved a complete charge-discharge cycle every seven hours to a 100% depth of discharge. During testing, laboratory prototypes withstood more than 2,500 cycles before failure. In comparison, most conventional lead-acid batteries intended for deep discharge applications are only able to survive 400 to 600 cycles under similar operating conditions.

More than eight years were devoted to R&D on various aspects of this technology. Work focused on optimizing the design, including:

- Characterizing baseline performance
- Developing proprietary treatment processes for the activated carbon used in the electrodes
- Developing proprietary designs and manufacturing techniques for electrode assemblies
- Fabricating a series of material and design evaluation prototypes ranging from single-cell to multi-cell batteries.

Conventional lead-acid batteries consist of two electrodes: a positive electrode made of lead dioxide(PbO_2) and a negative electrode made of sponge lead (Pb). Both the lead dioxide and sponge lead materials are pasted onto lead grids with conventional separators placed between cells that are connected in series.

The PbC battery is a hybrid device that uses the standard lead acid battery positive electrode and a supercapacitor negative electrode made of activated carbon. The specific type of activated carbon has an extremely high surface area (1500 m^2/g) and has been specifically formulated for use in electrochemical applications. During charge and discharge, the positive electrode undergoes the same chemical reaction that occurs in a conventional lead acid battery, i.e., lead dioxide reacts with acid and sulphate ions to form lead sulphate and water. The main difference in the PbC battery is the replacement of the lead negative electrode with an activated carbon electrode that does not undergo a chemical reaction at all. Instead, the very high surface area activated carbon electrode stores the protons (H+) from the acid in a layer on the surface of the electrode.

With conventional lead-acid batteries, the concentration of acid changes from being very concentrated in the charged state to somewhat diluteD in the discharged state as the acid is converted to water. In contrast, the PbC battery stores H+ in the negative electrode in the fully charged

17-4. Cross-section of a PbC battery.

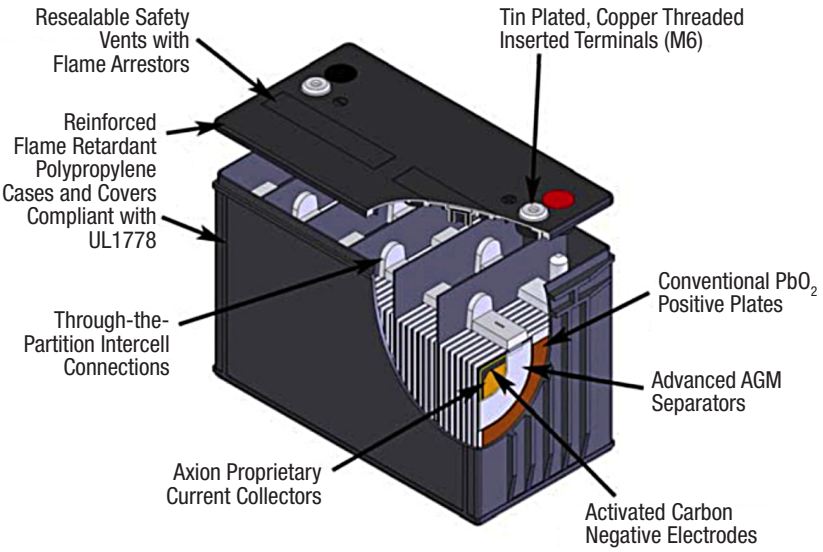

TABLE 17-2. DESIGN FEATURES OF AXION'S PBC TECHNOLOGY

Feature	Remarks
Rapid recharge	Well-suited to capture the intermittent power generated by renewable energy producers, resulting in improved performance, productivity, reliability, and profitability.
Heavy-duty design	Batteries for renewable energy designed and built for maximum energy storage and very long useful lives.
Minimal maintenance	Sealed unit and requires virtually no maintenance, resulting in low operating costs.
Sustainability	You can recycle existing lead-acid batteries, allowing the lead, plastic, and acid to be reused in the new PbC batteries.
Manufacturability	Designed to be manufactured in any of the dozens of existing lead-acid battery facilities in the U.S. as well as the hundreds of others worldwide. This eliminates the need for hundreds of millions of dollars in capital to build new advanced battery facilities in the U.S. Therefore, existing equipment can be utilized and it will not require new investments to manufacture the batteries.

17-5. PowerCube with PbC batteries providing 1MW for 30 minutes.

state, which moves to the positive electrode during discharge where they are neutralized to form water. The result is reduced acid concentration swings from the charged to discharged state, reducing grid corrosion on the positive electrode, leading to longer positive electrode life.

The rapid recharge and deep discharge capacity of the PbC battery are well-suited for intermittent power sources like wind and solar. When coupled with the ability to deliver longer cycle lives with minimal maintenance, grid connected systems based on our PbC technology will offer a greater total number of useful cycle lives. If battery cost per charge/discharge cycle is low enough, peak shaving and grid buffering for traditional utilities may also be cost effective. Table 17-2 lists the PbC battery's design features.

Axion has also developed the PowerCube, a mobile energy storage system using multiple PbC batteries that can be configured to deliver up to 1 MW for 30 minutes or 100 kW for 10 hours (Fig. 17- 5).

Solar Installation

For more than two and a half years, Axion's 500kW PowerCubes have been connected into the PJM grid utility network, one of the nation's largest power transmission organization serving more than 58 million people in all or parts of 13 states. Set up as a demand response and frequency regulation asset, Axion developed and tweaked a working model in a real-world setting utilizing the PowerCube's ability to participate 24/7 in the PJM frequency regulation application.

Following the initial installation, Axion received a follow-on order for four more PowerCube energy storage systems. The Cubes will provide storage for energy created by a commercial solar panel system and provide power storage and frequency regulation on the PJM grid. In addition, ancillary circuits provide seamless switching between the output of the solar-inverter and the utility's generators. The new order includes batteries, racks, wiring, a data communication system, and the electronics coordination needed to outfit and install the PowerCubes. Each of the PowerCubes will be tied to solar arrays that produce between 500kW and 700kW and the PowerCubes will each provide 500kW (both 500kW up and 500kW down) for frequency regulation.

Li-ion Batteries Compete

According to Marianne Boust, principal analyst, IHS Technology, massive cost reductions have permitted Li-ion technology to surpass lead-acid batteries in energy storage. Li-ion is even challenging sodium sulfur and flow for long-duration storage. Li-ion is also gaining traction in the grid-scale market for longer duration, which has been historically dominated by sodium sulfur and flow batteries. However, flow-battery manufacturers are scaling up their ambitions and betting on superior lifetime of flow-battery technology. While equipment costs keep falling, policies favorable to energy storage are being implemented in a larger number of countries, driving up new demand in the power sector.

Related Articles

1. Sam Davis, Book Review: Solar Energy Storage, powerelectronics.com, July 2015.
2. Sam Davis, Organic Mega Flow Battery Promises Breakthrough For Renewable Energy, powerelectronics.com, February 2014.
3. Sam Davis, Liquid Metal Battery Stores Power After Sun or Wind Retreat, powerelectronics.com, April 2014.
4. Sam Davis, Unique Battery Stores Wind or Solar Power for the Utility Grid, powerelectronics.com, July 2014.

5. Sam Davis, Flow-Battery Energy-Storage System Expands Capabilities, powerelectronics.com, January 2016.
6. Sam Davis, NASA Selects Proposals for Advanced Energy Storage Systems, powerelectronics.com, August 2014.
7. Sam Davis, Enhanced Sodium-Beta Batteries Boost Performance, Cut Cost for Large-Scale Energy Storage, powerelectronics.com, August 2014.
8. Sam Davis, Unique Battery Stores Wind or Solar Power for the Utility Grid, powerelectronics.com, August 2014.
9. Spencer Chin, Solar Energy System Generates Electricity On Demand, powerelectronics.com, January 2015.
10. Sam Davis, Revolutionary Solar-friendly Form of Silicon Shines, powerelectronics.com, December 2014.

☞ **BACK TO TABLE OF CONTENTS**

CHAPTER 18:

ELECTRONIC LIGHTING

Electronic lighting using LEDs is one of today's most rapidly evolving technologies. The major reason for this growth is the development of white LEDs whose efficiency keeps increasing. By 2020, the U.S. Department of Energy (DoE) estimates that commercial LED lighting efficiency will be as high as 258 lumens per watt, or two and a half times as efficient as today's fluorescent lamps, resulting in 90% energy savings. By then, the DoE predicts the cost of LEDs will fall by 80% and global penetration will be 60%.

With an average lifespan of over 100,000 hours, LEDs last more than 10 times longer than any other light source. However, LED lifetimes are rated differently than incandescent lights that fail when the filament breaks. One definition for an LED's typical lifetime is the average number of hours until light falls to 70% of initial brightness.

The commercial LED marketplace calls for low-cost lighting, which requires minimal cost components. LEDs operate with a dc voltage so the incoming ac must be rectified and reduced to a low voltage for the LED driver. The LED power circuit can be non-isolated so it may not need an input transformer. However, there is one component that must be chosen carefully, the electrolytic or tantalum capacitor used in the rectifier circuit. Although the LED may have a long lifespan, the capacitor's lifetime will probably be shorter. Electrolytic capacitor have a tendency of drying out and failing. Therefore, the manufacturer must minimize the capacitor's cost while selecting a capacitor with a long lifespan.

18-1. A new LED bulb from Cree is rated at 460 lumens for the 40-watt replacement and 815 lumens for the 60-watt replacement. Its two versions have a soft white (2700K) and daylight (5000K) color temperature.

Heating is an important design issue for LEDs and other lighting devices. An incandescent bulb gives off 90% of its energy as heat, and a compact fluorescent bulb wastes 80% as heat. LEDs don't heat as much as other light sources, but it is an issue that has required various heat-control techniques whose cost doesn't have a major impact on overall cost.

White LEDs

AlGaInP is one of the two types of LED materials now used for lighting systems. The other is indium gallium nitride (InGaN). Slight changes in the composition of these alloys changes the color of the emitted light. AlGaInP produces red, orange, and yellow LEDs. InGaN produces green, blue, and white LEDs.

Emergence of AlGaInP and InGaN materials for LEDs made commercial LED lighting feasible. These two materials allowed white light to be produced by mixing LEDs from different parts of the lighting spectrum.

Now, there are two approaches to creating white light. One is to mix the light from several colored LEDs to create a spectral power distribution that appears white. By locating red, green, and blue LEDs adjacent to one another, and properly mixing the amount of their output, the resulting light appears white.

Another approach to generating white light is to use phosphors for a short-wavelength LED. When illuminated by a blue LED light, one phosphor emits yellow light with

a broad spectral power distribution. The remaining blue light, when mixed with the yellow light, results in white light. Additional phosphors are being developed to produce soft white and bright white lighting.

Improved LED Bulb

Cree Inc. has introduced what it considers a better LED bulb, delivering an even better light with better performance, a longer life, and more energy savings (Fig. 18-1). The new Cree LED bulb is built to deliver true LED performance in color quality, light output, and dimming. It has an improved longer lifetime of over 27 years (30,000 hours), lasting as much as six times longer than some LED bulbs. Its proven 4Flow Filament Design, which ensures that it looks and lights like a traditional incandescent. The new bulb also provides consumers with a higher color rendering index of 83 to better display colors, true ENERGY STAR-compliant omnidirectional distribution for all-around light, and is fully dimmable with most standard dimmers and suitable for enclosed fixtures.

The new LED Bulb delivers 460 lumens for the 40-watt replacement and 815 lumens for the 60-watt replacement in soft white (2700K) and daylight (5000K) color temperatures inside a durable, shatterproof housing, and consumes up to 85 percent less energy during its lifetime. The new Cree LED bulb has achieved the ENERGY STAR certification by meeting all the high-performance requirements.

LED Drivers

Today's drivers operate in either constant current and constant voltage modes, with a number of variations. Constant current drivers usually tend to be used when one driver is required per light. The current will remain the same, regardless of the number of LEDs. Constant voltage drivers are best for applications where the user requires flexibility with the number of LEDs connected to one power supply. As lamps are added, the current will increase to the maximum limit.

The LT3744 from Linear Technology is a synchronous step-down dc/dc converter that delivers constant current to drive high-current LEDs (Fig. 18-2). The LT3744 uses two external switching MOSFETs, delivering up to 20A (80W) of continuous LED current from a nominal 12V input. In pulsed LED applications, it can deliver up to 40A of LED current or 160 watts from a 12V input. Delivering efficiencies as high as 95%, it can eliminate the need for external heat sinking.

The LT3744's peak current mode controller maintains ±3% LED current regulation over a wide voltage range from VEE to VIN. By allowing VEE to float to negative voltages, several LEDs can be driven from a single Li-Ion battery with a simple, single step-down output stage. Additionally, this enables a unique inverting step-down topology that allows a single common anode heat sink to be used for RGB LEDs. A frequency-adjust pin allows the user to program the frequency between 100 kHz and 1 MHz, optimizing efficiency while minimizing external component size. Combined with its 5mm × 6mm QFN package, the LT3744 offers a very compact 80-watt LED driver solution.

The LT3744 provides both PWM dimming and CTRL dimming, which offer 3,000:1 dimming capability for four LED current levels, ideal for color mixing applications, such as those required in DLP projectors. Similarly, its unique

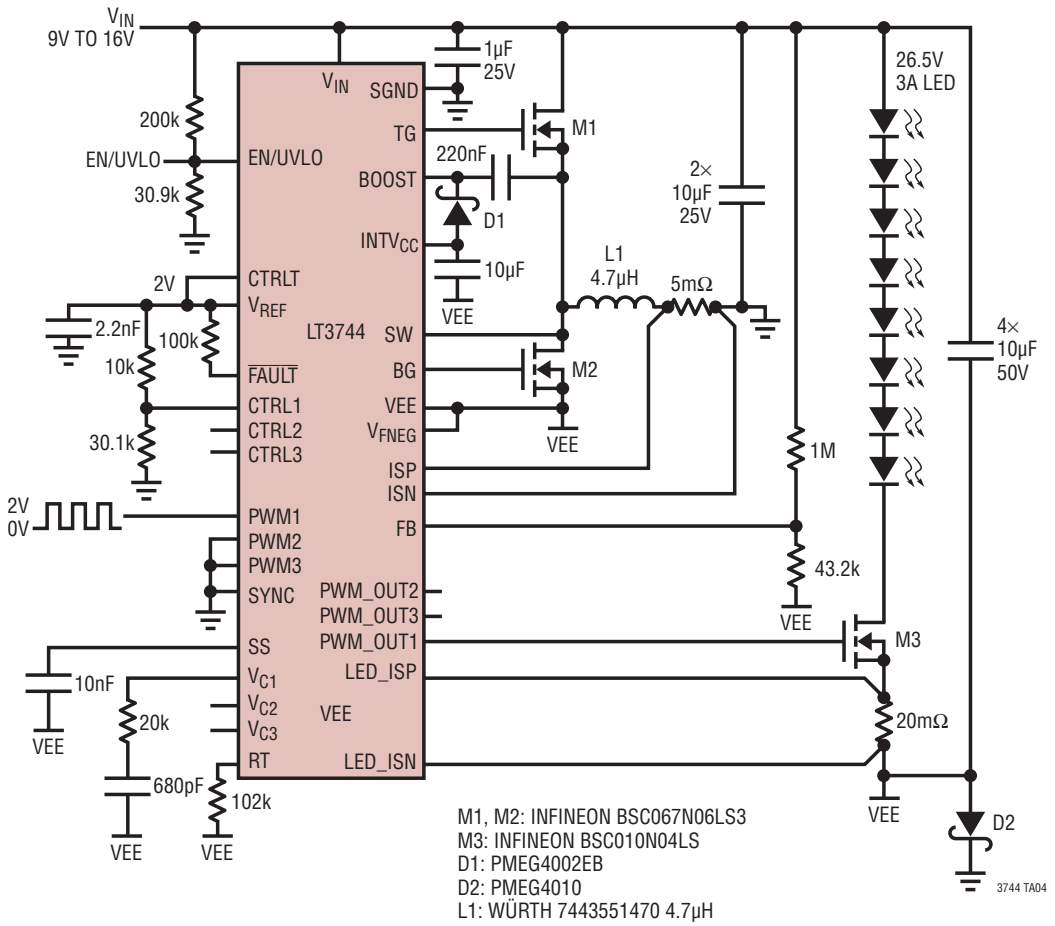

18-2. The LT3744 is burst-mode 3A LED driver with 98% efficiency.

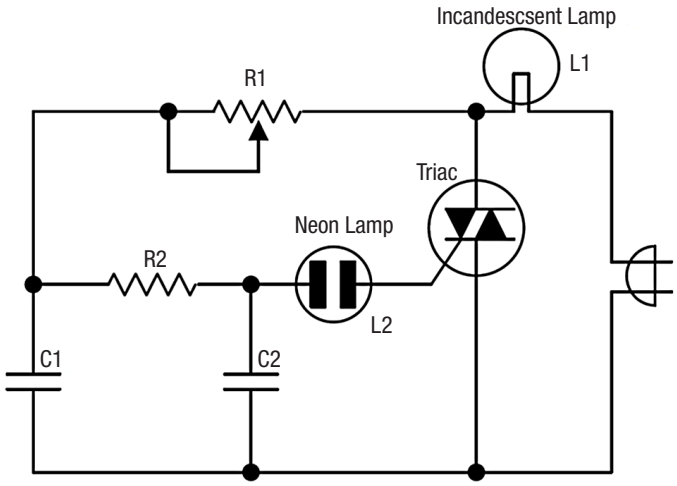

18-3. Triac dimmer circuit for an incandescent lamp.

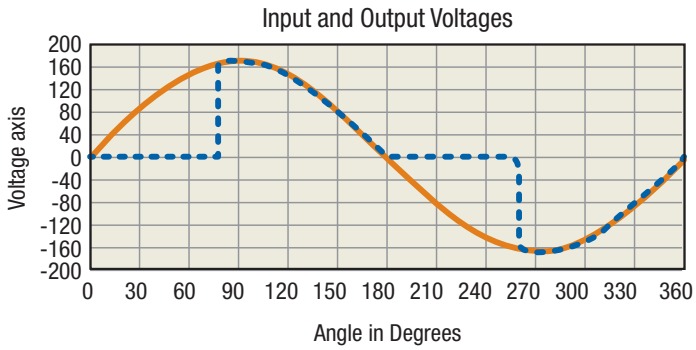

18-4. For the triac-based incandescent trimmer, the blue line indicates the switching of the triac.

topology enables it to transition between two regulated LED currents in less than 2µsec, enabling more accurate color mixing in RGB applications. LED current accuracy of ±3% is maintained to offer the most accurate brightness of light emitted from the LED. Additional features include output voltage regulation and open-LED and shorted-LED protection, open-drain output fault flag, frequency synchronization, and thermal shutdown.

With so many dimmers being used with incandescent lamps, several companies have shown conversion circuits that replace the incandescent with an LED. A typical triac lamp dimmer circuit for an incandescent lamp consists of the circuit in Fig. 18-3. The triac can conduct in either direction so it cuts both halves of the ac sine wave input, as shown in Fig. 18-4. Varying potentiometer (R1) varies the amount of the ac waveform that is cut, which varies the incandescent lamp brightness.

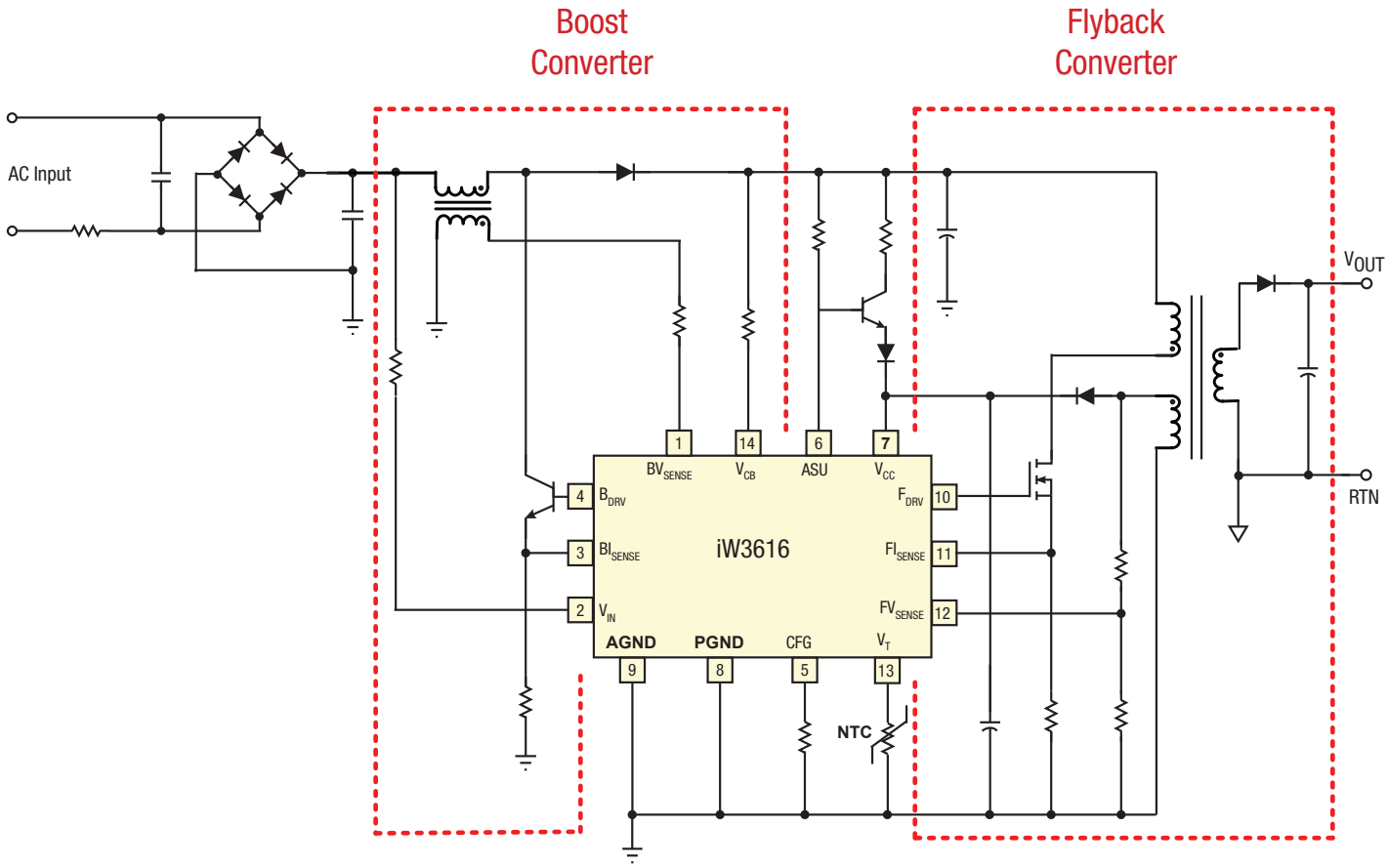

18-5. iW3616 control circuit converts a dimmer from an incandescent to an LED lamp.

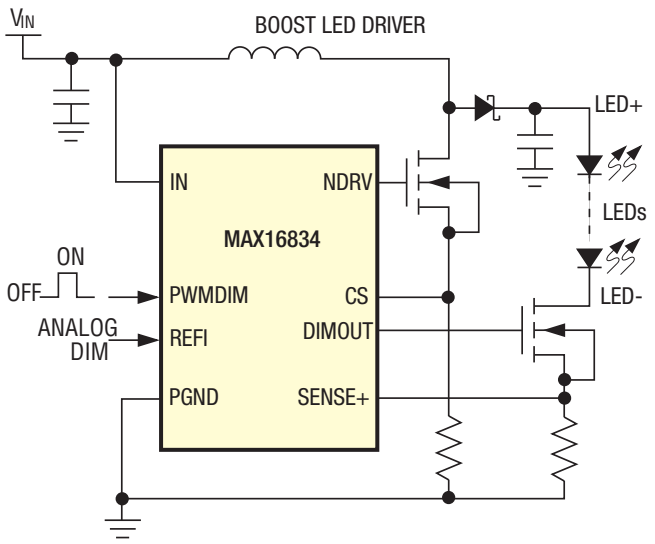

18-6. Maxim's MAX16834 current-mode, high-brightness LED (HB LED) driver.

An incandescent lamp is resistive so the voltage and current through the lamp have a linear relationship. Due to the thermal inertia of the incandescent lamp's filament, the pulsed input voltage of Fig. 18-4 does not cause the light output to flicker. In contrast, the LED is a nonlinear load in which lamp current and voltage depend on the diode-like performance of an LED. Furthermore, the LED responds much faster than an incandescent lamp to changes in applied voltage. Thus, the 120 Hz triac drive voltage can appear as flicker using an LED, unless a "smart" LED driver modifies the triac output to eliminate flicker.

Among the new "smart" LED drivers intended for use with existing triac dimmers are iWatt's iW3616 and iW3617 from iWatt (Fig. 18-5), now part of Dialog Semiconductor. They are two-stage ac/dc power-supply controllers optimized for dimmable LED luminaires. The iW3616 is rated at 12W and the iW3617 has a 25W rating. Both controllers are compliant with the IEC61000-3-2 standard for electromagnetic compatibility (EMC). Its proprietary Flickerless technology automatically detects the dimmer type and phase, providing compatibility with analog and digital dimmers.

Most LEDs can be dimmed using pulse width modulation (PWM). Incandescent lamps have thermal inertia that allows a relatively low PWM frequency to avoid visual flicker during dimming. In contrast, LEDs light up very quickly and require a higher frequency PWM to avoid flicker. There has been some concern that dimming light causes a loss of energy. However, the opposite is true. Driver efficiency may be reduced slightly during dimming, but it can also save significant energy. Plus, dimming lights to half power will save overall significant energy and actually extend LED lifespan.

The MAX16834 from Maxim Integrated is a current-mode, high-brightness LED (HB LED) driver designed to control a single-string LED current regulator with two external n-channel MOSFETs (Fig. 18-6). The MAX16834 integrates all the building blocks necessary to implement a fixed-frequency HB LED driver with wide-range dimming control. The MAX16834 allows implementation of different converter topologies such as SEPIC, boost, boost-buck, or high-side buck current regulator.

The MAX16834 features a constant-frequency, peak-current-mode control with programmable slope compensation to control the duty cycle of the PWM controller. A dimming driver offers a wide-range dimming control for the external n-channel MOSFET in series with the LED string. In addition to PWM dimming, the MAX16834 allows for analog dimming of LED current.

The MAX16834 switching frequency (100kHz to 1MHz) is adjustable using a single resistor from RT/SYNC. The MAX16834 disables the internal oscillator and synchronizes if an external clock is applied to RT/SYNC. The switching MOSFET driver sinks and sources up to 3A, making it suitable for high-power MOSFETs driving in HB LED applications, and the dimming control allows for wide PWM dimming at frequencies up to 20kHz.The MAX16834 is suitable for boost and boost-buck LED drivers.

The MAX16834 alone operates over a 4.75V to 28V input supply range. With a voltage clamp that limits the IN pin voltage to less than 28V, it can operate in boost configuration for input voltages greater than 28V. Additional features include external enable/disable input, an on-chip oscillator, fault indicator output (FLT) for LED open/short or overtemperature conditions, and an overvoltage protection circuit

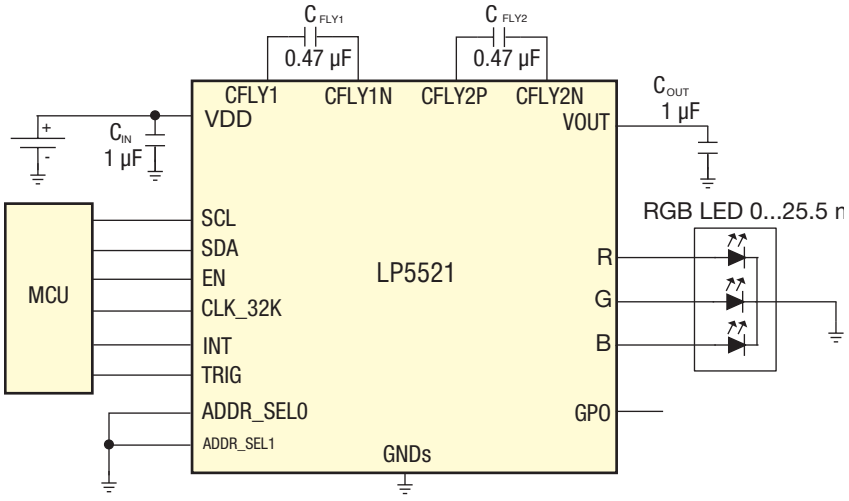

18-7. Texas Instruments' LP5521 is a three-channel LED driver designed to produce a variety of lighting effects.

for true differential overvoltage protection.

Texas Instruments' LP5521 is a three-channel LED driver designed to produce variety of lighting effects for mobile devices (Fig. 18-7). A high-efficiency charge pump enables LED driving over full Li-Ion battery voltage range. The device has a program memory for creating variety of lighting sequences. When program memory has been loaded, the LP5521 can operate autonomously without processor control allowing power savings.

The device maintains excellent efficiency over a wide operating range by automatically selecting proper charge pump gain based on LED forward voltage requirements. The LP5521 is able to automatically enter power-save mode, when LED outputs are not active and thus lowering current consumption.

Three independent LED channels have accurate programmable current sources and PWM control. Each channel has program memory for creating desired lighting sequences with PWM control.

The LP5521 has a flexible digital interface. A trigger I/O and 32-kHz clock input allow synchronization between multiple devices. Interrupt output can be used to notify the processor when LED sequence has ended. LP5521 has four pin-selectable I2C-compatible addresses. This allows connecting up to four parallel devices in one I2Ccompatible bus. GPO and INT pins can be used as digital control pins for other devices. The LP5521 requires only four small and low-cost ceramic capacitors.

Comprehensive application tools are available, including command compiler for easy LED sequence programming.

Texas instrument's LP5521 is a three-channel LED driver designed to produce variety of lighting effects for mobile devices. A high-efficiency charge pump enables LED driving over full Li-Ion battery voltage range. The device has a program memory for creating variety of lighting sequences. When program memory has been loaded, the LP5521 can operate autonomously without processor control allowing power savings.

The IC maintains excellent efficiency over a wide operating range by automatically selecting proper charge pump gain based on LED forward voltage requirements. The LP5521 is able to automatically enter power-save mode, when LED outputs are not active and thus lowering current consumption.

Three independent LED channels have accurate programmable current sources and PWM control. Each channel has program memory for creating desired lighting sequences with PWM control. The LP5521 has a flexible digital interface. A trigger I/O and 32-kHz clock input allow synchronization between multiple devices. Interrupt output can be used to notify processor, when LED sequence has ended. LP5521 has four pin-selectable I2C-compatible ad-

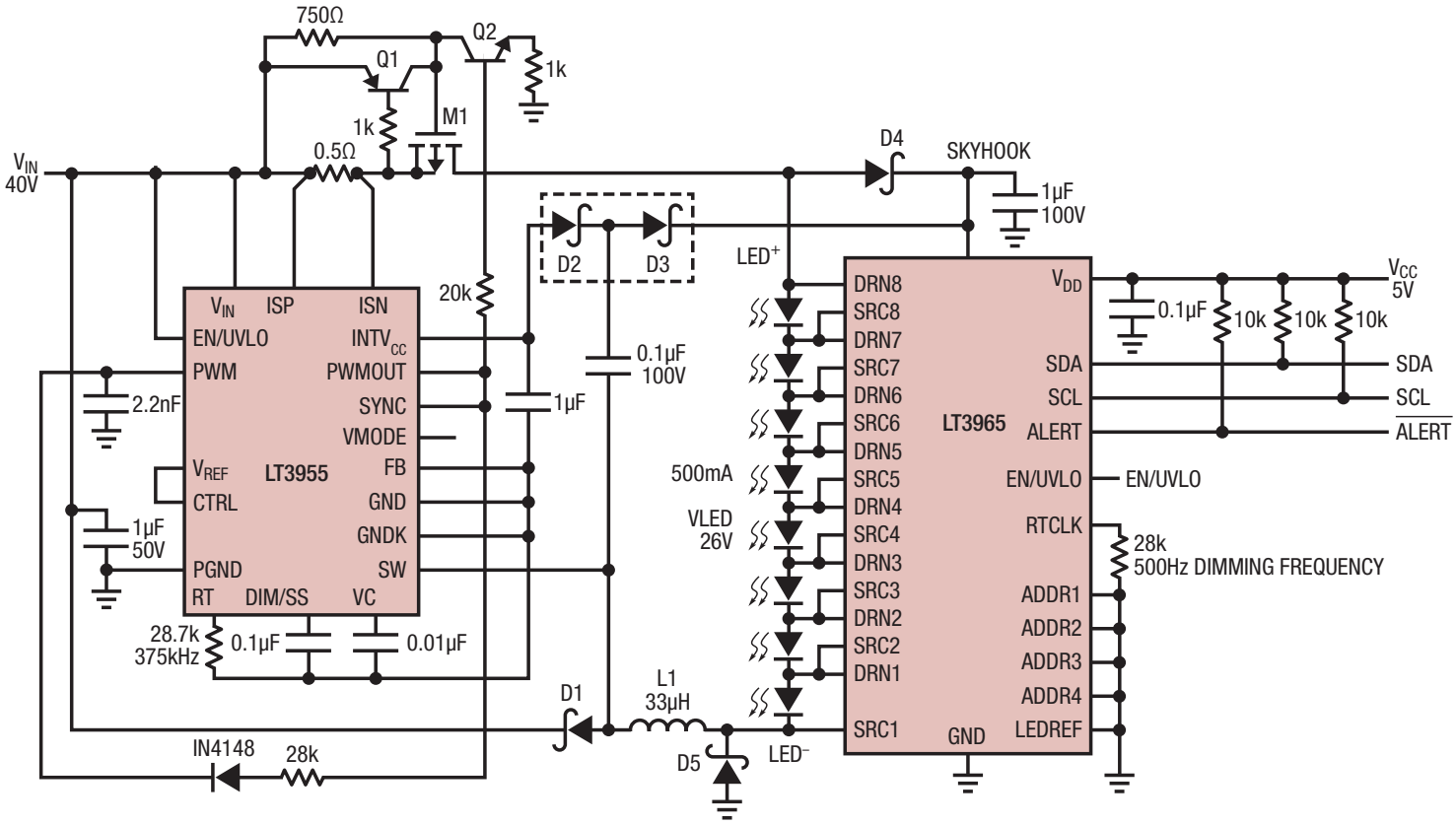

18-8. LT3965 with an external constant current LED driver (LT3955).

18-9. Mean Well's NPF-40D series, a single-output, waterproof switching power supply.

dresses. This allows connecting up to four parallel devices in one I2Ccompatible bus. GPO and INT pins can be used as a digital control pin for other devices.

The LP5521 requires only four small and low-cost ceramic capacitors. Comprehensive application tools are available, including command compiler for easy LED sequence programming.

Eight-Switch Matrix IC Controls On/Off/ Dimming and Diagnostics of LED Array

The LT3965 from Linear Technology is an LED bypass switching IC that contains a floating matrix of eight 17V/330mΩ NMOS switches (Fig. 18-8). You can connect the eight switches in parallel and/or in series to bypass current around any one of LEDs in a string. When interfaced with an external constant current driver IC, the combination can control dimming and diagnostics for up to eight individual LEDs or LED segments. An I^2C serial interface in the switch matrix provides the ability to control individual LEDs. Fig. 18-8 shows the LT3965 with an external constant current LED driver (LT3955). **You can independently program each of the eight channels to control each LED in the string in four different ways:**

- Constant LED on
- Constant LED off
- LED Dimming without fade transition
- LED Dimming with fade transition

The LT3965 operates over the VDD input supply range of 2.7V to 5.5V and V_{IN} range of 8V to 60V. A –40°C to 85°C junction temperature version, LT3965EFE, is housed in a 28-lead TSSOP thermally enhanced package that ensures a compact footprint for matrix dimming applications. An industrial temperature version, the LT3965IFE, guarantees operation from a –40°C to 125°C operating junction temperature range.

18-10. LED Test System

Typical applications include automotive matrix LED headlights, industrial lighting and large LED display lighting. TheI^2C serial interface enables digital programming with 256:1 dimming ratios with or without the 11-bit resolution fade transition between the dimming states. Each switch can control and monitor a single LED or a segment of up to 16V of series-connected LEDs. The LT3965's 8V to 60V input voltage range can accommodate a wide range of LED drivers commonly used in automotive and industrial applications.

LED Power Supplies

The emerging field of electronic lighting has produced families of power supplies specifically for LEDs. For example, Mean Well has introduced the NPF-40D series, a single-output, waterproof switching power supply (Fig. 18-9). Along with its LED driving function, the supply has built-in 3-in-1 dimming (0 to10VDC, PWM signal, or resistance), which simplifies brightness adjustment that allows light reduction and energy conservation. The entire series offers universal input range from 90VAC to 305 VAC and incorporates a PFC function. The enclosure is in a 94V-0 flame-retardant case. The interior is fully potted with silicone that enhances heat dissipation and allows the supply to meet the anti-vibration demand up to 5G. It also conforms to IP67 level, enabling the NPF-40D to be used in a very dusty and humid, harsh environment.

The supply has up to 90% efficiency and no load power consumption below 0.5W. It has protection for short circuit, overcurrent, overvoltage, and overtemperature. It can satisfy the energy-saving demand for the new generation of LED lighting. A double-insulation weather-resistant input cable allows users to install various types of lighting systems. The entire series can operate from -40°C to 70°C and comply with the relevant global lighting safety certification.

LED Testing

Because of their production processes, LEDs cannot be manufactured with 100% consistent optical properties. Brightness and color can vary substantially from component to component even in the same production batch. This is why LEDs have to be tested during production and in their final application. Comprehensive optical characterization is also essential during research and development of LEDs and for LED-based products. Tests are required to determine luminous intensity, luminous flux, color, spectrum, and spatial radiation pattern of LEDs.

The Instrument Systems' LED Tester (Fig. 18-10) is a

turnkey test system based on the company's CAS 140CT CCD Array Spectrometer, Keithley Series 2400/2600 Sourcemeter, and a control PC combined with tester software developed in-house. The interplay between all the components has been optimized for the tough conditions of continuous application in production environments.

This LED Tester can measure critical measuring parameters, e.g., color coordinates of white LEDs, extremely precisely and reproducibly. All calibrations are based on the PTB and NIST national reference standards. The Keithley 2600 delivers fast current supply to the LEDs and in this way permits short measurement times.

The tester software comprises a user-friendly interface with a multitude of functions. You can select different results and structure their display on the monitor to suit the application. The hardware setup is provided with an entering page in order to configure parameters and settings for each application.

Related Articles

1. Ed Rodriguez, Cooling LED Arrays and Power Converters Impacts Performance and Reliability, powerelectronics.com, April 2014.
2. Sam Davis, Intelligent LED Driver Employs Ledotron Digital Dimming, powerelectronics.com, February 2014.
3. Koenraad Rutgers, Overcoming Reliability Challenges in LED Streetlight Applications, powerelectronics.com, August 2013.
4. Sam Davis, LED Driver Micro-Module Needs No External Sensors, powerelectronics.com, July 2012.
5. Georgia Salis, LEDs Are Making Inroads on Automotive Lighting Systems, powerelectronics.com, July 2012.
6. Hector F. Arroyo, How to Add Analog Dimming to Virtually Any LED Driver, powerelectronics.com, January 2012.
7. Cathal Sheehan, Design Efficient Thermal Management for Added Reliability in LED Apps, powerelectronics.com, June 2011.
8. Kelvin Shih, Is the Thermal Resistance of LEDs Constant?, powerelectronics.com, April 2010.
9. Irene Signorino, Next-Generation Solid-State Lighting Fixtures Need Optimized LED Drivers, powerelectronics.com, September 2009.
10. Tsing Hsu, Simple, Constant-Current Drive Controls 16 LEDs, powerelectronics.com, February 2008.

BACK TO TABLE OF CONTENTS

CHAPTER 19:

MOTION-SYSTEM POWER MANAGEMENT

The key component in a motion system is the motor because it determines the design of the associated motion controller as well as the motor drive. From a power-management viewpoint, the important motion-system design considerations are providing the appropriate control signals as well as the required drive power for the specific motor. Each motion controller is unique for a specific motor. Fig. 19-1 shows the typical motion system that includes a motion controller and a motor drive.

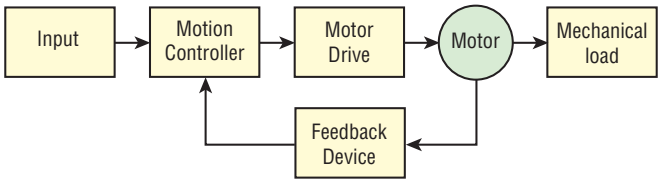

19-1.Typical motion system.

An electric motor is an electrical machine that converts electrical energy into mechanical energy. In normal motoring mode, most electric motors operate through the interaction between an electric motor's magnetic field and winding currents to generate force within the motor.

Electric motors are used to produce linear or rotary force (torque). That is, the motion controller controls the motor's rotary speed or its linear position. You can convert rotating motion to linear motion using mechanical components or use a linear motor to provide linear motion by itself.

The motor's moving part is the rotor that turns the shaft to deliver mechanical power. The stator is the stationary part of the motor's electromagnetic circuit and usually consists of either windings or permanent magnets. Windings are wires that

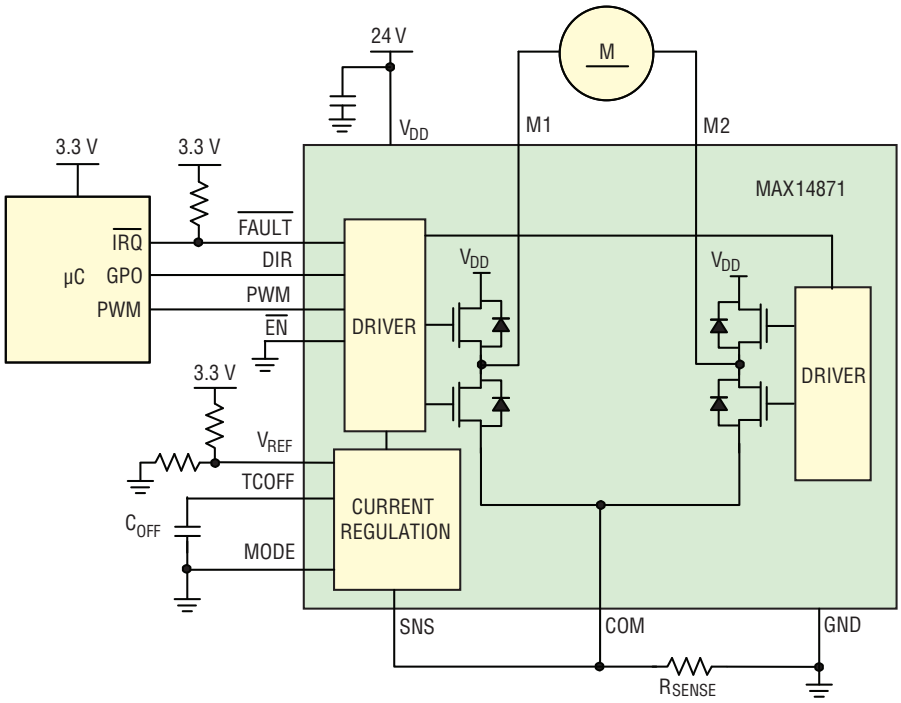

19-2. Maxim's MAX14871 dc motor driver provides a low-power and simple solution for driving and controlling brushed motors with voltages between 4.5V and 36V.

are laid in coils, usually wrapped around a laminated soft iron magnetic core to form magnetic poles when energized by current.

In a brushed motor, a commutator switches the input of most dc machines and certain ac machines consisting of slip-ring segments insulated from each other and from the electric motor's shaft. The motor's armature current is supplied through the stationary brushes in contact with the revolving commutator, which causes a current reversal and applies power to the machine in an optimal manner as the rotor rotates from pole to pole. In absence of such current reversal, the motor would brake to a stop.

The MAX14871 dc motor driver provides a low-power and simple solution for driving and controlling brushed motors with voltages between 4.5V and 36V. Very low driver on resistance reduces power during dissipation (Fig. 19-2).

The MAX14871 features a charge- pump-less design for reduced external components and low supply current. Integrated current regulation allows user-defined peak startup motor currents and requires minimal external components.

The MAX14871 includes three modes of current regulation: fast decay, slow decay, and 25% current ripple modes. Current regulation based on 25% ripple simplifies the design and enables regulation independent of motor characteristics. A separate voltage sense input (SNS) reduces current-sensing errors due to parasitic trace resistance.

The term "electronic commutator" is usually associated with self-commutated brushless dc motor and switched reluctance motor applications. Some problems with the brushed dc motor are eliminated in the brushless dc (BLDC) design. In this motor, the mechanical "rotating switch" or commutator is replaced by an external electronic switch synchronized to the rotor's position. BLDC motors are typically 85% to 90% efficient or more.

19-3. ON Semiconductor MC33035 brushless dc motor controller.

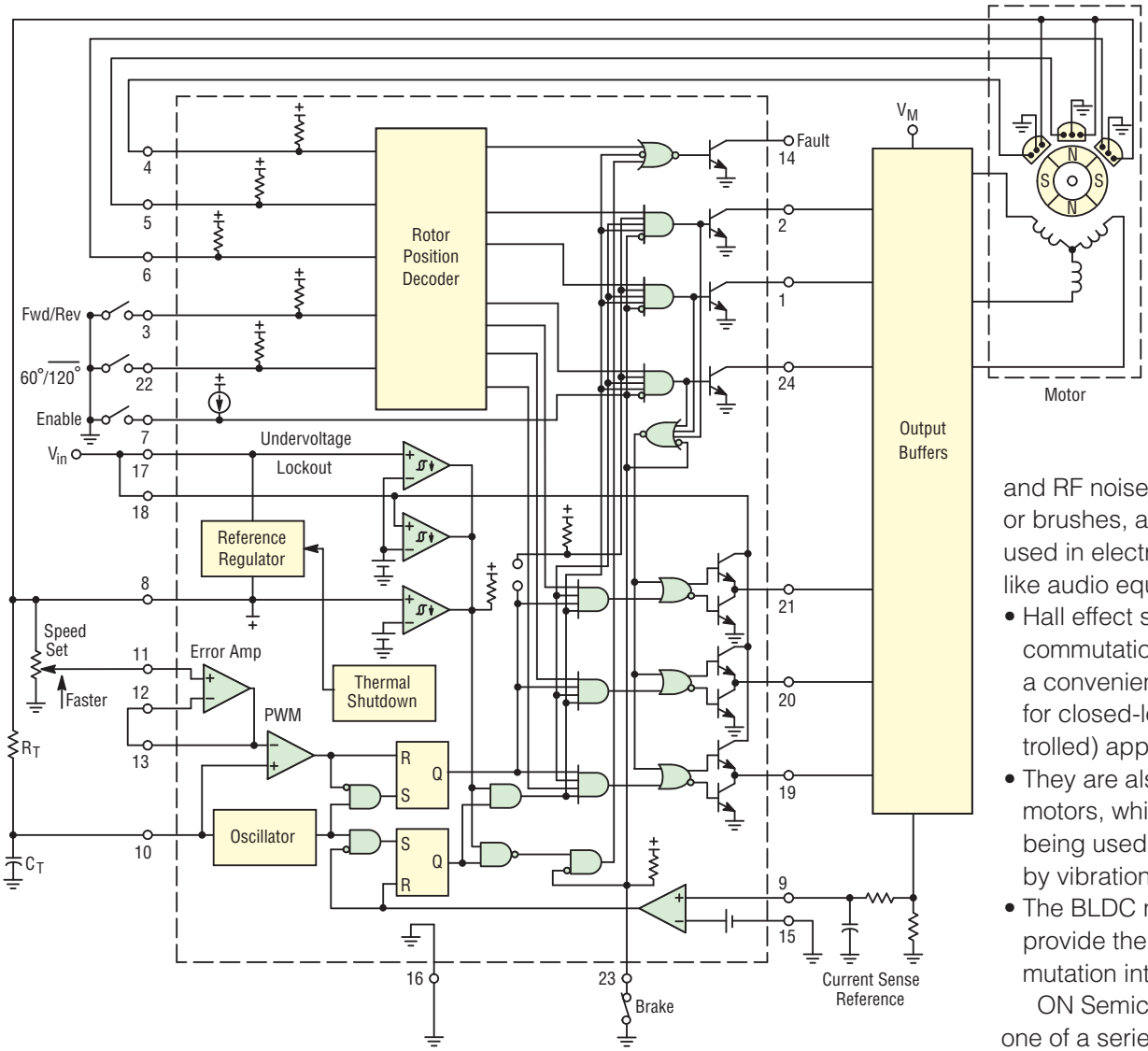

BLDC motors are commonly used where precise speed control is necessary. They have several advantages over conventional motors:

- Without a commutator to wear out, the life of a BLDC motor can be significantly longer compared to a dc motor using brushes and a commutator. Commutation also tends to generate electrical and RF noise. Without a commutator or brushes, a BLDC motor may be used in electrically sensitive devices like audio equipment or computers.
- Hall effect sensors provide the commutation and can also provide a convenient tachometer signal for closed-loop control (servo-controlled) applications.
- They are also acoustically quiet motors, which is an advantage if being used in equipment affected by vibrations.
- The BLDC motion controller must provide the proper electronic commutation interface.

ON Semiconductor's MC33035 is one of a series of high performance

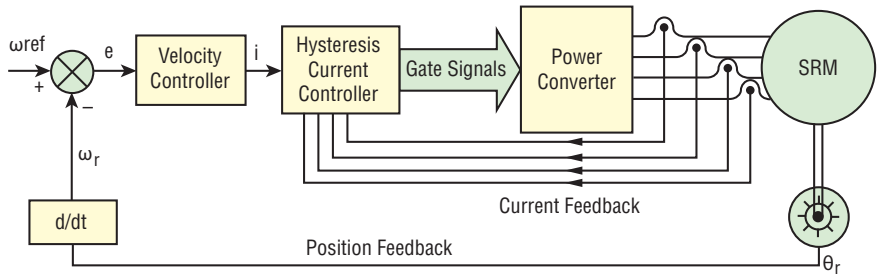

19-4. Control system for an SRM senses angular position, which is sent to the controller. Deriving the position in the time domain allows computing the angular speed of the rotor. The controller compares the actual speed with the reference value and calculates the error signal for the hysteresis comparator. Each phase is supplied within a certain rotor position range in order to maximize the developed torque. The hysteresis controllers send the gate signals to the power switches of the converter.

monolithic DC brushless motor controllers(Fig. 19-3). It contains all of the functions required to implement a full–featured, open loop, three or four phase motor control system. In addition, the controller can be made to operate DC brush motors. Constructed with Bipolar Analog technology, it offers a high degree of performance and ruggedness in hostile industrial environments. The MC33035 contains a rotor position decoder for proper commutation sequencing, a temperature compensated reference capable of supplying a sensor power, a frequency programmable sawtooth oscillator, a fully accessible error amplifier, a pulse width modulator comparator, three open collector top drive outputs, and three high current totem pole bottom driver outputs ideally suited for driving power MOSFETs.

Included in the MC33035 are protective features consisting of undervoltage lockout, cycle–by–cycle current limiting with a selectable time delayed latched shutdown mode, internal thermal shutdown, and a unique fault output that can easily be interfaced to a microprocessor controller.

Typical motor control functions include open loop speed control, forward or reverse rotation, run enable, and dynamic braking. In addition, the MC33035 has a 60°/120° select pin that configures the rotor position decoder for either 60° or 120° sensor electrical phasing inputs.

Switched Reluctance Motor (SRM)

The SRM has no brushes or permanent magnets, and the rotor has no electric currents (Fig. 19-4). Instead, torque comes from a slight misalignment of poles on the rotor with poles on the stator. The rotor aligns itself with the magnetic field of the stator, while the stator field stator windings are sequentially energized to rotate the stator field.

The magnetic flux created by the field windings follows the path of least magnetic reluctance, meaning the flux will flow through poles of the rotor that are closest to the energized poles of the stator, thereby magnetizing those poles of the rotor and creating torque. As the rotor turns, different windings will be energized, keeping the rotor turning. The SRM motion controller must provide the appropriate signals.

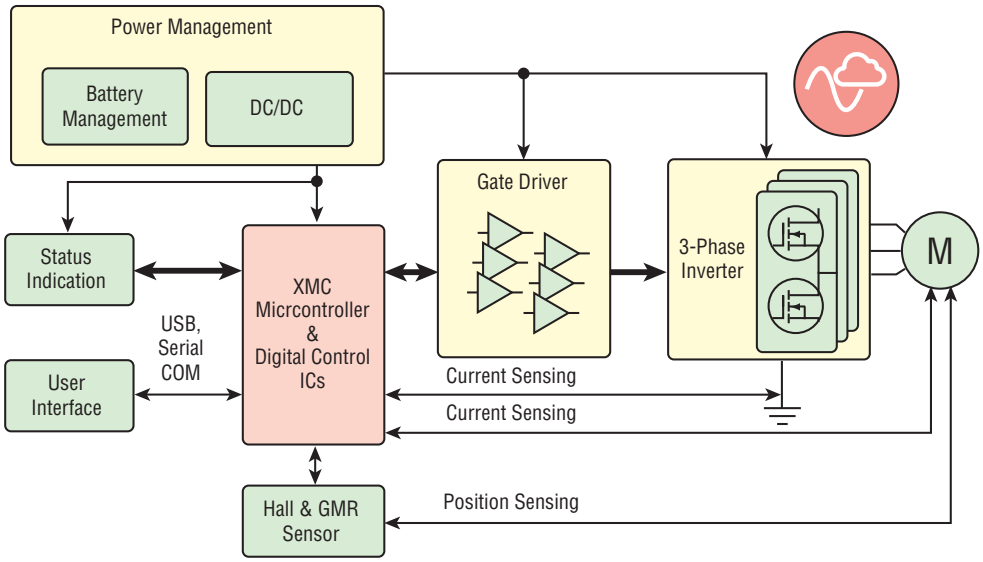

19-5. IRMCF143S from International Rectifier is a high-performance flash-based motion-control IC designed primarily for position servo applications based on an incremental encoder.

Induction Motor

An induction motor is an asynchronous ac motor where power is transferred to the rotor by electromagnetic induction, much like transformer action. An induction motor resembles a rotating transformer, because the stator (stationary part) is essentially the primary side of the transformer and the rotor (rotating part) is the secondary side. Polyphase induction motors are widely used in industry. Fig. 19-4 shows a microcontroller-based induction motor drive.

Currents induced into this winding provide the rotor magnetic field. The shape of the rotor bars determines the speed-torque characteristics. At low speeds, the current induced in the

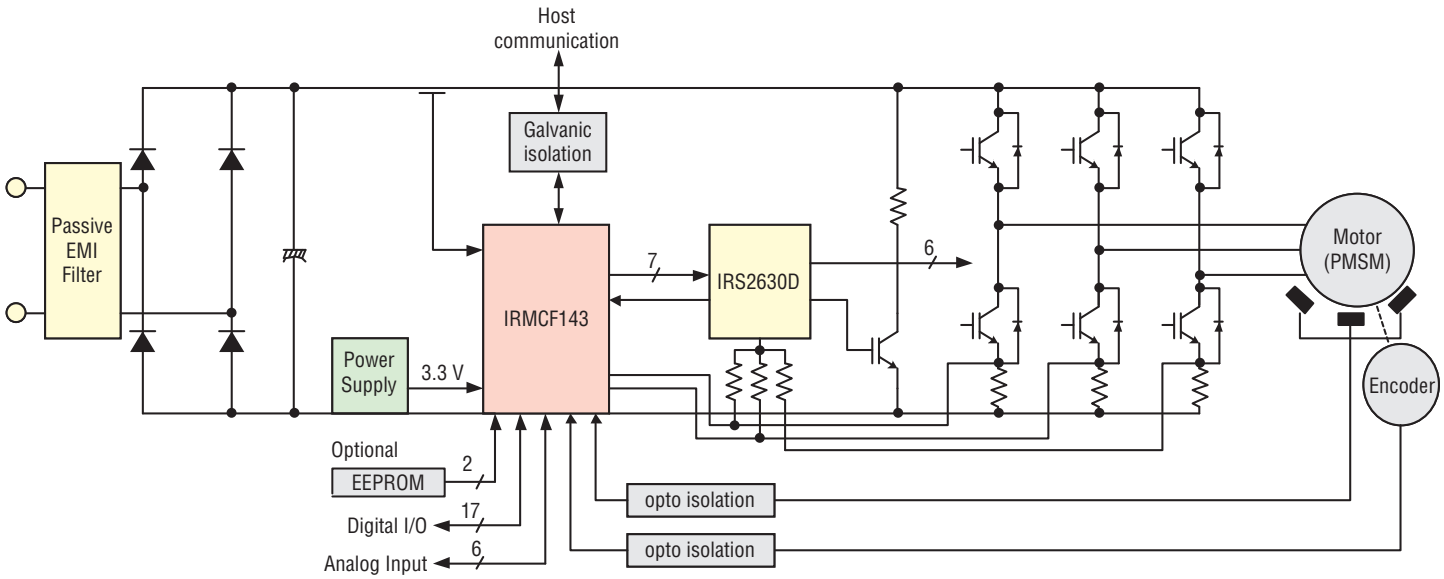

19-6. Texas Instruments' DRV8811 is a motor microstepping motor driver with two H-bridge drivers, as well as microstepping indexer logic to control a stepper motor.

squirrel cage is nearly at line frequency and tends to be in the outer parts of the rotor cage. As the motor accelerates, the slip frequency becomes lower, and more current is in the interior of the winding. By shaping the bars to change the resistance of the winding portions in the interior and outer parts of the cage, effectively a variable resistance is inserted in the rotor circuit. However, the majority of such motors have uniform bars.

Servo Motor

A servomotor is a motor, very often sold as a complete module, used within a position-control or speed-control feedback control system mainly to control valves, such as motor-operated control valves (Fig. 19-5). Servomotors are used in applications such as machine tools, pen plotters, and other process systems. Motors intended for use in a servomechanism must have well-documented characteristics for speed, torque, and power. The speed vs. torque curve is quite important and is high ratio for a servo motor. Dynamic response characteristics such as winding inductance and rotor inertia are also important; these factors limit the overall performance of the servomechanism loop. Large, powerful, but slow-responding servo loops may use conventional ac or dc motors and drive systems with position or speed feedback on the motor. As dynamic response requirements increase, more specialized motor designs such as coreless motors are used. AC motors' superior power density and acceleration characteristics compared to that of dc motors tends to favor PM synchronous, BLDC, induction, and SRM drive applications.

A servo system differs from some stepper motor applications in that the position feedback is continuous while the motor is running; a stepper system relies on the motor not to "miss steps" for short-term accuracy, although a stepper system may include a "home" switch or other element to provide long-term stability of control. For instance, when a typical dot matrix computer printer starts up, its controller makes the print-head stepper motor drive to its left-hand limit, where a position sensor defines home position and stops stepping. As long as power is on, a bidirectional counter in the printer's microprocessor keeps track of print-head position.

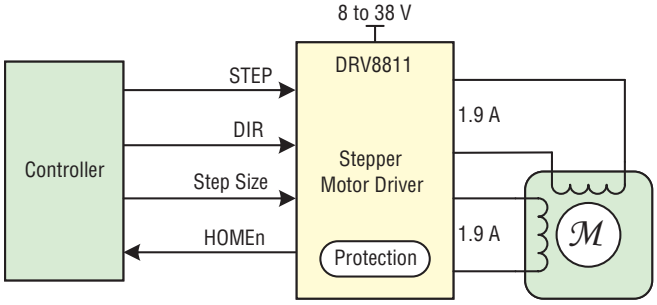

19-7. Texas Instruments' DRV8811 is a motor microstepping motor driver with two H-bridge drivers, as well as microstepping indexer logic to control a stepper motor.

Stepper Motor

Stepper motors are a type of motor frequently used when precise rotations are required. In a stepper motor, an internal rotor containing permanent magnets or a magnetically soft rotor with salient poles is controlled by a set of external magnets that are switched electronically. A stepper motor may also be thought of as a

cross between a dc electric motor and a rotary solenoid. As each coil is energized in turn, the rotor aligns itself with the magnetic field produced by the energized field winding. Unlike a synchronous motor, in its application, the stepper motor may not rotate continuously; instead, it "steps"—starts and then quickly stops again—from one position to the next as field windings are energized and de-energized in sequence. Depending on the sequence, the rotor may turn forward or backward, and it may change direction, stop, speed up, or slow down arbitrarily at any time.

Simple stepper motor drivers entirely energize or entirely de-energize the field windings, leading the rotor to "cog" to a limited number of positions; more sophisticated drivers can proportionally control the power to the field windings, allowing the rotors to position between the cog points and thereby rotate extremely smoothly. This mode of operation is often called "microstepping" (Fig. 19-6). Computer controlled stepper motors are one of the most versatile forms of positioning systems, particularly when part of a digital servo-controlled system.

Piezoelectric motor

A piezoelectric motor or piezo motor is a type of electric motor based upon the change in shape of a piezoelectric material when an electric field is applied. Piezoelectric motors make use of the converse piezoelectric effect whereby the material produces acoustic or ultrasonic vibrations in order to produce a linear or rotary motion. In one mechanism, the elongation in a single plane is used to make a series stretches and position holds, similar to the way a caterpillar moves.

Related Articles

1. Ryan Scott, Motor Control System Efficiency with IGBTs, powerelectronics.com, September 2012.
2. Alberto Guerra, Multichip QFN IPM Provides Efficient Drive for Low Power Motors, powerelectronics.com, September 2012.
3. Randy Frank, Motion Controls Move Vehicles in a New Direction, electronicdesign.com, January 2012.
4. Ali Husain, Run a Single-Phase Induction Motor with a Three Phase Inverter, powerelectronics.com, May, 2011.
5. Roger Allan, Smart Motor Controllers Take Charge of Expanding Applications,, powerelectronics.com, March 2011.
6. Kaushik Rajashekara, Cryogenic Power For Transportation Heats Up, powerelectronics.com, June 2014.
7. White Paper, Power Analysis of PWM Motor Drives, powerelectronics.com, April 2014.
8. Alberto Guerra, Optimized IPM Spawns Energy-Efficient Motors, electronicdesign.com, May 2012.
9. Tom Rowan, Versatile Microstepper Driver ICs Provide Next Generation Stepper, powerelectronics.com, September 2010.
10. Sam Davis, Monolithic 500-V, 1-A Three-Phase Motor Drive IC Fits SMT SOP, powerelectronics.com, July 2009.

BACK TO TABLE OF CONTENTS

CHAPTER 20:

COMPONENTS AND METHODS FOR CURRENT MEASUREMENT

Current measurement components and methods must provide an accurate output signal as well as preventing damage to the associated printed circuit board.
Reprinted by permission of ***Power Electronics Technology*** *and* ***Penton Media*** *from Jan. 6, 2012*

Bryan Yarborough | ***Power Electronics***

Current sensing is used to perform two essential circuit functions. First, it is used to measure "how much" current is flowing in a circuit, which may be used to make decisions about turning off peripheral loads to conserve power or to return operation to normal limits. A second function is to determine when it is a "too much" or a fault condition. If current exceeds safe limits, a software or hardware interlock condition is met and provides a signal to turn off the application, perhaps a motor in a stalled condition or short circuit. It is essential to choose the appropriate technology with the necessary robustness to properly withstand the extreme conditions that can exist during a fault.

A signal to indicate the "how much" condition and the "too much" condition is available in a variety of measurement methods:

1. Resistive (Direct)
    a. Current Sense Resistors
    b. Inductor dc resistance
2. Magnetic (Indirect)
    a. Current Transformer
    b. Rogowski Coil
c. Hall Effect Device
3. Transistor (Direct)
    a. $R_{DS(ON)}$
    b. Ratio-metric

Each method has advantages for current measurement, but also comes with tradeoffs that can be critical to the end reliability of the application. They can also be classified into two main categories of measurement methods; direct or indirect. The direct method means that it is connected directly in the circuit being measured and that the measurement components are exposed to the line voltage, whereas the indirect method provides isolation that may be necessary for design safety.

Current Sense Resistor

The resistor is a direct method of current measurement that has the benefit of simplicity and linearity. The current sense resistor is placed in line with the current being measured and the resultant current flow causes a small amount of power to be converted into heat. This power conversion is what provides the voltage signal. Other than the favorable characteristics of simplicity and linearity, the current sense resistor is a cost-effective solution with stable Temperature Coefficient of Resistance (TCR) of < 100 ppm/°C or 0.01%/°C and does not suffer the potential of avalanche multiplication or thermal runaway. Additionally, the existence of low resistance (< 1 mΩ is available) metal alloy current sense products offer superior surge performance for reliable protection during short circuit and overcurrent events.

Inductor DC Resistance

The dc resistance of an inductor can also be used to provide a resistive current measurement. This method is considered "lossless" because of the low resistance value of the copper, typically < 1 mΩ and because it is providing a secondary use of an existing component. In higher current applications; a 30 amp current would provide a 30 mV signal for a 1 mΩ resistance value. This method has two draw-

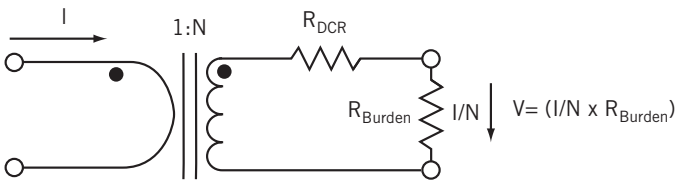

Ideal current transformer circuit

20-1. In the ideal current transformer ac current passes through the copper wind¬ings with very little resistive losses.

backs; first copper has a high TCR (temperature coefficient of resistivity) of approximately 3900 ppm, which causes the resistance value to increase by 39% for a 100°C rise above room temperature. Because of this high TCR, the temperature must be monitored and compensated to provide an acceptable current measurement. The second drawback is the variance in the resistance of the copper due to dimensional changes that occur due to the conductor being wider or thinner from one lot to the next.

Current Transformer

A current transformer's three key advantages are that it provides isolation from the line voltage, provides lossless current measurement, and the signal voltage can be large providing a measure of noise immunity. This indirect current measurement method requires a changing current, such as an AC, transient current, or switched DC; to provide a changing magnetic field that is magnetically coupled into the secondary windings (Fig. 20-1). The secondary measurement voltage can be scaled according to the turns ratio between the primary and secondary windings. This measurement method is considered "lossless" because the circuit current passes through the copper windings with very little resistive losses. However, a small amount of power is lost due to transformer losses from the burden resistor, core losses, and primary and secondary dc resistance.

Rogowski Coil

The Rogowski coil is similar to a current transformer in that a voltage is induced into a secondary coil that is proportional to the current flow through an isolated conductor. The exception is that the Rogowski coil (Fig. 20-2) is an air core design as opposed to the current transformer that relies upon a high permeability core, such as a laminated steel, to magnetically couple to a secondary winding. The air core design has a lower inductance providing a faster signal response and very linear signal voltage. Because of its design, it is often used as a temporary current measurement method on existing wiring such as a handheld meter. This could be considered a lower cost alternate to the current transformer.

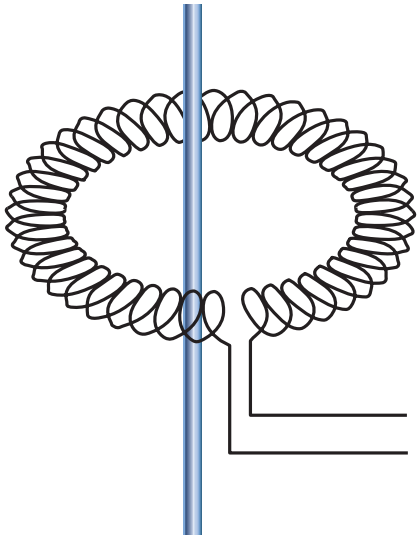

Rogowski Coil

20-2. Rogowski coil is an air core design that has a lower inductance providing a faster response.

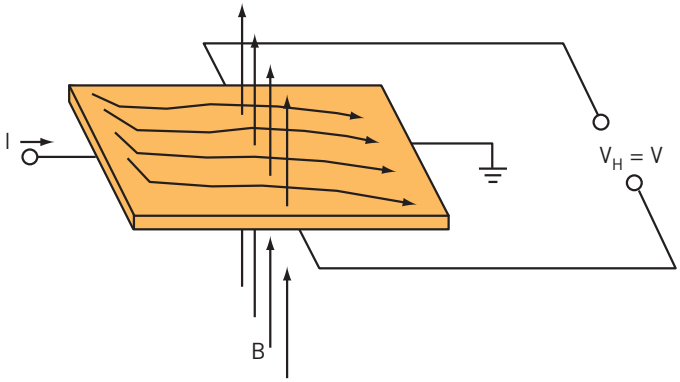

Hall effect principle, magnetic field present

20-3. Hall-Effect devices are capable of measuring large currents.

Hall Effect

When a current carrying conductor is placed in a magnetic field, as shown in Fig. 20-3, a difference in potential occurs perpendicular to the magnetic field and the direction of current flow. This potential is proportional to the magnitude of the current flow. When there is no magnetic field and current flow exists, then there is no difference in potential. However, when a magnetic field and current flow exists the charges interact with the magnetic field, causing the current distribution to change, which creates the Hall voltage.

The advantage of Hall effect devices is that they are capable of measuring large currents with low power dissipation. However, there are numerous drawbacks that can limit their use, including non-linear temperature drift requiring compensation, limited bandwidth, low range current detection requires a large offset voltage that can lead to error, susceptibility to external magnetic fields, and high cost.

Transistors

Transistors are considered a "lossless" overcurrent detection method since they are standard control components to the circuit design and no further resistance or power dissipating devices are required to provide a control signal. Transistor datasheets provide the on-resistance for

the drain-to-source, {$R_{DS(ON)}$, with a typical resistance in the mΩ range for power MOSFETs (Fig. 20-4). This resistance comprises several components that begin with the leads connecting to the semiconductor die through the resistance that makes up the numerous channel characteristics. Based on this information, the current passing through the MOSFET can be determined by $I_{Load} = V_{RDS(ON)} / R_{DS(ON)}$.

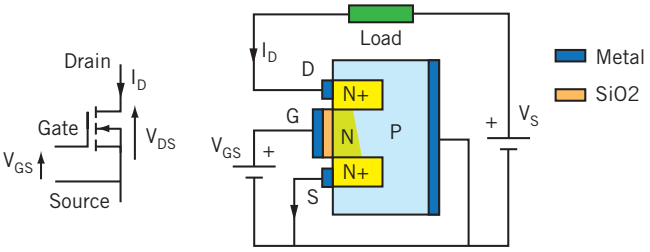

20-4. Power MOSFET's on-resistance provides current sensing capability.

Each constituent of the} $R_{DS(ON)}$ contributes to measurement error that is due to minor variations in the resistances of the interface regions and TCR effects. The TCR effects can be partially compensated by measuring temperature and correcting the measured voltage with anticipated change in resistance due to temperature. Often times, the TCR for MOSFETs can be as large as 4000 ppm /°C, which is equivalent to a 40% change in resistance for 100°C rise. Generally, this method provides a signal with approximately 10% to 20% accuracy. Depending on the accuracy requirements, this may be an acceptable range for providing overcurrent protection.

Ratiometric Current Sense MOSFETs

The MOSFET consists of thousands of parallel transistor cells that reduce the on-resistance. The current sensing MOSFET shown in Fig. 20-5 uses a small portion of the parallel cells and connects to the common Gate and Drain, but separate Source. This creates a second isolated transistor; a "sense" transistor. When the transistor is turned on, the current through the sense transistor will be a ratio comparable to the main current through the other cells.

Depending on the transistor product, the accuracy tolerance range can vary from as low as 5% or as wide as 15%-20%. This is not suitable for current control applications that typically require 1% measurement accuracy, but is intended for overcurrent and short circuit protection.

Resistor Technology Benefits

Thin film is not typically used for current sense applications, but is included in this discussion to provide breadth to the topic. Generally these resistive products are for precision applications because of the resistive layer ranges from 0.000001 in. to 0.000004 in. thick. They are quite surge-tolerant in the appropriate application, but are not designed for the high currents typically associated with the applications mentioned here.

Thick film, typically 0.0005 to 0.002 in. thick, is nearly 100 times thicker than thin Film. The increased thickness equates to a greater mass that is better able to carry the relatively high currents and dissipate the heat across the substrate, as well as better able to manage transients. Another advantage of the thick film products is the flexibility to request standard resistance values because of the process efficiency of laser trimming. The tradeoff of thick film is that these products are not as capable of the very tight tolerances of thin film products.

Foil technology has a larger cross section still and is a uniform resistive alloy, which is different from the thick-film technology that employs resistive materials suspended in a glass matrix. By comparison, the foils tend to withstand larger surge transients as compared to the previous versions. The principle advantage with this technology is the low range ohmic values with low TCRs.

Bulk alloy resistor technology has the greatest surge tolerance because of its large current carrying mass. It is available in resistance values as low as 0.000 5 Ω with low TCR. Bulk alloy tends to be the best choice for high current power supplies, or for where fault conditions can result in extreme currents. These products do not have as wide of a resistance offering as the Thick Film products, because the resistor alloy has limited resistivities to reach high range values, as well as needing the mechanical strength to tolerate process handling.

Product-Specific Features

High-current applications require the resistance value to be very low to minimize power losses and yet provide the necessary signal level to provide a voltage signal high enough to exceed noise levels. These low ohmic values often times need a four-terminal connection to reduce errors that may result due to the contact resistance that occurs when the part is mounted to the board.

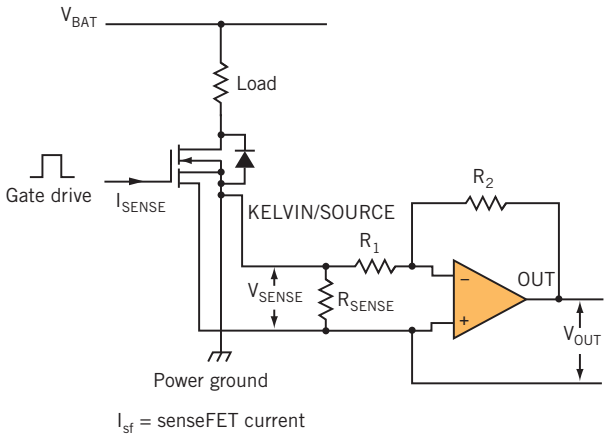

20-5. SenseFET uses a small portion of its parallel MOSFET cells to sense current.

The CSL (Fig. 20-6a) offers four terminals by design, but other standard surface-mount devices

(a)

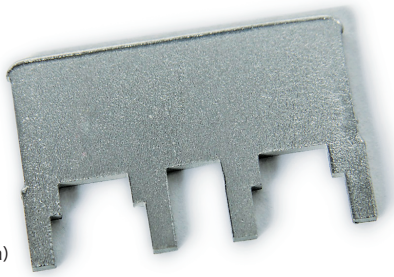

20-6a. Shows a four-terminal resistor for current sense applications.

(b)

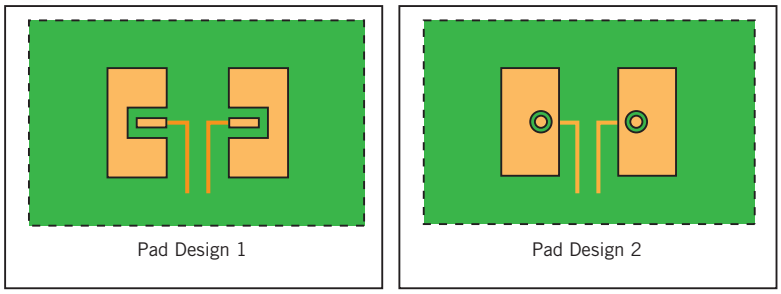

20-6b. Two pad designs, (1) with isolated pad regions, and (2) with a plated through-hole.

can benefit from a four-terminal pad design. These parts offer physically separated connection points for current and voltage, which reduces contact related measurement error. In the case of the CSL, the current will flow through the inner pins and voltage is sensed on the outer pins and is recommended for best accuracy with the LRF3W to be configured as a cross flow arrangement with current on diametrically opposing corners (e.g., pin 2 to pin 3).

The pad layout (Fig. 20-6b) creates separate regions for measuring signal voltage from the current carrying portion, which reduces error. Pad Design 1 illustrates one method that creates an isolated pad region within the pad layout, but this design may reduce the pad area below necessary limits to carry high currents through the copper trace. Pad Design 2 uses a plated through-hole to connect under the pad and connects to an internal or outer trace for measurement; this maximizes the pad space to carry current to the resistor. The contact point places the signal line as close to the current channel as possible; minimizing measurement error.

(a)

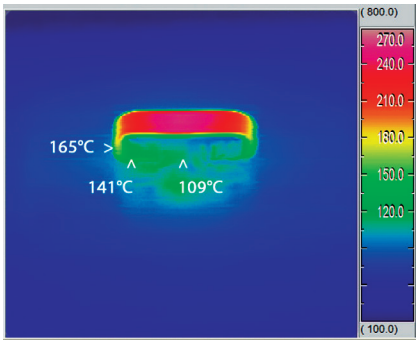

(b)

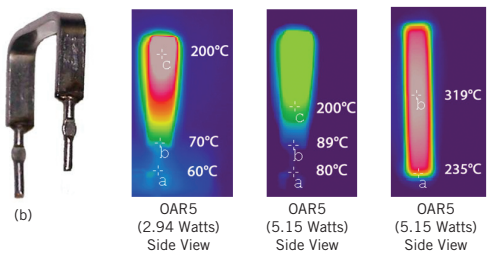

20-7. Thermal images illustrating the isolation performance of the OARand OARS product.

Thermal Isolation

The OARS (Open Air Resistor Surface Mount) is a unique design that elevates the hot spot of the resistive material well above the circuit-board material. This places the hottest region of the part into the available airstream, which dissipates the maximum amount of heat energy to the air instead of the PCB.

This provides two key advantages for thermal design, which affects the PCB material and the other neighboring power or semiconductor components. Typical FR4 PCB material is only rated to 130°C; a power resistor that is traditionally against the board could cause damage to the material during power excursions or reduces the upper temperature performance limits of the circuit. An elevated current sense prevents damage to the circuit material and permits the solder joint to run cooler. The second benefit by dissipating the heat to the air instead of the PCB is the improved performance of nearby heat-affected devices. These effects may include lifetime rating, power handling, luminous output, accuracy, and reliability.

The thermal images shown in Fig. 20-7 help illustrate the isolation performance of the OAR and OARS products. These tests were conducted on FR4 board material with no ambient airflow; airflow would improve system thermal performance. Observe the temperature of the solder joint with respect to the hot spot. These temperatures are based on reaching thermal equilibrium, however in the application these results may be extended to be considered as the thermal performance characteristics for an overcurrent protection condition. The FR4 will not exceed its temperature rating, though extreme circuit conditions exist.

Solder Joint Stress

The OARS resistive product family's elevated and curved construction permits the resistor to flex. This construction reduces the stress generated by differences in thermal expansion coefficients between the heat producing metal and the dissipating circuit board material. Surface-mount components that are flat and parallel to the circuit board will apply shear forces to the solder joint that can lead to failure

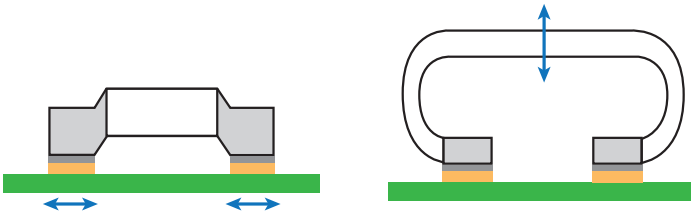

Figure 20-8. Differences in the thermal expansion coefficient between the metal materials of the current sense resistor and the circuit board materials dissipate forces on each part.

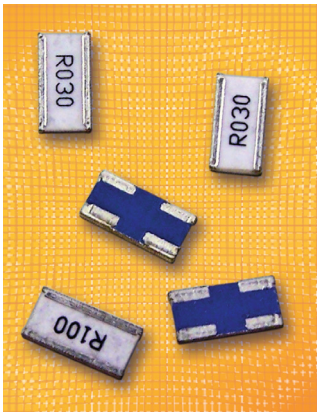

Figure 20-9. LRF3W from TT electronics uses side terminations to achieve a 3W rating.

TABLE 20-1. COMPARISON OF CURRENT MEASUREMENT METHOD

Measurement Method	Accuracy	Isolation	EMI (Tamper Resistance)	Robust	Size	Cost
Resistive (Direct)						
Sense Resistor	High	No	High	High	Small	Low
Inductor DC resistance	Low	No	Moderate	High	Small	Low
Transistor (Direct)						
RDSon	Low	No	Moderate	Moderate	Small	Low
Ratio Metric	Moderate	No	Moderate	Moderate	Small	Moderate
Magnetic (Indirect)						
Current Transformer	High	Yes	Moderate	High	Large	Moderate
Rogowski Coil	High	Yes	Moderate	High	Large	Moderate
Hall Effect	High	Yes	High	Moderate	Moderate	High

or changes in performance. In high thermal cycling applications, the OARS has been preferred to other similar all-metal construction parts because of this flexibility feature (Fig. 20-8).

The LRF3W (Fig. 20-9) from TT electronics provides several design benefits derived from its 1225 aspect ratio with the termination along the long side of the component. The side termination extends the power rating to 3 Watts, eliminating the need to reduce the circuit traces as required by the traditional 2512 footprint. It also reduces solder joint stresses due to differences in the temperature coefficient of expansion between the ceramic and PCB material. The 1225 aspect ratio reduces the distance between the center / hot spot region of the part and the thermally dissipative circuit board material. This permits a high 3W rating and lessens the stress on the solder joint due to the differences in the temperature coefficients of expansion between the ceramic substrate and the thermal mass of the printed circuit board material.

Table 20-1 compares the current measurement methods.

Related Articles

1. Timothy Hegarty, 3D-Integrated MOSFETs with Ultra-Low DCR Inductor Provide High-Efficiency DC/DC Regulator, powerelectronics.com, November 2013.

2. Hong Lei Chen, Protect IGBTs by Sensing Current Using Optical Isolation Amplifiers, powerelectronics.com, April 2012.

3. Jerry Steele, Current Sensing For Server Power Monitoring: MOSFET Or Shunt?, powerelectronics.com, July 2011.

4. Sam Davis, 2-Terminal Current Source Boasts High Accuracy, Programmability and Stability, powerelectronics.com, May 2009.

5. Alfredo H. Saab, Current-Sense Amplifier Doubles as High-CM IA, powerelectronics.com, November 2008.

6. Tom Morris, Current-Sense Resistors Heed Call for More Power, powerelectronics.com, September 2008.

7. Maurizio Gavardoni, Improving High-Side Current Measurements, powerelectronics.com, August 2008.

8. Alfredo H. Saab, Extend Range of Current-Sense Amplifiers, powerelectronics.com, May 2008.

9. Donna Schaefer, Copper Alloy Inductors Stabilize Current Sensing, powerelectronics.com, April 2008.

10. Alfredo H. Saab, Current-Sense Amp Offers Four-Quadrant Operation, powerelectronics.com, February 2008.

CHAPTER 21:

THERMOELECTRIC GENERATORS

A thermoelectric generator, TEG, is a solid-state device that converts heat directly into electrical energy through a phenomenon called the Seebeck effect. Thermoelectric generators consist of three major components: thermoelectric materials, thermoelectric modules, and thermoelectric systems that interface with the heat source.

Thermoelectric materials generate power directly from heat by converting temperature differences into a dc voltage. To be good thermoelectric materials these materials must have both high electrical conductivity and low thermal conductivity. Having low thermal conductivity ensures that when one side is made hot, the other side stays cold, which helps to generate a large voltage while in a temperature gradient.

The typical efficiency of TEGs is around 5% to 8%. Older devices used bimetallic junctions and were bulky. More recent devices use highly doped semiconductors made from bismuth telluride(Bi_2Te_3), lead telluride (PbTe), calcium manganese oxide ($Ca_2Mn_3O_8$), or combinations thereof, depending on temperature. Maximizing the efficiency (or, conversely, the total power output) of requires trade-offs between total heat flow through the thermoelectric modules and maximizing the temperature gradient across them. The design of heat-exchanger technologies to accomplish this is one of the most important aspects of engineering of a thermoelectric generator.

Three semiconductors are known to have both low thermal conductivity and high power factor:

- Low temperature materials (up to around 450K): alloys based on Bismuth (Bi) in combinations with Antimony (Sb), Tellurium (Te), or Selenium (Se).
- Intermediate temperature (up to 850K): such as materials based on alloys of Lead (Pb).
- Highest-temperatures material (up to 1300K): materials fabricated from silicon germanium (SiGe) alloys.

Although these materials still remain the cornerstone for commercial and practical applications in thermoelectric power generation, significant advances have been made in synthesizing new materials and fabricating material structures with improved thermoelectric performance. Recent research has focused on improving the material's figure-of-merit (zT), and hence the conversion efficiency, by reducing the lattice thermal conductivity.

Researchers are trying to develop new thermoelectric materials for power generation by improving the figure-of-merit zT. One example of these materials is the semiconductor compound ß-Zn_4Sb_3, which possesses an exceptionally low thermal conductivity and exhibits a maximum zT of 1.3 at a temperature of 670K. This material is also relatively inexpensive and stable up to this temperature in a vacuum, and can be a good alternative in the temperature range between materials based on Bi_2Te_3 and PbTe.

Besides improving the figure-of-merit, there is increasing focus to develop new materials by increasing the electrical power output, decreasing cost and developing environmentally friendly materials. For example, when the fuel cost is low or almost free, such as in waste-heat recovery, then the cost per watt is only determined by the power per unit area and the operating period. As a result, it has initiated a search for materials with high power output rather than conversion efficiency. For example, the rare earth compound YbAl3 has a low figure-of-merit, but it has a power output of at least double that of any other material, and can operate over the temperature range of a waste-heat source.

Many challenges are confronted when designing a reliable TEG system that operates at high temperatures. Achieving high efficiency in the system requires extensive engineering design in order to balance between the heat flow through the modules and maximizing the temperature gradient across them. To do this, designing heat-exchanger technologies in the system is one of the most important as-

pects of TEG engineering. In addition, the system must minimize the thermal losses due to the interfaces between materials at several places. Another challenging constraint is avoiding large pressure drops between the heating and cooling sources.

When selecting materials for thermoelectric generation, a number of other factors need to be considered. During operation, ideally the thermoelectric generator has a large temperature gradient across it. Thermal expansion will then introduce stress in the device, which may cause fracture of the thermoelectric legs, or separation from the coupling material. The mechanical properties of the materials must be considered and the coefficient of thermal expansion of the n- and p-type material must be matched reasonably well.

21-1. TG8-1.0 Thermoelectric Module from GMZ.

Thermoelectric generators can be applied in a variety of applications. Frequently, thermoelectric generators are used for low-power remote applications or where bulkier but more efficient heat engines such as Stirling engines would not be possible. Unlike heat engines, the solid-state electrical components typically used to perform thermal to electric energy conversion have no moving parts. The thermal to electric energy conversion can be performed using components that require no maintenance, have inherently high reliability, and can be used to construct generators with long service-free lifetimes. This makes thermoelectric generators well suited for equipment with low to modest power needs in remote uninhabited or inaccessible locations such as mountaintops, the vacuum of space, or the deep ocean.

Besides low efficiency and high cost, two general problems exist in such devices: high output resistance and adverse thermal characteristics.

- High output resistance. In order to get a significant output voltage, a very high Seebeck coefficient is needed (high V/°C). A common approach is to place many thermo-elements in series, causing the effective output resistance of a generator to be very high (>10Ω). Thus, power is only efficiently transferred to loads with high resistance; power is otherwise lost across the output resistance. This problem is solved in some commercial devices by putting more elements in parallel and fewer in series.
- Adverse thermal characteristics. Because low thermal conductivity is required for a good thermoelectric generator, this can severely dampen the heat dissipation of such a device (i.e., thermoelectric generators serve as poor heat sinks). They are only economical when a high temperature (>200 °C) can be used and when only small amounts of power (a few watts) are needed.

Most thermoelectric generator module manufacturing companies use many thermoelectric couples that are sandwiched between two pieces of non-electrically conductive materials. It is also necessary for this material to be thermally conductive to ensure a good heat transfer; usually two thin ceramic wafers are used to form what is called a "thermoelectric module."

Each module can contain dozens of pairs of thermoelectric couples called thermoelectric generator modules, TEC modules, and sometimes Peltier or Seebeck modules, which simply denotes whether they are being used to generate electricity (Seebeck) or produce heat or cold (Peltier). Functionally there is no difference between the two. They both are capable of producing heat and cold or generating electricity, depending on whether heat is applied or an electrical current.

There are differences in performance between various modules depending on what they were manufactured for. For example, if a module is being manufactured for use in a 12-volt dc automotive cooler, the thermoelectric couples will be of a thicker gauge and so will the wire connecting the modules to the 12-volt dc power source. In most cases, the module itself is quite large. This is simply because the module will be conducting a heavy load of current and will need to be able to handle the load. Although these type modules can be used to produce electricity, they are not well suited for the task because they have a high internal resistance (lowering output) and lower temperature solder that may melt if used for Seebeck purposes. This means the electrical connection may fail when the higher heat needed to produce significant amounts of electricity is applied to the module.

GMZ-Energy

GMZ-Energy's TG16-1.0 thermoelectric module is capable of producing twice the power of the company's first product, the TG8 (Fig. 21-1). The highly efficient TG16-1.0 directly converts waste heat into usable electricity and is well suited for extremely high-temperature environments, such as those in boilers and furnaces.

By doubling the power density, GMZ's new module substantially increases performance while maintaining a minimal footprint. The TG16-1.0 will augment the TG8, enabling dramatic efficiency improvements and new functionalities in products requiring high power density. Now, with two product offerings, GMZ is capable of providing a solution to even more OEM partners around the world.

GMZ Energy's proprietary platform technology enables low-cost manufacturing of bulk thermoelectric materials. The company's patented nano-structuring process reduces thermal conductivity while maintaining electrical conductivity, enhancing the performance ("figure of merit," zT) by 30% to 60% across multiple classes of thermoelectric materials, including bismuth telluride, lead telluride, skutterudites, silicon germanium, and half-Heusler materials.

The company has recently applied its nano-structuring process to half-Heusler materials, yielding a unique combination of high performance, high strength and low cost. GMZ's proprietary method of bulk manufacturing TE materials of less than 1 micron in size is more cost-effective than known nanowire or thin-film manufacturing methods for temperatures of 550°C to 650°C on the hot side and 100°C on the cold side.

A demonstration of the TEG's ability to convert a vehicle's waste heat into electricity was performed for the Army's TARDEC (Tank Automotive Research, Development and Engineering Center) program. For that program, GMZ Energy successfully demonstrated a 1,000W TEG designed for diesel engine exhaust heat recapture. The company integrated five 200W TEGs into a single 1,000W diesel engine solution that directly converts exhaust waste heat into electrical energy, which increases fuel efficiency and lowers overall costs.

The GMZ TEGs demonstrated continuous output power with no degradation in performance over the test period. To simulate vehicle performance, the unit was tested by connecting directly to the exhaust of a 15-liter V8 diesel engine inside an engine test cell. At approximately 80 liters (2.8 ft^3), GMZ's TEG was less than one-third of the TARDEC program's specified size requirement.

The operating temperature range of a TEG depends on the materials employed. For example, a bismuth-tellurium system is suitable for relatively low temperature operation (room temperature to 200 °C), whereas silicon-germanium alloys work best for high-temperature applications (>800°C). For moderate temperature (T = 500°C to 800°C) heat sources such as a vehicle's exhaust and industrial waste heat, half-Heusler types are the material of choice.

The GMZ TEGs demonstrated continuous output power with no degradation in performance over the test period. To simulate vehicle performance, the unit was tested by connecting directly to the exhaust of a 15-liter V8 diesel engine inside an engine test cell. At approximately 80 liters (2.8 ft^3), GMZ's TEG was less than one-third of the TARDEC program's specified size requirement.

With this demonstration, GMZ successfully reached an important milestone in the $1.5 million vehicle-efficiency program sponsored by TARDEC and administered by the U.S. Department of Energy (DOE). With battlefield fuel costs ranging from $40 to $800 per gallon, the U.S. military is especially interested in thermoelectric technologies, which are physically robust, have long service lives, and require no maintenance due to their solid-state design.

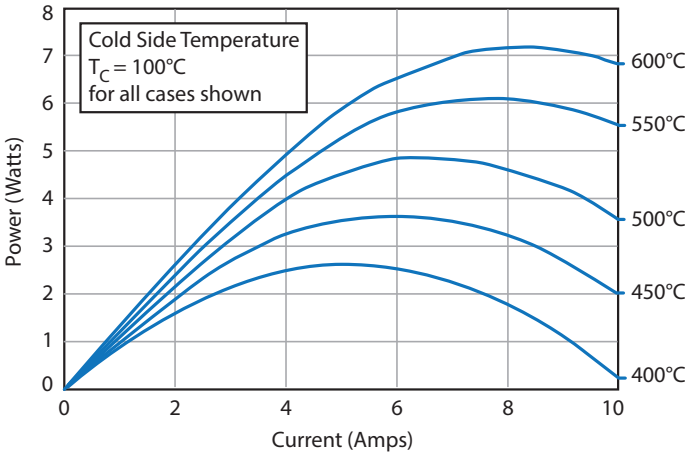

21-2. TG8-1.0 power output as a function of temperature and output current.

GMZ's patented half-Heusler material is uniquely well suited for military applications. The 1000W TEG features enhanced mechanical integrity and high-temperature stability thanks to a patented nano-structuring approach. GMZ's TEG also enables silent generation, muffles engine noise, and reduces thermal structure. Half-Heusler is environmentally friendly and mechanically and thermally robust, although cost may be an eventual issue.

The TARDEC TEG incorporates GMZ's TG8-1.0 modules, which are the first commercially available modules capable of delivering power densities greater than one Watt/cm^2 while operating at 600°C. Fig. 21-2 shows the power output of a TG8-1.0 module as a function of current and temperature. The TARDEC 1000W TEG consists of 400 TG8-1.0 modules with associated cold-side and hot-side heat exchangers and manifolds. GMZ did the engineering and CFD simulation to project performance. The technology's uniqueness is its ability to operate at high-temperature gradients (high ΔT), which allows the extraction of more power per unit area of the TEG modules.

The next phase of this program will be testing in a Bradley Fighting Vehicle. Besides saving money and adding silent-power functionality for the U.S. military, this TEG can increase fuel efficiency for most gasoline and diesel engines. This low-cost TEG technology fits into a broad array of commercial markets, including long-haul trucking, heavy equipment, and light automotive.

Due to the high currents involved, GMZ usually employs series connections to maximize voltage and minimize current as much as possible as well as to minimize I^2R losses. Because diesel exhaust is less than 600°C and the module

hot-side temperature is even lower than the flow temperature, the modules do not give their full power output the way they do in other applications. However, even with the derating to account for the lower hot-side temperature, the economics of incorporating these systems is very compelling with payback times typically less than 12 to 24 months.

A high ΔT capability can result in higher efficiency in some cases. However, what really matters is the $/Watt. When the input energy is free, the cost of the output energy is driven entirely by the cost of the generator. GMZ designed the system to minimize the $/W in order to maximize their utility to the largest possible set of prospective users. Because any thermoelectric material generates more power with higher ΔT, GMZ focused on half-Heusler material systems, which have very high temperature capability. GMZ modules are rated for 600°C continuous hot-side capability with 700°C intermittent. This maximizes power per device, which minimizes the $/W. In volume production, GMZ expects its TEG systems to be below $1/W.

GMZ Energy's proprietary platform technology enables low-cost manufacturing of bulk thermoelectric materials. The company's nano-structuring process reduces thermal conductivity while maintaining electrical conductivity, enhancing the performance (figure of merit, zT) by 30% to 60% across multiple classes of thermoelectric materials, including bismuth telluride, lead telluride, skutterudites, silicon germanium, and half-Heusler materials.

Compared to thin-film and nanowire materials, GMZ's nano-structured bulk materials have superior mechanical integrity and high-temperature (20°C-800°C) thermal stability. GMZ's TEG materials and processes also allow direct bonding to interconnect without the need for metallization, which lowers costs and increases module durability and life cycle. This enables the module to provide consistent energy over long-term cycling, even in the most challenging environments.

The 1000W TEG is composed of 400 TG8 modules with associated cold-side and hot-side heat exchangers and manifolds. GMZ did the engineering and CFD simulation to project the performance. GMZ's uniqueness is its ability to operate at high-temperature gradients (high ΔT), which allows the extraction of more power unit area of its TE modules.

The 1000W test unit included 400 modules. In general, GMZ tries to do series connections (maximize voltage and minimize current) as much as possible in order to minimize I^2R losses due to the high currents involved. Because diesel exhaust is less than 600°C and the module hot-side temperature is even lower than the flow temperature, the modules do not give their full power output the way they do in applications like self-powered boilers. However, even with the derating to account for the lower hot-side temperature, the economics of incorporating these systems is very compelling with payback times typically less than 12 to 24 months.

High ΔT capability of the TG8-1.0 can result in higher efficiency in some cases. However, what really matters is the $/Watt. When the input energy is free, the cost of the output energy is driven entirely by the cost of the generator. The system is designed to minimize the $/W in order to maximize the largest possible set of prospective users. Because any thermoelectric material generates more power with higher ΔT, GMZ has focused on half-Heusler material systems that have very high temperature capability. Modules are rated for 600°C continuous hot-side capability with 700°C intermittent. This maximizes the power per device and minimizes $/W. In volume production, GMZ expects to sell its TEG systems at or below $1/W.

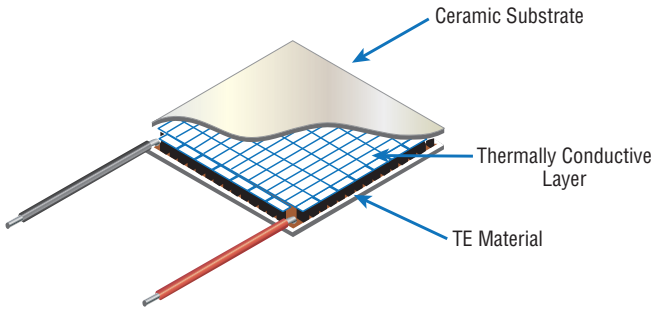

21-3. Laird's PCS series of thermoelectric modules are intended for thermal cycling applications.

Test and Measurement

In certain applications, thermoelectric modules (TEMs) are typically used to achieve the rapid temperature changes. The advantages of thermoelectric modules over other types of thermal cycling devices are precise temperature control, compactness, faster temperature ramp rates, and efficiency.

The PC Series TEMs from Laird are proven to perform for more than 800,000 temperature cycles and can operate in temperatures up to 120°C. This exceeds the requirements for certain applications and provides a lower total cost of ownership.

These TEMs are constructed with multiple layers between the ceramic substrates, copper buss bars, and semiconductor couples (Fig. 21-3). To reduce thermally induced stress, a flexible and thermally conductive "soft layer" is inserted between the cold-side ceramic substrate and copper buss bars. The integration of the polymer into the thermoelectric modules absorbs the mechanically induced stresses caused by rapid temperature cycling. As a result, the stress induced on the semiconductor couples and solder joints is significantly reduced, extending the overall operational life of TEM.

Thermal cycling exposes TEMs to mechanical stresses as the module contracts and expands from repeated cooling and heating cycles. The high-temperature diffusion of impurities and mechanical stresses over time significantly reduces the operational life of a standard TEM. The PC Series is designed to handle hundreds of thousands of thermal cycles with minimal degradation.

Among its features:

- Designed to pass rigorous testing
- Robust construction developed for thermal cycling applications
- 800K+ thermal-cycle operating life
- Superior temperature control stability
- RoHS compliant

Related Articles

1. PET, High-Power-Thermoelectric-Module, powerelectronics.com, December 2014.
2. PET, Harvesting Unused Energy with Flat Thermoelectrics, powerelectronics.com, January 2013.
3. PET, Outdoor Thermoelectric Cooler Series, powerelectronics.com, March 2013.
4. PET, Thin-Film Thermoelectric Modules, powerelectronics.com, February 2013.
5. PET, Thermoelectric Power Generators for Energy Harvesting, powerelectronics.com, February 2013.
6. PET, Thin Film Thermoelectric Module Product Line, powerelectronics.com, February 2013.
7. PET, High Performance Air-To-Air Thermoelectric Assembly, powerelectronics.com, June 2012.
8. PET, Thermoelectric Tester, powerelectronics.com, January 2013.
9. PET, Mismatched alloys could lead to better thermoelectric generators, PV, powerelectronics.com, September, 2010
10. PET, Thermoelectrics Target Hot CPUs: Are Power Semis Next?, powerelectronics.com, December 2002.

☞ **BACK TO TABLE OF CONTENTS**

CHAPTER 22:

FUEL CELLS

Fuel cells convert the chemical energy from a fuel into electricity through a chemical reaction of positively charged hydrogen ions with oxygen or another oxidizing agent. They differ from batteries because they require a continuous source of fuel and oxygen or air to sustain the chemical reaction. Fuel cells produce electricity continuously as long as these inputs are supplied. In a battery, the chemicals present in the battery react with each other to generate a voltage. They are used for primary and backup power for commercial, industrial, and residential buildings and in remote or inaccessible areas. They can also be used to power vehicles, including forklifts, automobiles, buses, boats, motorcycles, and submarines.

All fuel cells consist of an anode, cathode, and electrolyte that allows positively charged hydrogen ions (or protons) to move between the two sides of the fuel cell. The anode and cathode contain catalysts that cause the fuel to undergo oxidation reactions that generate positively charged hydrogen ions and electrons. The hydrogen ions are drawn through the electrolyte after the reaction. At the same time, electrons are drawn from the anode to the cathode through an external circuit, producing direct current electricity. At the cathode, hydrogen ions, electrons, and oxygen react to form water.

Individual fuel cells produce relatively small electrical potentials, about 0.7 V, so cells are "stacked," or placed in series, to create sufficient voltage to meet an application's requirements. Besides electricity, fuel cells produce water, heat, and, depending on the fuel source, very small amounts of nitrogen dioxide and other emissions. The energy efficiency of a fuel cell is generally between 40% to 60%, or up to 85% efficient in cogeneration if waste heat is captured for use. The most widely used types are:

- Proton Exchange Membrane Fuel Cells (PEMFC)
- Solid Oxide Fuel Cells (SOFC)

Fuel-Cell Applications

Automobiles—As of 2015, two fuel-cell vehicles have been introduced for commercial lease and sale in limited quantities: the Toyota Mirai and the Hyundai ix35 FCEV. Additional demonstration models include the Honda FCX Clarity and Mercedes-Benz F-Cell. General Motors and its partners estimated that per mile traveled, a fuel-cell electric vehicle running on compressed gaseous hydrogen produced from natural gas could use about 40% less energy and emit 45% less greenhouse gases than an internal combustion vehicle. A lead engineer from the Department of Energy whose team is testing fuel-cell cars said in 2011 that the potential appeal is that "these are full-function vehicles with no limitations on range or refueling rate so they are a direct replacement for any vehicle."

Forklifts—Fuel-cell forklifts lift and transport materials. In 2013, there were over 4,000 fuel-cell forklifts used in material handling in the United States. Most companies in Europe and the U.S. do not use petroleum-powered forklifts, as these vehicles work indoors where emissions must be controlled and instead use electric forklifts. Fuel-cell-powered forklifts can provide benefits over battery-powered forklifts as they can work for a full eight-hour shift on a single tank of hydrogen and can be refueled in three minutes. Fuel-cell-powered forklifts can be used in refrigerated warehouses, because lower temperatures do not degrade their performance.

Motorcycles and bicycles—In 2005, a British manufacturer of hydrogen-powered fuel cells, Intelligent Energy (IE), produced the first working hydrogen-run motorcycle called the ENV (Emission Neutral Vehicle). The motorcycle holds enough fuel to run for four hours, and to travel 160 km (100 mi) in an urban area, at a top speed of 80 km/h (50 mph).

Airplanes—Boeing researchers and industry partners throughout Europe conducted experimental flight tests in February 2008 of a manned airplane powered only by a fuel cell and lightweight batteries. The fuel-cell demonstrator airplane, as it was called, used a (PEM) fuel-cell/lithium-ion battery hybrid system to power an electric motor, which was coupled to a conventional propeller. In 2003, the world's first propeller-driven airplane to be powered entirely

by a fuel cell was flown. The fuel cell was a stack design that allowed it to be integrated with the plane's aerodynamic surfaces.

UAVs—A Horizon fuel-cell UAV set the record distance flown for a small UAV in 2007. The military is interested in this application because of its low noise, low thermal signature, and ability to attain high altitude. In 2009, the Naval Research Laboratory's (NRL's) Ion Tiger utilized a hydrogen-powered fuel cell and flew for 23 hours and 17 minutes. Fuel cells are also in use to provide auxiliary power in aircraft, replacing fossil-fuel generators that were previously used to start the engines and power on-board electrical needs.

Boats—The HYDRA fuel-cell boat used an AFC system with 6.5 kW net output. Iceland committed to converting its vast fishing fleet to use fuel cells to provide auxiliary power and, eventually, to provide primary power in its boats. Amsterdam recently introduced its first fuel-cell-powered boat that ferries people around the city's canals.

Submarines—German and Italian submarines use fuel cells to remain submerged for weeks without the need to surface. The U212A is a non-nuclear submarine developed by German naval shipyard Howaldtswerke Deutsche Werft. The system consists of nine PEM fuel cells, providing between 30 kW and 50 kW each. The ship is silent, giving it an advantage in the detection of other submarines.

Portable Power Systems—Fuel cells can be used in the leisure sector (i.e., RVs, cabins, marine), the industrial sector (i.e., power for remote locations including gas/oil wellsites, communication towers, security, weather stations), and in the military sector. SFC Energy is a German manufacturer of direct methanol fuel cells for a variety of portable power systems. Ensol Systems Inc. is an integrator of portable power systems, using the SFC Energy DMFC.

The most important design features in a fuel cell are

- The electrolyte substance. The electrolyte substance usually defines the type of fuel cell.
- The fuel that is used. The most common fuel is hydrogen.
- The anode catalyst breaks down the fuel into electrons and ions. The anode catalyst is usually made up of very fine platinum powder.
- The cathode catalyst turns the ions into waste chemicals like water or carbon dioxide. The cathode catalyst is often made up of nickel, but it can also be a nanomaterial-based catalyst.

A typical fuel cell produces a voltage from 0.6 V to 0.7 V at full-rated load. Voltage decreases as current increases, due to several factors:

- Activation loss.
- Ohmic loss (voltage drop due to resistance of the cell components and interconnections).
- Mass transport loss (depletion of reactants at catalyst sites under high loads, causing rapid loss of voltage).

To deliver the desired amount of energy, the fuel cells can be combined in series to yield higher voltage, and in parallel to allow a higher current to be supplied. Such a design is called a "fuel-cell stack." The cell surface area can also be increased, to allow higher current from each cell. Within the stack, reactant gases must be distributed uniformly over each of the cells to maximize the power output.

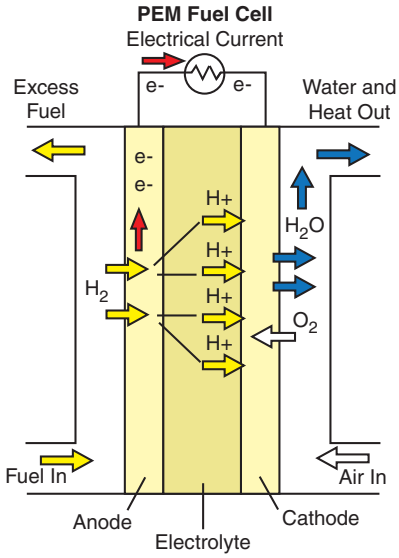

22-1. Proton exchange membrane fuel cell

Proton Exchange Membrane Fuel Cells (PEMFCs)

In the archetypical hydrogen-oxide proton-exchange membrane fuel-cell design, a proton-conducting polymer membrane contains the electrolyte solution that separates the anode and cathode sides (Fig. 22-1).

On the anode side, hydrogen diffuses to the anode catalyst where it later dissociates into protons and electrons. These protons often react with oxidants, causing them to become what are commonly referred to as multi-facilitated proton membranes. The protons are conducted through the membrane to the cathode, but the electrons are forced to travel in an external circuit (supplying power) because the membrane is electrically insulating. On the cathode catalyst, oxygen molecules react with the electrons (which have traveled through the external circuit) and protons to form water.

The materials used for different parts of the fuel cells differ by type. The bipolar plates may be made of different types of materials, such as, metal, coated metal, graphite, flexible graphite, C–C composite, carbon–polymer composites, etc. The membrane electrode assembly (MEA) is referred as the heart of the PEMFC and is usually made of a proton exchange membrane sandwiched between two catalyst-coated carbon papers. Platinum and/or similar type of noble metals are usually used as the catalyst for PEMFC. The electrolyte could be a polymer membrane.

Phosphoric Acid Fuel Cell (PAFC)

In these cells, phosphoric acid is used as a non-con-

ductive electrolyte to pass positive hydrogen ions from the anode to the cathode. These cells commonly work in temperatures of 150°C o 200°C. This high temperature will cause heat and energy loss if the heat is not removed and used properly. This heat can be used to produce steam for air-conditioning systems or any other thermal energy-consuming system. Using this heat in cogeneration can enhance the efficiency of phosphoric acid fuel cells from 40% to 50% up to about 80%. Phosphoric acid, the electrolyte used in PAFCs, is a non-conductive liquid acid that forces electrons to travel from anode to cathode through an external electrical circuit. Since the hydrogen ion production rate on the anode is small, platinum is used as a catalyst to increase this ionization rate. A key disadvantage of these cells is the use of an acidic electrolyte. This increases the corrosion or oxidation of components exposed to phosphoric acid.

Solid Oxide Fuel Cells

Solid oxide fuel cells (SOFCs) use a solid material, most commonly a ceramic material called yttria-stabilized zirconia (YSZ), as the electrolyte (Fig. 22-2). Because SOFCs are made entirely of solid materials, they are not limited to the flat-plane configuration of other types of fuel cells and are often designed as rolled tubes. They require high operating temperatures (800°C-1,000°C) and can be run on a variety of fuels including natural gas.

SOFCs are unique in that negatively charged oxygen ions travel from the cathode (positive side of the fuel cell) to the anode (negative side of the fuel cell) instead of positively charged hydrogen ions traveling from the anode to the cathode, as is the case in all other types of fuel cells. Oxygen gas is fed through the cathode, where it absorbs electrons to create oxygen ions. The oxygen ions then travel through the electrolyte to react with hydrogen gas at the anode. The reaction at the anode produces electricity and water as byproducts. Carbon dioxide may also be a byproduct depending on the fuel, but the carbon emissions from an SOFC system are less than those from a fossil-fuel combustion plant.

SOFC systems can run on fuels other than pure hydrogen gas. However, since hydrogen is necessary for the reactions listed above, the fuel selected must contain hydrogen atoms. For the fuel cell to operate, the fuel must be converted into pure hydrogen gas. SOFCs are capable of internally reforming light hydrocarbons such as methane (natural gas), propane, and butane. These fuel cells are at an early stage of development.

Challenges exist in SOFC systems due to their high operating temperatures. One such challenge is the potential for carbon dust to build up on the anode, which slows down the internal reforming process. Research to address

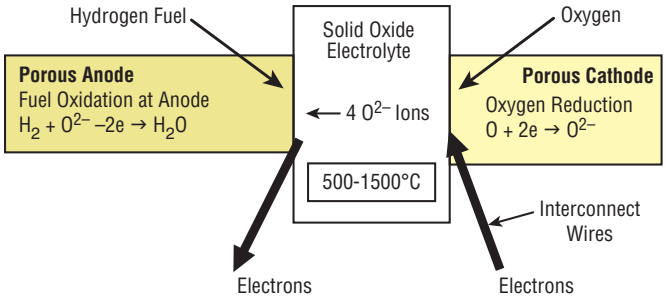

22-2. Solid oxide fuel cell.

this "carbon coking" issue at the University of Pennsylvania has shown that the use of copper-based cermet (heat-resistant materials made of ceramic and metal) can reduce coking and the loss of performance. Another disadvantage of SOFC systems is slow startup time, making SOFCs less useful for mobile applications. Despite these disadvantages, a high operating temperature provides an advantage by removing the need for a precious metal catalyst like platinum, thereby reducing cost. Additionally, waste heat from SOFC systems may be captured and reused, increasing the theoretical overall efficiency to as high as 80% to 85%.

The high operating temperature is largely due to the physical properties of the YSZ electrolyte. As temperature decreases, so does the ionic conductivity of YSZ. Therefore, to obtain optimum performance of the fuel cell, a high operating temperature is required. According to its website, Ceres Power, a UK-based SOFC fuel-cell manufacturer, has developed a method of reducing the operating temperature of their SOFC system to 500°C to 600°C. They replaced the commonly used YSZ electrolyte with a CGO (cerium gadolinium oxide) electrolyte. The lower operating temperature allows Ceres Power to use stainless steel instead of ceramic as the cell substrate, which reduces cost and startup time of the system.

Theoretical Maximum Efficiency

The energy efficiency of a system or device that converts energy is measured by the ratio of the amount of useful energy put out by the system (output energy) to the total amount of energy that is put in (input energy) or by useful output energy as a percentage of the total input energy. In the case of fuel cells, useful output energy is measured in electrical energy produced by the system. Input energy is the energy stored in the fuel. According to the U.S. Department of Energy, fuel cells are generally between 40% to 60% energy-efficient. This is higher than some other systems for energy generation. For example, the typical internal combustion engine of a car is about 25% energy-efficient. In combined heat and power (CHP) systems, the heat produced by the fuel cell is captured and put to use, increasing the efficiency of the system to up to

85%–90%.

The theoretical maximum efficiency of any type of power generation system is never reached in practice, and it does not consider other steps in power generation, such as production, transportation, and storage of fuel and conversion of the electricity into mechanical power. However, this calculation allows the comparison of different types of power generation. The maximum theoretical energy efficiency of a fuel cell is 83%, operating at low power density and using pure hydrogen and oxygen as reactants (assuming no heat recapture). According to the World Energy Council, this compares with a maximum theoretical efficiency of 58% for internal combustion engines. While these efficiencies are not approached in most real-world applications, high-temperature fuel cells (solid oxide fuel cells or molten carbonate fuel cells) can theoretically be combined with gas turbines to allow stationary fuel cells to come closer to the theoretical limit. A gas turbine would capture heat from the fuel cell and turn it into mechanical energy to increase the fuel cell's operational efficiency. This solution has been predicted to increase total efficiency to as much as 80%.

Solid-oxide fuel cells produce exothermic heat from the recombination of the oxygen and hydrogen. The ceramic can run as hot as 800°C. This heat can be captured and used to heat water in a micro combined heat and power (m-CHP) application. When the heat is captured, total efficiency can reach 80% to 90% at the unit, but does not consider production and distribution losses. CHP units are being developed today for the European home market.

Power

Stationary fuel cells are used for commercial, industrial, and residential primary and backup power generation. Fuel cells are very useful as power sources in remote locations, such as spacecraft, remote weather stations, large parks, communications centers, rural locations including research stations, and in certain military applications. A fuel-cell system running on hydrogen can be compact and lightweight, and has no major moving parts. Because fuel cells have no moving parts and do not involve combustion, in ideal conditions they can achieve up to 99.9999% reliability. This equates to less than one minute of downtime in a six-year period.

Since fuel-cell electrolyzer systems do not store fuel in themselves, but rather rely on external storage units, they can be successfully applied in large-scale energy storage, rural areas being one example. There are many different types of stationary fuel cells so efficiencies vary, but most are between 40% and 60% energy-efficient. However, when the fuel cell's waste heat is used to heat a building in a cogeneration system, this efficiency can increase to 85%. This is significantly more efficient than traditional coal power plants, which are only about one third energy-efficient. Assuming production at scale, fuel cells could save 20% to 40% on energy costs when used in cogeneration systems. Fuel cells are also much cleaner than traditional power generation; a fuel-cell power plant using natural gas as a hydrogen source would create less than one ounce of pollution (other than CO2) for every 1,000 kW·h produced, compared to 25 pounds of pollutants generated by conventional combustion systems. Fuel cells also produce 97% less nitrogen oxide emissions than conventional coal-fired power plants.

Steel Cell

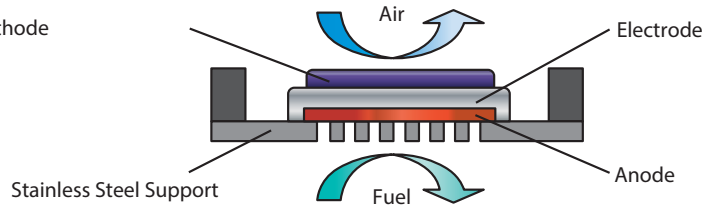

22-3. Ceres Steel Cell combines unique technology, durable low-cost materials, and existing manufacturing processes.

Ceres Power Holdings Plc's steel-cell technology uses the existing infrastructure of natural gas mains and is manufactured using commodity materials such as steel and standard processes already used in the photovoltaic industry, meaning that it can be mass produced at an affordable price for domestic, business, and other applications in multiple markets.

The patented Ceres steel cell (Fig. 22-3) is a combination of unique technology, durable low-cost materials, and existing manufacturing processes. The steel cell is unique because it operates at temperatures of 500° C to 600°C, allowing use of low-cost steel and abundant ceramics with cost-effective mass manufacturing, at the same time as delivering high performance.

The steel cell is made by screen printing layers of ceramic ink onto a drilled sheet of steel. Achieving these high-quality ceramic layers at low temperature on steel is protected through extensive registered intellectual property and know-how. Exclusive to Ceres is the use of Ceria in the anode and electrolyte. Ceria is as abundant as copper and is used industrially for dyeing glass, self-cleaning ovens, and catalytic converters in cars. Steel needs no introduction as the backbone of modern life, used in 75% of household applications.

This steel-cell technique is a very efficient way of generating power from gas and can use the existing gas

22-4. The Ballard Power Systems FCgen-1020ACS has no moving parts and high efficiency, producing clean dc power with a low thermal and acoustic signature.

infrastructure. Overall efficiency of fossil-fuel use can be improved from around 35% to 40% up to 80% to 90%. This means that regular users could reduce the carbon footprint of their home by 30% and even more for the modern always-on business. The combination of these factors makes the steel cell an efficient, cost-effective, and cleaner way of giving people control over their energy supply.

A fuel cell is the most efficient way of converting fuel energy into electricity. It doesn't matter whether the fuel is natural gas or hydrogen. Fuel cells convert fuel and air directly into power and heat in a chemical reaction. This makes the process efficient, reliable, and quiet.

Fuel passes over the anode side and air passes over the cathode. Sandwiched between the anode and cathode is the very thin electrolyte layer. An external circuit connects the anode to the cathode and provides the mechanism to take power from the fuel cell to power electrical devices.

A single cell can power a low-energy light bulb. Approximately 100 cells are combined to create a stack. One stack could supply up to 90% of a home's electricity needs and all of its hot water. The steel cell is completely scalable; 200 stacks can supply a large office, apartment block, or supermarket.

FCgen-1020ACS

Ballard Power Systems offers an air-cooled, scalable proton exchange membrane fuel-cell stack suitable for a wide range of light-duty applications where durability, reliability, and a simplified balance of plant are key requirements.

The FCgen-1020ACS fuel cell (Fig. 22-4) has been engineered to incorporate advanced open cathode technology and state of the art self-humidifying membrane electrode assemblies. These features completely eliminate the need for humidification systems and simplify system integration. The result is a simple, low-cost design delivering reliable operation over a wide range of challenging conditions.

With no moving parts and high efficiency, the FCgen-1020ACS produces clean dc power with a low thermal and acoustic signature. The FCgen–1020ACS stack can be scaled to meet power requirements from 450W to 3kW and integrated into various end-user applications. The FCgen-1020ACS fuel-cell product is available in a number of cell-configuration options.

Delphi Solid Oxide Fuel-Cell StackEL CELLS

Delphi's Solid Oxide Fuel Cell (SOFC) technology is commercially ready for a wide range of high-volume stationary power-generation and transportation-industry applications. Delphi's innovative fuel cell is robust, fuel-flexible, and highly efficient (Fig. 22-5). A single Delphi Gen 4 SOFC Stack can provide 9 kW of electrical power and it features a modular design, ideal for integration into large power plants.

Delphi has developed two stack sizes that can be implemented into a stationary or transportation application. They provide increased efficiency and reliability while decreasing emissions when compared to conventional technology. Delphi's low-cost solid oxide fuel-cell stacks are designed for high-volume manufacturing. Processes are developed and critical suppliers have been identified for all components.

Delphi's fuel-cell technology can operate with natural gas, hydrogen, gasoline, diesel fuel, bio fuels, or other hydrocarbon fuels. The fuel is converted directly to electrical energy without thermal-mechanical conversion. Therefore, potential efficiency is not limited by the Carnot Cycle and

22-5. Delphi's two stack sizes can be implemented into a stationary or transportation application. Compared to conventional technology, they provide increased efficiency and reliability while decreasing emissions.

the fuel cell can achieve higher efficiency than internal combustion engines and other conventional power sources. Additional benefits to the fuel-cell technology are the reduction in operating noise and a low level of emissions.

Among other benefits:

- High quality, reliable power:
- Delphi Gen 4 Stack produces up to 9 kW
- Delphi Gen 3 Stack produces 1.5 kW
- Optimum cell sizes (active area) for a range of packaging requirements
- 403}cm^3 with the Delphi Gen 4 Stack
- 105cm^3 with the Delphi Gen 3 Stack
- Power density at 500mW/cm^2
- Stable cell performance
- Equivalent of 40,000 hours of operation
- Delphi has produced more than 30,000 fuel cells
- Thermal Cycle Capability is >200
- High mechanical robustness, achieving the equivalent of 3 million miles in a vibration test schedule.

Related Articles

1. Sam Davis, Book Review: High Temperature Solid Oxide Fuel Cells for the 21st Century (2nd Edition), powerelectronics.com, January 2016.

2. Peter Podesser, Fuel-Cell/Battery Hybrid is a Leaner Portable Power Solution, powerelectronics.com, October 2009.

3. Sam Davis, Getting Fuel-Cells from Concept Cars to Showrooms, powerelectronics.com, March 2014.

4. Sam Davis, Potential Future of Electricity Generation, powerelectronics.com, September 2013.

5. Mark Valentine, PEM Fuel Cells Emerge from Niche Markets, powerelectronics.com, May 2006.

6. Jonathan W. Kimball, Power Converters for Micro Fuel Cells, powerelectronics.com, October 2004.

7. Gregg Makuch, Micro Fuel Cells Strive for Commercialization, powerelectronics.com, February 2004.

8. Ashok Bindra, Can Micro Fuel Cells Supplant Batteries?, powerelectronics.com, October 2003.

BACK TO TABLE OF CONTENTS

CHAPTER 23:

POWER MANAGEMENT OF TRANSPORTATION SYSTEMS

Power management plays a vital role in transportation systems that travel on land, air, and sea. Regardless of the particular application or technology, power management regulates, controls, and distributes power throughout that system.

Land transportation includes the automotive industry, whose requirements are specific and different from most industrial and commercial applications. Some of these power-management requirements are similar to the general requirements for power supplies, whereas some are exclusive to the automotive industry: reverse polarity protection, load dump, alternator overvoltage, peak current, water resistance, and vibration. The main issues for electronic equipment in the automotive industry are:

- Cost
- Reliability
- Electromagnetic compatibility (EMC).

The requirements for the automotive industry are much closer to military requirements, but the cost must be significantly lower. List 23-1 lists the main requirement and conditions of electronic equipment for the automotive industry.

Semiconductors

At the heart of an automotive power converter are the power semiconductors. Clearly, the main types of power semiconductors used in the automotive industry are MOSFETs, IGBTs, and bipolar transistors. For automotive applications, it is preferable to use semiconductors with a gate threshold voltage of 2-4V or higher. With a lower gate threshold, semiconductor reliability will be reduced or the cost of the gate drive will increase significantly. Consider semiconductors with logic level threshold or GaN type devices, although GaN has the additional penalty of higher cost. For low voltage, below 200V, obviously a MOSFET is straightforward to use. For high voltage, there is a choice: MOSFETs, IGBTs, bipolar transistors, or a combination thereof.

During the last 15 years the EMI requirements for electronic units for automotive applications has become more stringent, from CISPR25 class 2 to class 4. The main reason is the demand for compatibility. A contemporary vehicle has many electronics units on board and the tendency is for these numbers to grow. Each unit needs to operate without interfering with other units on the vehicle. The next point about EMI is the slew rate of voltage. This slew rate shouldn't be higher than 2500V/µS, and it's better when it is 1500V/µS or less. In this case, EMI will be reduced, reliability will be increased, and the cost of the EMI filter itself and shielding will be reduced.

Troubleshooting is included in the cost of the product. If the product is more reliable, it results in a cost reduction of the product for the customer. In the automotive industry, this requirement is much stronger because of the price of troubleshooting is much higher than in the industrial and commercial markets. That's why more reliable design is preferable.

List 23-1. Requirements and Conditions for Automotive Electronic Equipment

1. *Sources: battery and alternator*
2. *Load dump overvoltage from alternator*
3. *Reverse polarity protection*
4. *Jump-start stresses*
5. *High efficiency under light load and low consumption at idle and key off*

23-1. Tesla predicts that its Roadster 3.0 will have a 400-mile driving range.

6. Peak currents up to 2900A at 12V
7. Overvoltage spikes to 800V
8. Electromagnetic compatibility
9. CAN-bus communication capability
10. Life time, reliability
11. Mechanical challenges:
Water resistance and vibration
12. Operational temperature -40°C to +110°C
13. Development cycle-time pressures

Roadster Strives for 400-Mile Range

EV pioneer Tesla Motors will employ several improvements that could achieve a 40% to 50% improvement on range between the original Roadster and the new Roadster 3.0 (Fig. 23-1). There is a set of speeds and driving conditions where the company is confident it can drive the Roadster 3.0 over 400 miles on a single charge.

The company notes that battery technology has had continued steady improvement in recent years, as it has also had in optimizing total vehicle efficiency through Model S development. The company has wanted to apply the experience gained from its first vehicle, and are going to do that with the prototype Roadster 3.0 package. It consists of three main improvement areas.

The original Roadster battery was the very first lithium ion battery put into production in any vehicle. It was state of the art in 2008, but cell technology has improved substantially since then. It has identified a new cell that has 31% more energy than the original Roadster cell. Using this new cell, it has created a battery pack that delivers roughly 70kWh in the same package as the original battery.

Aerodynamics

The original Roadster had a drag coefficient (Cd) of 0.36. Using modern computational methods it expects to make a 15% improvement, dropping the total Cd down to 0.31 with a retrofit aero kit.

The original Roadster tires have a rolling resistance coefficient (Crr) of 11.0 kg/ton. New tires for the Roadster 3.0 have a Crr of roughly 8.9 kg/ton, about a 20% improvement. It is also making improvements in the wheel bearings and residual brake drag that further reduce overall rolling resistance of the car.

Appointments for upgrading Roadsters will be taken this spring once the new battery pack finishes safety validation. Tesla is confident that this will not be the last update the Roadster will receive in the many years to come.

In addition, CEO Elon Musk said, “We are actually working on a charger that automatically moves out from the wall and connects like a solid metal snake. This can be used with all existing Model S cars, not just future ones.”

Last year, Tesla produced more than 22,000 cars; this year it is on track to build about 35,000. By the end of 2015, it will have increased production by another 50%. With Model X on the horizon, Dual Motor Model S now in production, and increasing global demand, the company decided to temporarily pause production in order to increase capacity at the Tesla Factory in Fremont, Calif.

During the pause in production, the company:

- Upgraded the assembly line
- Added capacity to the body shop
- Enhanced powertrain assembly
- Revamped facilities for its employees.

The result of this retooling phase, which complemented ongoing upgrade work, is a much-expanded operation that allows the company to produce more cars, faster, while increasing automation and providing a more inviting work environment.

Musk said that the most dramatic changes are to be found in general assembly, where Tesla eliminated a lot of overhead steel and mechanical structures in favor of advanced robots that can lift and maneuver entire cars with optimum precision while taking up less room. Soon, these new robots will even be able to install battery packs in the cars, relieving humans of the most labor-intensive operation in the factory and reducing installation time from four to two minutes.

Alongside the robots, Tesla created a more efficient floor plan with significantly more automation. In addition, the cars now move down the assembly line as associates work on them, enabling a streamlined and more consistent workflow. The line is now running at about 1,000 cars a week with the potential for significantly more with minor adjustments.

In the powertrain department, Tesla added conveyors and advanced robots that have given them the capacity to process 1 million battery cells per day, up from 800,000. In body-in-white, they’ve added new welding equipment and improved production uptime by 5% to 10%, thanks in part to a 13-car buffer that guards against bottlenecks. Also added are 24 new tire and export docks to the perimeter of

23-2. An autonomous Volvo lets the "driver" relax.

the main building, increasing the speed with which it can deliver cars overseas.

As well as making the plant brighter by installing skylights, replacing fluorescent lights with energy-saving LED lamps, and painting previously gray walls and floors a bright white, they've added a few novel touches. For instance, they wrapped several pillars with climbing plants to add some greenery to the surroundings. They had a comic artist depict the manufacturing process in a series of illustrations, which were printed on the glass walls enclosing some of the robots. And they've added a wall of framed photos showing the factory building in different guises over its 54-year existence.

Sit Back and Enjoy the Ride …. to Work

At the 2016 Consumer Electronics Show (CES), Volvo revealed that it is developing intelligent, high-bandwidth streaming capabilities with its technology partner, Ericsson, that will ensure drivers and passengers get the most out of their time traveling in an autonomous Volvo (Fig. 23-2). Power management is an important design consideration for autonomous cars because of the different voltages necessary for sensors and mechanical controls.

Volvo recently unveiled its design vision for fully autonomous cars with Concept 26. Now it is actively working on future solutions to deliver the best user experience in fully autonomous mode. Imagine a highway full of autonomous cars with their occupants sitting back watching their favorite TV shows in high definition. "This new way of commuting will demand new technology, and a much broader bandwidth to ensure a smooth and enjoyable experience," said Anders Tylman, general manager, Volvo Monitoring & Concept Center at Volvo Car Group.

Volvo Cars' ongoing research into autonomous driving has confirmed what we all know—that the daily commute is taking the joy out of driving. It is during the commute and on long-haul motorway trips that people are most willing to delegate the act of driving to their car.

With this in mind, Volvo has developed Concept 26, named to reflect the average daily commute to work of 26 minutes—time that could be spent doing something more meaningful than sitting in stop-and-go traffic. Volvo has set out to bring choice and freedom back to the driver; to enjoy the driving experience when they want to, or to delegate driving to the car when they want to do something else.

By learning the most common routes and times of travel and understanding media preferences, future Volvo cars will be able to provide one-click navigation and a customized preference based list of potential media—allowing customers to choose routes and select content tailored to the amount of autonomous time that is available during their commute.

"With our future autonomous drive technology, we will provide people with the freedom to choose the way they would like to commute and the content they would like to experience," said Tylman.

Drive, Create, Relax

"It's all about people," said Robin Page, vice president of Interior Design at Volvo Cars.

"Our research clearly shows that some people will want to use their commuting time creatively when they have full autonomous drive available, while others will want to just sit back and relax, watch online media, or listen to music. Autonomous drive will make all of this possible. This is what Concept 26 has captured by reimagining the entire car experience."

Concept 26 is based around an all-new patented seat design that actively cradles the driver during the transformation phase into one of the three modes: Drive, Create or Relax. With these three modes, the concept creates a new autonomous drive innovation platform that can adapt to new needs and technologies over time.

When the driver wishes to delegate driving to the car the steering wheel retracts, the seat reclines, and a large display emerges from the dashboard, allowing the driver to enjoy the time spent in the car as they like. Concept 26 embraces the need for radical change of the basic design of car interiors and provides a space that can be used as the driver/passenger wishes.

Concept 26 opens up a new paradigm of possibilities in the car—from entertainment to service provision and beyond, using the technology that is now a natural part of our everyday lives. It also signals the huge potential for new business opportunities and high-tech collaborations that autonomous drive will bring.

"We have gone to great lengths to understand the challenges and opportunities that autonomous cars will bring to people in coming years, and our flexible approach to engineering and design, enabled by our new Scalable Product Architecture, means that we can readily bring this from concept to reality," said Dr. Peter Mertens, senior vice president, research and development at Volvo Car Group.

Volvo Cars' ongoing Drive Me research project, which will see an extended fleet of fully autonomous cars driving real customers on the roads of Gothenburg, Sweden, in 2017 is further proof that Volvo is a leader in autonomous drive technology, building firmly on its foundation of safety.

"Volvo Cars is among the first to address the subject of self-driving cars and liability. We firmly believe that car makers should take full responsibility for the actions of the car when it is driving in full autonomous mode. If a manufacturer does not accept liability, it clearly implies that they are not confident about their autonomous drive technology," said Mertens.

Taking Flight Powered by the Sun

Air transportation today includes Solar Impulse, the solar-powered airplane that flew across the U.S. and landed in New York's Kennedy airport. It includes high-tech and innovative power electronics subsystems, including solar panels, batteries, and motors.

Solar Impulse is a one-of-a-kind aircraft whose technology highlights the exclusive use of sun power for a transcontinental flight (Fig. 23-3). "Our airplane is not designed to carry passengers, but to carry a message," said pilot Bertrand Piccard. Pilot Andre Borschberg noted that "from the very start of the project we understood that our primary goal was to save energy."

The first Solar Impulse from San Francisco, and made stops in Phoenix, Dallas, St. Louis, Cincinnati, and Washington, D.C., before landing in New York City in May 2013. The 3,511-mile journey took 105 hours and 41 minutes in the air. Average speed was 33.14 mph. Piccard and Borschberg alternated piloting the airplane.

The U.S. flight employed version HB-SIA of the Solar Impulse; actually a prototype of what is envisioned as the forerunner of an airplane that will circumnavigate the world, the HB-SIB (Solar 2), whose construction began in 2011. The HB-SIB will have a larger cockpit that will allow the pilot to fully recline during flights lasting four to five days. It will have an increased payload, its electrical circuits will be isolated to enable flights in rain, and system redundancy will improve reliability. Its advanced avionics will allow trans-oceanic travel. Wingspan of the HB-SIB is 262.5 ft. compared to 208 ft. for the HB-SIA.

Solar Impulse HB-SIB required development of new materials and new construction methods. For example, Solvay has invented electrolytes that increase the batteries energy density. Bayer Material Sciences is allowing the project to make use of its nanotechnologies. The fuselage is using carbon fibers that weigh less than any previously seen. The carbon fiber sheets are only 25g/m2, which is three times lighter than paper. By using carbon fiber construction, the aircraft will weigh about the same as an average automobile.

23-3. The wing of the HB-SIA is filled with solar cells used to charge the batteries that power the motors and cockpit electronic systems.

The aircraft will undergo the same structural strength and vibration testing as the HB-SIA. Flight testing was done in 2014, and a round-the-world flight began in 2015.

Solar Panels

There were about 12,000 solar cells on the HB-SIA's wings and horizontal stabilizer. The HB-SIB will have 15,000 of them. This is more impressive than it appears because the panel-building process is all handmade. Plus, the cells are 150 microns thick and rated at 45kW, peak power. Cells were selected for their lightness, flexibility, and efficiency, which is 22%. SunPower Corp. provides the cells, which are then meticulously put together one by one. The process begins when a new batch of solar cells arrives, then are tested three times to verify their output voltage.

After 70 healthy cells are tested and accepted, they are strung together in series, providing 300 V. Following this is a layering process that places a plastic resin under a glass foil, and so forth, eventually laminating the strings. The "sandwich" is then cooked at 95°C for seven hours before being placed on a mold that bends the cells into the desired shape, slightly rounded for the wings. Care is taken to ensure that nothing falls on the panels during the curing process. Any microscopic piece of hair, dust, or an insect could potentially cause a failure, rendering the panel unusable. It takes 10 to 15 hours to make a panel and 48

are needed for the HB-SIB.

A thin fluorine copolymer film protects the solar cells. These cells are brittle and have no mechanical resistance, but when covered with this film, they can be molded into the wing curvature without breaking. The resin is UV-resistant, waterproof, and only 17 microns thin.

Batteries

Solar panels charge the batteries many times during a typical long flight. Because they are part of the airframe, their weight is critical. Plus, their efficiency and lifespan impact the success of the mission. A set of unique batteries will be employed in the HB-SIB. Made by the Korean producer Kokam, they required extensive research to push their performance limits. The key lies in the complex chemical formula that has improved that battery's oxidation issue, because they age faster and lose efficiency when oxidized. This technology is two years ahead of the industry, but it is the most that can be disclosed at this time. Ameliorating this usual aging process allows Solar Impulse to have batteries able to guarantee 2,000 flight hours for the HB-SIB, compared with only 500 for the HB-SIA. Energy density of the HB-SIA batteries is 260kW/kg (348 HP).

Each of the battery cells is a little different from the other. These cells do not like stress, and extremely hot or cold temperatures impact their performance. Some days a cell is more efficient than others because of certain parameters that were applied the day before. Lithium-polymer can be charged up to 4.35V, but that doesn't necessarily mean that on Friday it will exploit its full potential as it did on Thursday. Battery output voltage depends on the temperature conditions as well as the type of charge and discharge.

To ensure that lithium-polymer cells are fit for the aircraft, they must undergo numerous tests. These tests check the cell's behavior in extreme temperatures, how much energy they can store, and for how long. Tests are also done for a better understanding of their reaction to different situations. The challenge is to find the optimum balance between usable lifespan and energy, which depends on temperature, cell voltage, and current. For example, it was found that keeping a constant temperature of 25°C inside the motor gondolas provides the ideal environment for optimized battery efficiency.

Solar Impulse uses Etel torque motors. Torque motor quality operating in extreme environmental conditions is an important characteristic. Performance must be maintained optimal and constant during non-stop flights for many hours. In addition, motor efficiency must be high to maximize use of precious solar/battery energy. These motors can reach efficiencies of 96%, and they weigh less than other types of motors.

The power plant for the HB-SIA consists of four torque motors, each of which is powered by 21 kWh (300 V) lithium-polymer batteries, providing 7.5kW (10 HP) for twin-bladed propellers. Batteries associated with each of the four motors are housed in gondolas under the wing. The gondola also includes a power-management subsystem that controls charge/discharge and temperature. Thermal insulation conserves the heat radiated by the batteries to keep them functioning at very low temperatures encountered at high altitudes. Each motor is fitted with a reducer that limits propeller rotation to a 3.5 meter diameter within the range of 200 to 4,000 rpm.

Over an ideal 24-hour cycle, HB-SIA motors delivered a combined average of about 8 HP (6 kW). That's roughly the power used by the Wright Brothers aircraft in 1903. The HB-SIB will employ more powerful motors and batteries.

Flight Instruments

The cockpit's electronic instruments have three main functions:

- Monitor the power supplied by solar panels to the motors and batteries.
- Communicate to the pilot the necessary information for controlling the airplane.
- Provide real-time information to the mission team that is monitoring the aircraft's flight path and behavior from the ground.

A revolutionary new instrument was developed for the HB-SIA with collaboration from Omega and Claude Nicollier, who heads the Solar Impulse test flight team. Its primary function is to inform the pilot within an accuracy of one degree, the bank angle of the aircraft (the turn or change of direction when it banks or inclines) must be below five degrees. For this reason, the Omega instrument is connected to gyroscopes that are used to provide stability or maintain a fixed orientation.

Another key function of the Omega instrument is to inform the pilot of his real flight direction. This is important because the HB-SIA's huge wingspan, combined with lightness, makes it very sensitive to air movements, especially crosswinds, which can cause it to drift. LEDs on the front panel indicate the flight direction to one degree. This also helps align the aircraft in the axis of the runway for landing.

On-board electronics have been optimized to combine lightness and maximum efficiency. In flight, the electronic systems undergo significant temperature variations between low and high altitudes; this must not affect their performance. Therefore, prototype circuits and devices have been destruction-tested with the test results used directly in the manufacturing process of the final systems.

Due to the repair work to the aircraft's main spar, Solar Impulse 2's circumnavigation of the earth was delayed from 2012 to 2015. The aircraft was delivered to Masdar in Abu

23-4. Elektra One has a maximum power of16-20 kW, and range is more than 400 km (249 miles) with a flight time of up to more than three hours.

Dhabi for the World Future Energy Summit in late January 2015, and it began the journey on March 9, 2015. It was scheduled to return to the same location in August 2016. A mission-control center for the circumnavigation was established in Monaco, utilizing satellite links to gather real-time flight telemetry and remain in constant contact with the aircraft and the support team.

The route being followed by Solar Impulse 2 is entirely in the northern hemisphere; its closest approach to the equator was expected to be a flyby of Honolulu at 21.3° N. Twelve stops were originally planned to allow the alternation and rest periods of pilots Borschberg and Piccard, and to ensure good weather conditions for each take-off and landing site along the route. For most of its time airborne, Solar Impulse 2 has been cruising at a ground speed of between 50 and 100 kilometers per hour—usually at the slower end of that range at night to save power. The legs of the flight crossing the Pacific and Atlantic oceans are the longest stages of the circumnavigation, and were each expected to take about five days. On multi-day flights, the pilots take 20-minute naps and use Yoga or other exercises to promote blood flow and maintain alertness.

By the end of May 2015, the plane had traversed Asia. It made an unscheduled stop in Japan to await favorable weather over the Pacific, increasing the expected number of legs of the journey to 13. The aircraft began the flight from Japan to Hawaii on June 28, 2015 (June 29, Japan local time). With Borschberg in the cockpit, it reached Hawaii on July 3, setting new records for the world's longest solar-powered flight both by time (117 hours, 52 minutes) and distance (7,212 km; 4,481 mi). The flight's duration was also a record for longest solo flight, by time, for any aircraft. During that leg, however, the plane's batteries were damaged by overheating caused by being packed in too much insulation. New parts had to be ordered, and as it was late in the season, the plane was grounded in Hawaii, and the U.S. Department of Transportation is storing the aircraft in a hangar at Kalaeloa Airport on Oahu.

New batteries have been made and were installed in the plane in the early weeks of 2016. Test flights began in February, and the circumnavigation resumed in April 2016, when northern hemisphere days lengthen enough to permit multi-day solar-powered flights.

Electric Aircraft

For several years, all-electric power assisted gliders and hang gliders have been available. Advantages of electric aircraft include improved maneuverability due to the greater torque from electric motors, increased safety due to decreased chance of mechanical failure, less risk of explosion or fire in the event of a collision, and less noise. There will be environmental and cost benefits associated with the elimination of consumption of fossil fuels and resultant emissions.

Electric aircraft are available from several sources worldwide. As with on-road vehicles, the major problem with electric aircraft is range—the best of both being 160 to 400 km (about 100 to 250 miles) in a practical manned configuration. Following are descriptions of these aircraft.

The battery and solar-panel powered Elektra One (Fig. 23-4) is built of lightweight fiber composite structures. Maximum power is 16-20 kW, and range is more than 400 km (249 miles) with a flight time of up to more than three hours. Its wingspan is 8.6m, and it can carry up to a 90kg payload.

23-5. Cri-Cri uses composite materials instead of metal to reduce overall weight and make room for the high-energy-density lithium batteries that provide power to four brushless electric motors—two mounted back-to-back on nose pods on each side—with counter-rotating propellers.

Cri-Cri (Fig. 23-5) uses composite materials instead of metal to reduce overall weight and make room for the high-energy-density lithium batteries that provide power to four brushless electric motors—two mounted back-to-back on nose pods on each side—with counter-rotating propellers. Projected perfor-

mance is 30 minutes of cruise flight at 110 km/h (68 mph); 15 minutes of full aerobatics at up to 250 km/h (155 mph); and a climb rate of approximately 5.3 m/sec (1,020 fpm.

Yuneec's E430 (Fig. 23-6) is a two-seat, V-tailed, composite aircraft with a high-aspect ratio wing. Take-off speed is 40 mph, cruise speed is 60 mph, and max speed is 95 mph. The company claims that the battery packs have an expected lifespan of 1,500 hours and cost $7,000 each, with the aircraft carrying three to five battery packs, giving two to two and half hours endurance. The batteries can be recharged in three to four hours from a 220V outlet.

Sonex is the prototype of a Waiex E-Flight Electric-powered plane resulting from a partnership between Sonex Aircraft LLC and AeroConversions. This electric plane (Fig. 23-7) will use a dc cobalt motor, controller, and highly efficient battery and charging system. The emphasis will be placed solely on power-plant research and development to develop an efficient sturdy and efficient power system.

The Puffin is a vertical-takeoff and landing aircraft, taking off like a helicopter and flying like a plane. Just 60 horsepower gets pilot and craft airborne. It is 12 feet high with a 13.5-feet wingspan and its rotors are nearly 7.5 feet in diameter. Rather than tilting the rotors forward for horizontal flight, the whole craft, cockpit and all, pitches forward, so the pilot flies from a prone position. During takeoff and landing, the tail splits into four legs that serve as landing gear, and flaps on the wings deploy to keep the aircraft stable as it lifts and descends. It can cruise at 150 miles per hour and sprint at more like 300 miles per hour. Its range is 50 miles, which is related to its battery density. Using carbon composite construction, the Puffin weighs less than 400 pounds including the lithium phosphate batteries. Fig. 23-8 shows the Puffin parked in its vertical position and Fig. 23-9 shows the Puffin in flight.

Battery-Powered Unmanned Aircraft

AeroVironment's Puma AE (All Environment) is a small unmanned aircraft intended for land-based and maritime operations (Fig. 23-10). Capable of landing in the water or on land, the Puma AE empowers the operator with operational flexibility.

The Puma AE is durable with a reinforced fuselage construction, portable for ease of mobility, and requires no auxiliary equipment for launch or recovery operations. The system is quiet to avoid detection and operates autonomously, providing persistent intelligence, surveillance, reconnaissance, and targeting data (ISRT).

The Puma AE delivers 3.5-plus hours of flight endurance, with versatile smart-battery options to support diverse mission requirements. Its powerful propulsion system and aerodynamic design make it efficient and easy to launch, especially in high altitudes and hotter climates. A

23-6. The E430 uses three lithium polymer battery packs that allow it to fly for two hours in an "optimum cruise" with two people on board.

23-7. The Sonex electric airplane will use a dc cobalt motor, controller, and highly efficient battery and charging system. It will emphasize power-plant research and development.

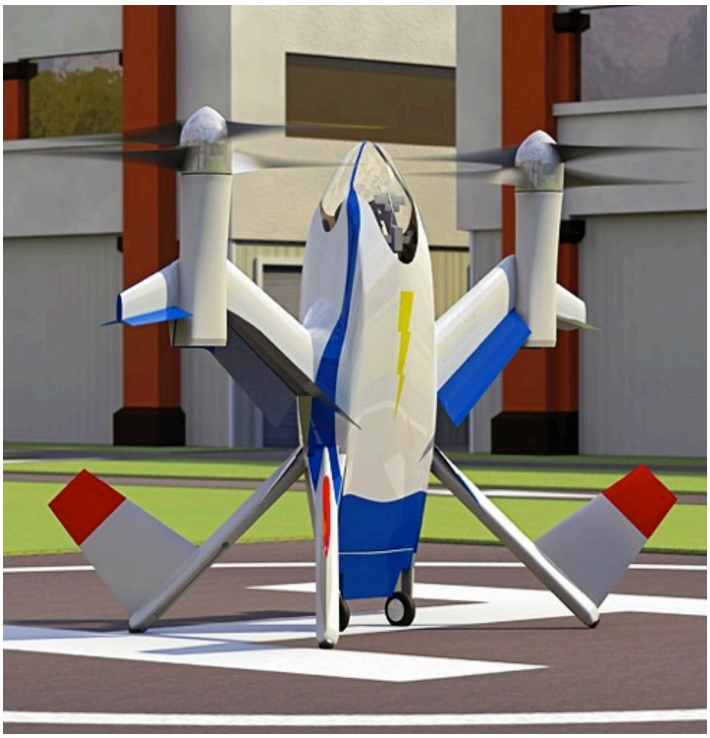

23-8. The Puffin is a vertical-takeoff and landing aircraft, taking off like a helicopter and flying like a plane. It uses carbon composite construction and weighs less than 400 pounds, including the lithium phosphate batteries. It is shown parked in its vertical position.

23-9. Puffin in flight showing the pilot in the prone position.

plug-and-play power adapter is provided for easy integration of future extended endurance options, such as, solar and fuel cell solutions.

It carries both an electro-optical (EO) and infrared (IR) camera plus illuminator on a lightweight mechanical gimbaled payload, allowing the operator to keep "eyes on target." For increased payload capacity, an optional under-wing Transit Bay is available for easy integration of third-party payloads such as communications relay, geo locations, or laser marker to meet the diverse needs of military or civilian applications.

The precision navigation system with secondary GPS provides greater positional accuracy and reliability of the Puma AE. The UAV is operated from AeroVironment's battle-proven ground control station (GCS) with a communications range of 15 km. The GCS allows the operator to control the aircraft manually or program it for GPS-based autonomous navigation.

23-10. AeroVironment's Puma battery-powered unmanned aircraft.

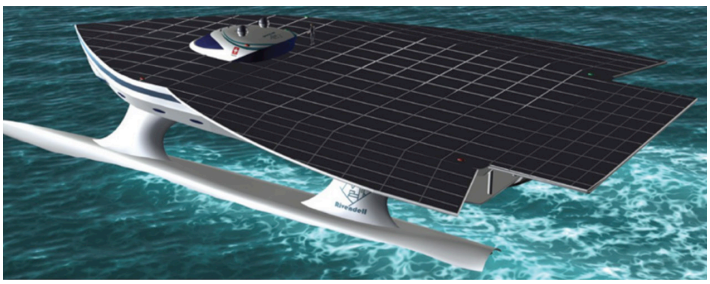

Solar-Powered Ship Travels the World

The MS Tûranor PlanetSolar, the world's largest solar-powered boat (Fig. 23-11), was the first boat to circumnavigate the world powered exclusively using solar energy. It docked on May 4, 2012, after sailing for 584 days and traveling over 60,000 km.

This initial version of the solar boat is a 31-meter three-hull catamaran. Its deck has over 500 square meters of 18.8% efficient solar panels rated 93 kW. Panels charge 648 series and parallel connected lithium-ion batteries that produce 388 V and 2910 Ah. The batteries power two 10kW (maximum), 1000 rpm permanent magnet synchronous motors in each hull. The boat's shape allows it to reach speeds up to 14 knots. Its carbon-fiber composite hull was model tested in wind tun¬nels and was tank tested to determine its hydrodynamics and aerodynamics. Construction cost was 12.5 million euros. Its name, derived from J.R.R. Tolkien's novel The Lord of the Rings, translates to "The Power of the Sun."

Its two years of solar circumnavigation were instructive for PlanetSolar and led to an initial assessment of the vessel's performance. This assessment indicated where optimizations were needed to make the boat more efficient and maneu¬verable. These improvements will expand and diversify the boat's applications and uses; notably, enabling it to navigate to the northernmost part of the Atlantic, near the Arctic, for the first time.

The ship recently went to sea with a team of scientists who will monitor the air and water of the Atlantic Ocean's Gulf Stream, a current that influences the climates of North America's east coast and Europe's west. The team of scientists will monitor ocean phenomena such as eddies and whirlpools that, in the right environment, help to power the so-called ocean conveyor belt that drives circulation in the oceans.

This new four-month scientific expedition will take the Tûranor out of the Mediterranean headed toward Miami, Fla., at the southwestern tip of the Gulf Stream. From there, physicists, biologists, and climatologists from the University of Geneva, led by Professor Martin Beniston, director of the Institute of Environmental Sciences at the university, will begin continuous monitoring of the air and water in a project dubbed PlanetSolar Deep Water.

Built in Kiel, Germany, the catamaran runs exclusively on solar energy. After two years of design and construction, PlanetSolar was responsible for many technological advances, notably in the domain of com¬posite material

23-11. MS Tûranor PlanetSolar, the world's largest solar-powered boat.

manufacturing and solar energy storage.

In preparation for its 2013 expedition, the MS Tûranor PlanetSolar underwent major maintenance upgrades. Among the extensive maintenance tasks and optimizations car¬ried out, most notable was the cabin refurbishment, the creation of a walkway on the solar bridge, an increase in water tank capacity, and improve¬ment to the rudder. The most significant optimization was a change to the propulsion system—replacing the surface propellers with a completely immerged system.

This project is under the direction of the University of Geneva, Switzerland. Founded in 1559, the University of Geneva (UNIGE) ranks among the top 100 universities in the world. UNIGE welcomes approximately 16,000 stu¬dents each year to its eight colleges, dealing with the essen¬tial domains of science, medicine, literature, economic and social sciences, law, theology, psychology, education, transla¬tion, and interpretation sciences.

U.S. Navy's DDG 1000 Incorporates an Integrated Power System

The future USS Zumwalt (DDG 1000) has begun sea trials in the Atlantic Ocean (Fig. 23-12). The largest destroyer ever built for the U.S. Navy and the first of three Zumwalt-class destroyers, DDG 1000 will be the first U.S. Navy surface combatant to employ an integrated power system (IPS) to generate the total ship electric power requirements, then distribute and convert it for all ship loads from common gas turbine generators. This power flexibility allows for potentially significant energy savings and is well suited to enable future high-energy weapons and sensors. The IPS is a unique design integrating a power system with fight-through power and allowing automatic reconfiguration if there is damage to the power distribution system.

Integrated Power System (IPS)

An integrated power system is an all-electric architecture that provides electric power to the total ship (propulsion and ship service) with an integrated plant. IPS enables a ship's electrical loads, such as pumps and lighting, to be powered from the same electrical source as the propulsion system (e.g., electric drive). This eliminates the need for separate power-generation capabilities for these loads. In commercial applications, this is known as the "power station" concept.

Anticipated benefits of IPS include:

- Fewer prime movers: Usually allows a reduction from a total of seven to five prime movers in the traditional gas-turbine surface combatant.
- Reduced costs of ownership: Results in significant fuel savings (15%-19% in a typical gas-turbine combatant). Fewer engines installed results in less maintenance and manning.
- Naval architectural flexibility: Provides flexibility in locating prime movers, allowing space previously used for uptakes to be put to better use.
- Improved survivability and stealth: Quiet propulsion motors can better meet current acoustic requirements. Smaller main machinery spaces allow for improved damage control.
- Improved warfighting: Integrated power makes large amounts of power available throughout the life of the ship. This power can be reallocated to accommodate future combat systems. Advances in power conversion are making it possible to provide uninterrupted power, advanced fault isolation, and fight-through capabilities beyond what is currently available.

23-12. The U. S. Navy's DDG-1000 has an integrated power system with an all-electric architecture that provides electric power to the total ship (propulsion and ship service) with an integrated plant.

In a typical mechanical-drive propulsion system, the propulsion prime movers are connected to long shafts running through the ship to large reduction gears that rotate the ship's propellers. With electric drive, the prime movers rotate electric generators that are connected through cabling to motor drives and electric motors that rotate a ship's propellers. Electricity is the medium for transmitting the energy of the prime mover. It enables "cross connecting" of any available prime mover/generator combination by breaking the physical link between the power-generation and power-utilization components.

IPS provides for all of a ship's electrical needs, including propulsion and ship service loads. Traditional electric drives only provide for propulsion. They do not include power for ship service loads.

The Navy has used electric drive in many ships, including early aircraft carriers, a number of ships during World War II, and many of the current inventory of smaller auxiliary ships. In fact, the Navy is leveraging as much as possible from the cruise-ship industry, where nearly all new ships employ integrated electric systems. What is new and

significant is the application of these concepts in a fully electrically integrated (no mechanical takeoffs for power) power system on a surface combatant. These ships have higher speed and lower noise requirements than any of the other ships, as well as large combat systems to support. Commercial cruise ships would be too big and too noisy for a surface combatant, and do not have a power-system architecture to let them survive damage and continue to fight.

Training Required

The new crew trained on components including main and auxiliary turbine generators, propulsion motors and drives, dynamic braking resistors, auxiliary control panels, and high-voltage switchboards. They also spent time working with harmonic filters, neutral ground resistors, the Integrated Fight-Through Power System (IFTP), power conversion modules, and an emergency diesel generator.

Equipment operation was conducted at the local control level, as well as the remote supervisory Engineering Control System (ECS). The ECS system provides a significant advancement in machinery control with automation for system transitions and power management to support the reduced manning concept for the DDG 1000.

DDG 1000's power allocation flexibility allows for potentially significant energy savings and is well-suited to enable future high-energy weapons and sensors.

Its wave-piercing Tumblehome ship design has provided a wide array of advancements. The composite superstructure significantly reduces cross-section and acoustic output, making the ship harder to detect by enemies at sea. The design also allows for optimal manning with a standard crew size of 158 sailors (including air detachment), thereby decreasing lifecycle operations and support costs.

DDG 1000 will employ active and passive sensors and a Multi-Function Radar (MFR) capable of conducting area air surveillance, including over-land, throughout the extremely difficult and cluttered sea-land interface.

Related Articles

1. Peter Harrop, 21st Century Technology Propels Electric Aircraft into the "Blue Yonder," powerelectronics.com, October 2010.
2. Don Tuite, Understanding U.S. and European Standards for Electric-Vehicle Charging, electronicdesign.com, March 2012.
3. Solar-Powered Ship Travels the World, powerelectronics.com, May 2013.
4. Sam Davis, Powered by the Sun, Solar Impulse Takes Flight, powerelectronics.com, August 2013.
5. Sam Davis, Volvo Car Group Embeds Batteries, Supercaps in Carbon Fiber Body, powerelectronics.com, October 2013.
6. Sam Davis, Getting Fuel-Cells from Concept Cars to Showrooms, machinedesign.com, March 2014.
7. Alexander Isurin, Philosophy of Topology and Components Selection for Cost and Performance in Automotive Converters., powerelectronics.com, September 2014.
8. Sam Davis, Tesla Updates its Roadster to Achieve 400 Mile Range on a Single Charge, powerelectronics.com, January 2015.
9. Sam Davis, U.S. Navy's DDG 1000, Incorporating an Integrated Power System, Will Make Waves, powerelectronics.com, December 2015.
10. Sam Davis, Sit Back and Enjoy the Ride . . . to Work, powerelectronics.com, January 2016.

BACK TO TABLE OF CONTENTS

CHAPTER 24:

POWER-MANAGEMENT TEST AND MEASUREMENT

Power management involves test and measurement in three different levels:

- System
- Subsystem
- Component

At the system level, there are ac and dc power analyzers. At the subsystem level, a considerable amount of test and measurement systems can ensure a power supply is working properly. Testing at the component level mostly involves the power semiconductors employed in the system.

AC Power Glossary

RMS (Root mean squared value) is the most commonly used and useful means of specifying the value of both ac voltage and current. The RMS value of an ac waveform indicates the level of power that is available from that waveform, which is one of the most important attributes of any ac source.

RMS value = Peak Value/$\sqrt{2}$

Crest Factor is the relationship between peak and RMS.

Crest Factor = Peak Value/RMS Value

For a sinusoid: Crest factor = $\sqrt{2}$

Because the output current of a switch-mode power supply is not sinusoidal, the crest factor of the current waveform can be much greater than $\sqrt{2}$

Average Value can only have real meaning over one half cycle of a symmetrical waveform.

Average Value= Area enclosed by one half cycle/
Length of base over one half cycle

Real Power is the power available to the load to do real work and is given in Watts. With a pure resistive load, you can multiply the RMS voltage and RMS current to get real power.

Apparent Power equals the product of the RMS voltage and RMS current.

Apparent Power= V_{RMS} Y= I_{RMS}

Reactive Power is the vector difference between Apparent Power and Real Power and is measured in Volt-Amperes (VA). This is correct for sinusoidal waveforms.

Power Factor for sinusoidal voltage and current waveforms is the cosine of the phase angle (θ) between the voltage and current waveforms.

Power Factor = Real Power/Apparent Power

Harmonic Distortion on an ac powerline is a non-sinusoidal current waveform that consists of a fundamental component at the supply frequency plus a series of harmonic frequencies that are integral multiples of the fundamental frequency (Fourier Analysis).

Total Harmonic Distortion (THD) is a figure of merit that quantifies the level of harmonics in non-sinusoidal ac voltage or current waveforms.

System: AC and DC Power Analyzers

Power analyzers accurately measure electrical power characteristics of devices that generate, convert, or consume electricity. There are now two types of power analyzers: ac and dc. A dc power analyzer allows engineers to gather and configure multiple instruments to complete dc sourcing and measurement tasks. AC power analyzers provide precise measurements of true power (watts), power factor, harmonics and efficiency in power-conversion equipment. Reliable ac power analyzers enable engineers to minimize energy loss due to distorted, transient waveforms

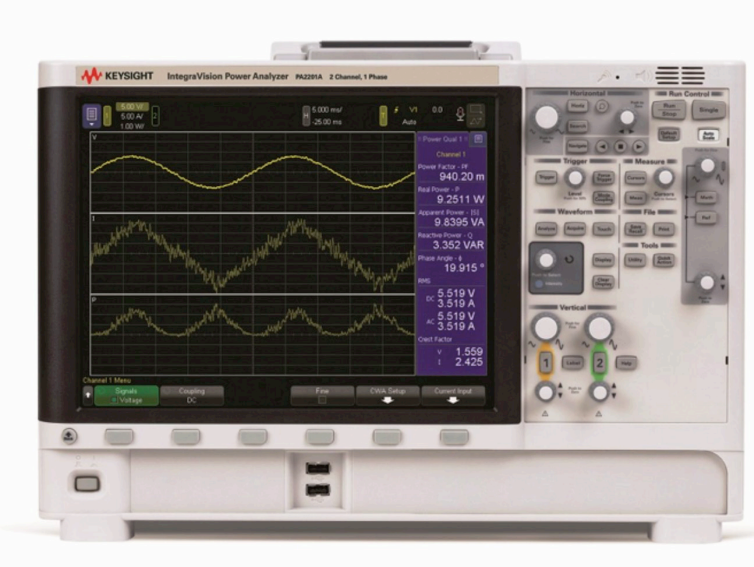

24-1. The Keysight Integravision ac power analyzer provides oscilloscope-like ability and ac power analysis.

in power electronics such as inverters, motors, lighting circuits, and power supplies.

Engineers working on electronic power-conversion systems need high-accuracy measurements to identify and characterize incremental efficiency improvements. Precision ac power analyzers offer high accuracy and ease of connection to the DUT, making them ideal for steady-state measurements of power consumption, efficiency, and power quality. For these measurements, the accuracy of the power analyzer gives R&D engineers the measurement integrity they need. With floating inputs and directly connected measurements, precision power analyzers make it easy for engineers to connect to their DUTs.

Traditionally, only oscilloscopes offer the single-shot measurement capability necessary for dynamic measurements during functional test. Furthermore, by offering a visual picture of what is happening, oscilloscopes allow engineers to gain insight into their DUTs and to identify issues. However, their lower accuracy means that making critical efficiency measurements on high-efficiency converters may be impossible. Because oscilloscopes have ground-referenced, non-isolated front ends, probes are required for floating and current measurements. Probes further reduce measurement accuracy and make oscilloscopes harder to connect to the DUT for high-accuracy, power-related measurements.

R&D engineers may have to switch between these two instruments depending on the type of measurement they need to make. They would use a power analyzer to make accurate measurements and an oscilloscope to visualize repetitive and single-shot events such as turn-on and occurrences of transients.

Keysight's PA2000 Series ac power analyzer provides oscilloscope-like ability and ac power analysis (Fig. 24-1). It supports the capture of voltage, current, and power waveforms over specific periods of time, with measurements made based on cursors placed on the captured waveforms. This helps in examining transient phenomena and in the design of periodically controlled equipment. To ensure that the DUT complies with energy standards, for instance, it is vital to measure power consumption across a range of different modes from sleep to full activity—and all the transient states in between.

Abnormal phenomena can often be hard to isolate, disappearing from the screen almost as soon as they appear. Like a traditional oscilloscope, you can set up the PA2000 ac power analyzer to make single-shot measurements to capture and measure transient phenomena, including inrush, cycle dropouts, blackouts/brownouts, and other line disturbances.

Power analyzers use mathematical transformations to analyze signals. For precision, the measurement window cannot have any discontinuities or gaps. Continuous Whole-Cycle Analysis (CWA) used by the PA2000 Series is a gapless measurement technique that always performs measurements on a positive integer number of signal cycles.

Tektronix' PA3000 is a one- to four-channel power analyzer optimized for testing single- and multi-phase, high-efficiency power-conversion products and designs (Fig. 24-2). Use it to quickly visualize, analyze, and document power efficiency, energy consumption, and electrical performance to the latest regional and international standards, including Level VI, EnergyStar, CEC, IEC 62301, CQC-3146, and more.

Key features

- One to four channels support single- and three-phase applications
- 10 mW standby power measurement
- 1 MHz bandwidth

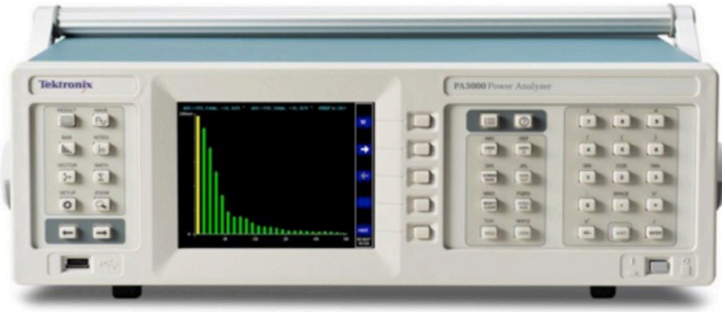

24-2. The Tektronix PA3000 is a one- to four-channel power analyzer optimized for testing single- and multi-phase, high-efficiency power-conversion products and designs.

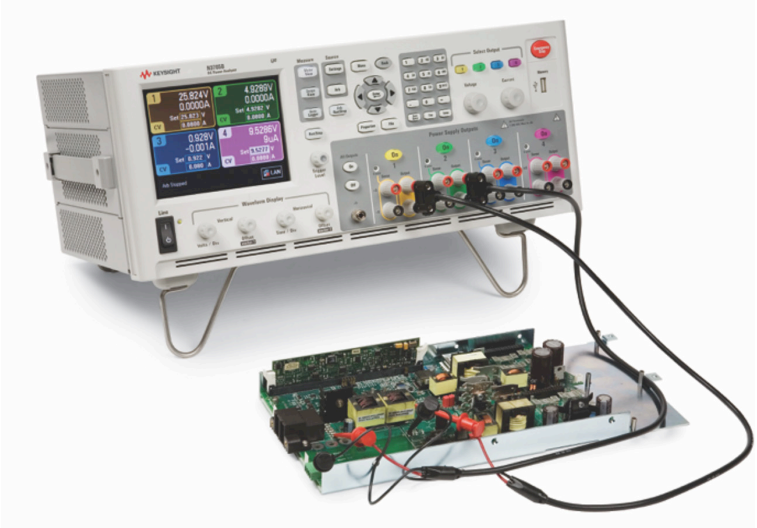

24-3. Keysight's N6705 DC Power Analyzer provides insights into the DUT's power consumption in minutes without writing a single line of code.

- 1 MS/s sampling rate
- 16 bit A/D
- Harmonic analysis to 100th order ±0.04% basic voltage and current accuracy
- Measurements to 30 Arms and 600 Vrms Cat II (2000 Vpk)
- USB and LAN interfaces standard (GPIB option)
- Free PWRVIEW software
- Full color graphical display for intuitive readouts of measured values, waveforms, harmonics, and energy integration plots.

The essential power-measurement tool for R&D and validation

- High accuracy supports testing to Level VI efficiency standards for external ac/dc power supplies
- Dedicated energy consumption testing in integration mode for standards like Energy Star and CEC
- Complete solution for full compliance testing to IEC 62301 standby power requirements
- 1 MHz bandwidth supports the LED module energy certification requirements of CQC-3146 as well as harmonic analysis of designs with higher fundamental frequencies
- More than 50 standard measurement functions, including harmonics, frequency, and star-delta computation
- Multiple analog and digital inputs for sensor data such as thermocouples, speeds sensors, and torques sensors.
- Built-in ±15 V supplies for external transducers to support high-current applications.

Applications

- AC/DC power supplies and LED drivers
- Appliances and consumer electronics
- UPS systems, inverters, and dc/ac conversion systems
- Wireless battery charging
- Three phase motors and drives.

Keysight's N6705 DC Power Analyzer represents an entirely new instrument category for R&D engineers (Fig. 24-3). It provides productivity gains when sourcing and measuring dc voltage and current into a DUT. Using the N6705 DC Power Analyzer, R&D engineers can gain insights into the DUT's power consumption in minutes without writing a single line of code. It provides an easy-to-use interface, with all sourcing and measuring functions available from the front panel.

When executing these complex tasks, which can involve simultaneously connecting to and physically interacting with multiple test instruments, the risk of error increases. In response, R&D engineers may choose to automate tests that are too complex to do manually. Unfortunately, while automating tasks reduces human error, writing and debugging programs adds more work to already overloaded R&D engineers.

The N6705 DC power analyzer makes measurement tasks easy, right from the front panel:

- Set up and view critical turn-on/turn-off sequences.
- Measure and display voltage, current versus time to visualize power into the DUT.
- Control dc bias supply ramp-up/down rates.
- Generate dc bias supply transients and disturbances (arbs).
- Log data for seconds, minutes, hours, or even days to see current/power consumption or capture anomalies.
- Save data and screen shots to internal storage or external USB memory devices.
- Save and name your setup and tests for easy reuse.
- Share setups with colleagues.

The Keysight 14585A control and analysis software is a companion PC application that lets you control any of the N6700 family's dc power modules when installed in up to four N6705 mainframes from a single PC control screen. This software provides improved data visualization and data management.

Subsystem: Power Supply Testing Test Probes

Designing a power supply requires the testing of various parameters to ensure its proper operation and that it meets system specifications. In addition, some of the same measurements must be employed in troubleshooting a defective power supply. In most cases, these measurements must be made without influencing the performance of the circuit under test.

Along with a vector network analyzer (VNA) and the appropriate probes, you can measure power supply parameters, non-invasively. The probes work for regulators, POLs, converters, and voltage references.

24-4. Picotest's 1-Port probe is used to make an output impedance measurement of a voltage reference.

Picotest probes are referred to as PDN probes because they can measure low and ultra-low impedances found in Power Distribution Networks. PDN probes are 50Ω passive transmission-line probes. Their small and lightweight probe heads are intended for easy handling and high-performance measurement. The small form-factor probe tip and variable pitch ground lead allow designers to easily browse different device outputs, component footprints, and test points. There are two types of probes, the 1-port (Fig. 24-4) and 2-port (Fig. 24-5).

Transmission line probes are a special class of passive probe that use a precision transmission line to replace the high-impedance probe cable, found in a traditional passive probe. The probe characteristic impedance matches the 50Ω impedance of a VNA or oscilloscope's input. This reduces the input capacitance to a fraction of a picofarad, minimizing the loading of sensitive outputs with high-frequency signals.

Input impedance of the Picotest probes remain nearly constant over their entire frequency range, whereas a traditional ÷10 passive probe has a high input impedance at dc and drops rapidly with frequency, passing below the input impedance of a transmission line probe at <100MHz.

Transmission-line probes are useful in applications that produce fast-rising, narrow pulses with amplitudes that exceed the dynamic range of active probes. They also tend to have less parasitic effects on frequency response and so they are ideal for measuring impedance. By providing a simple, elegant, and flexible solution to probing high-frequency signals, Picotest's 1- and 2-Port probes preserve signal fidelity and allow high-bandwidth test equipment to properly measure circuit characteristics.

The PDN probes have a wide dynamic range and can measure levels up to 5 V (RMS) without distortion. Their low inherent noise enables measurement of small signal levels. The comprehensive accessory set allows these probes to be connected to a wide variety of DUTs without impairing their very high bandwidth, though the length of the ground lead should be kept as short as possible.

High-speed applications put pressure on the measurement of power-supply buses to unprecedented frequencies. As an example, the measurement of PDN impedance for FPGAs, ASICs, and high-speed digital devices generally requires the measurement of impedance levels in the milliohm scale at frequencies exceeding 1GHz. Measuring the high-speed step-load response in power systems using 2-ports is difficult because of the need to connect two 50Ω transmission lines to the output capacitor. Compounding this difficult task is that these measurements often need to be made on very small circuits such as cell phones, solid-state disk drives, and computer tablets, etc.

These PDN probes are bi-directional. They can be used like a traditional probe to record signals or used to inject stimulus. For example, you can use a 1-port probe to inject a wide-band signal into your power rails in order to look for power-plane resonances or troubleshoot EMI problems. The 2-port probe can be used to transmit a stepped-load current pulse through one port, while measuring the voltage response from the other port, simultaneously.

These probes alleviate many physical testing challenges associated with traditional probes while maintaining precision 50Ω characteristics for a wide variety of measurements. **Among the important power-supply functional measurements are:**

- Control loop stability
- Power supply rejection ratio (PSRR)
- Ripple and noise
- Bandwidth
- Rise time
- Output impedance.

Electronic Loads

24-5. The Picotest 2-port probe.

24-6. Chroma System Solutions' 63200 electronic load.

An electronic load is a test instrument that emulates dc or ac resistance loads normally required to perform functional tests of batteries, power supplies, or solar cells. Programmability allows tests like load regulation, battery-discharge curve measurement, and transient tests can be fully automated and load changes for these tests can be made without introducing switching transient that might change the measurement or operation of the power source under test.

The electronic load electrically "looks like"a programmable resistor. These most commonly use one transistor/FET, or an array of parallel connected transistors/FETs for more current handling, to act as a variable resistor. Internal circuitry in the equipment monitors the actual current through the transistor/FET, compares it to a user-programmed desired current, and through an error amplifier changes the drive voltage to the transistor/FET to dynamically change its resistance. This negative feedback results in the actual current always matching the programmed desired current, regardless of other changes in the supplied voltage or other variables. Most commercial dc loads are equipped with microprocessor front-end circuits that allow the user to not only program a desired current through the load (constant current, or CC), but the user can alternatively program the load to have a constant resistance (CR) or constant power dissipation (CP).

Chroma System Solutions' 63200A (Fig. 24-6) is a high-power electronic load intended for testing power-conversion products including ac/dc and server power supplies, dc/dc converters, EV batteries, automotive charging stations, and other power electronics components. Built-in digital signal microprocessors (200MHz) provide optimal speed and control performance. These loads can be synchronously paralleled and dynamically synchronized for generating complex multi-channel transient profiles. The 300% peak overpower capability provides extra headroom for fault-condition simulations in automotive batteries and fuel cells.

Advantages of the 63200A series include ultra-high density power (6kW@4U), built-in digital microprocessors, master/slave parallel control, sine wave dynamic loading, and an industry leading measurement accuracy achieving 0.015%+0.015% F.S., 0.04%+0.04% F.S., and 0.1%+0.1% F.S. accuracy for voltage, current, and power measurement, respectively.

The front panel includes iconic function selectors via rotary knob or arrow keys and a vacuum fluorescent display. For pain-free viewing and access, the entire front panel tilts upward on 7U, 10U, and 13U models. Operation can be achieved by the front panel or from a remote workstation via standard USB or optional Ethernet and GPIB interfaces.

The 63200A series is complete with 150V, 600V, and 1200V voltage ranges and 3kW to 24kW power ranges. The maximum current of a single unit is 2000A and up to 480kW when paralleled. These high-power dc electronic loads are designed for testing server power supplies, A/D power supplies, batteries and energy storage systems, EV/EVSE, solar, and other power electronics.

Components: Power Semiconductors

Typical power semiconductor data sheets usually describe device behavior, but only over a limited range of operating conditions. This makes the operating conditions even more complicated because improved power MOSFETs and IGBTs can now operate at several hundred volts and hundreds of amps. This challenges the designer to obtain his/her own accurate power device measurement data over a broader range of operating conditions than those provided in data sheets.

Test measurements necessary to support the choice of the optimum power MOSFET in terms of power dissipation, reliability and efficiency, include:

- Static characterization (breakdown, $R_{DS(ON)}$, leakage, etc.)
- Characterization based on bias and temperature conditions experienced by devices in the actual end item system
- Drain (collector) voltage dependency of FET junction capacitances
- Gate charge characteristics
- Power losses.

For best results, use a test instrument that provides wide current and voltage measurements. To minimize device heating, testing the power semiconductor at high currents must be done using a series of short pulses. Fig. 24-7 shows a typical a plot of I_C vs, V_{CE} and Fig. 24-8 shows the breakdown voltage characteristics of a power MOSFET.

Although no current should flow in the off-state of high-power applications, there can often be small leakage currents. This means that even sub-nanoamp current measurements on the power devices may be necessary to

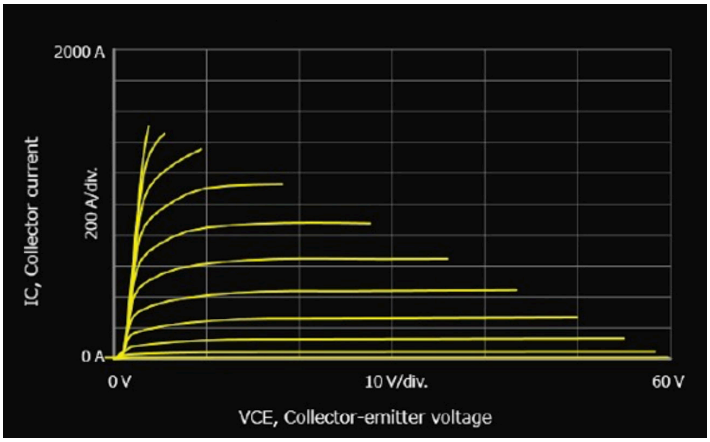

24-7. Typical plot of IC vs. V_{CE} presented on a Keysight B1506A.

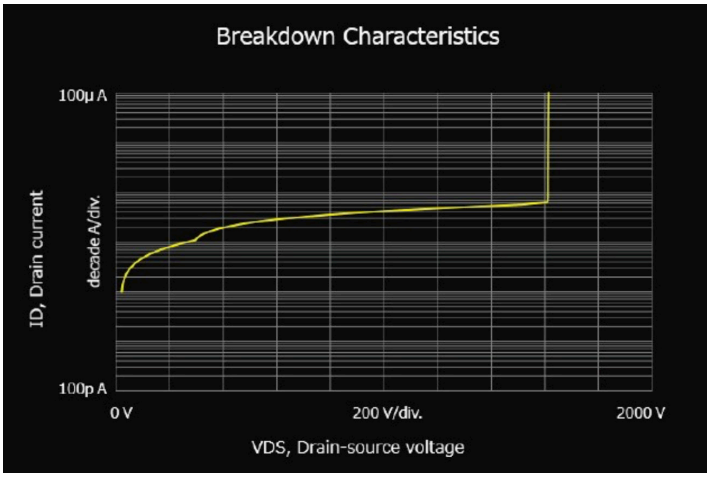

24-8. Breakdown characteristics of a power MOSFET presented on a Keysight B1506A.

guarantee the energy efficiency of the end product. Understanding the maximum current when a device is on and the leakage current when a device is off is important because the test instrument must be able to measure currents as low as picoamps and voltages as low as microvolts as well as much higher operating currents and voltages.

Besides measuring general device characteristics over temperature, the designer may also want to screen various devices because they can look fine at room temperature, but be out of spec at a low or high temperature. Unfortunately, temperature characterization of power devices is not easy. Special measurement techniques must be used because these tests require a thermal test chamber whose temperature can take a long time to stabilize, and long cables leading from the chamber to the test equipment can create resistive and inductive oscillation problems. And, some applications may require performing device tests at temperature extremes, such as -50°C to 250°C. Fig. 24-9 is an example of temperature dependence of a power MOSFET that shows the variation of on-resistance

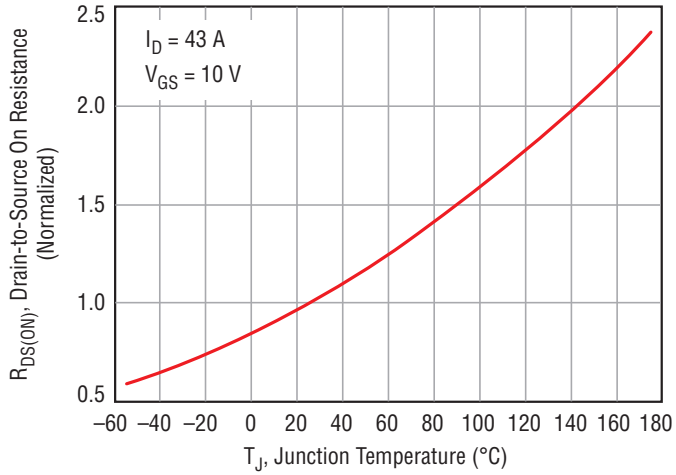

24-9. Variation of on-resistance ($R_{DS(ON)}$) vs. temperature presented on a Keysight B1506A.

vs. temperature.

For all levels of current and voltage, it is important to obtain accurate and reliable measurement results. The larger the measurement error is in device evaluation, the larger the negative impact it has on circuit operating margins and peripheral circuit design. However, test data taken using traditional power device measurement equipment (such as curve tracers) is suspect in terms of measurement accuracy and reliability. Therefore, many circuit designers only use curve tracers to verify gross device functionality, and take the numerical measurement results as only a rough indication of device behavior. Obviously, when the need arises to compare the characteristics of multiple devices or to verify whether a device meets a manufacturer's specifications, an approximate device characterization data is not meaningful.

A key parameter to determine from testing is total gate charge (Q_G), which is the total amount of charge necessary to turn on a power MOSFET. It is an extremely important parameter when estimating the driving loss during circuit operation. The driving loss consists of the product of Q_G, the gate voltage (V_G), and the switching frequency. Accurate Q_G evaluation allows precise driving loss calculation as well as optimized design of the driving circuit. Fig. 24-10 shows a plot of V_{GS} (gate-source voltage) vs. Q_G for a super junction MOSFET.

Q_G also provides other useful information to help with switching operation analysis. For example, when a circuit does not meeting performance expectations, examining the Q_G curve can offer valuable insights that identify the source of the problem.

Because Q_G varies with the output voltage and current, it should be evaluated under in-circuit bias conditions. The Q_G characteristics shown on a device data sheet only provides an approximation of the value of Q_G during actual circuit operation. Therefore, a designer must be able to ac-

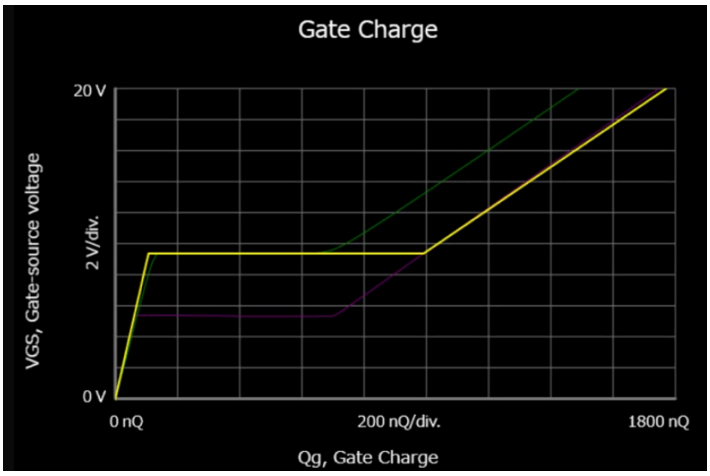

24-10. V_{GS} (gate-source voltage) of a super junction MOSFET that indicates QG presented on a Keysight B1506A.

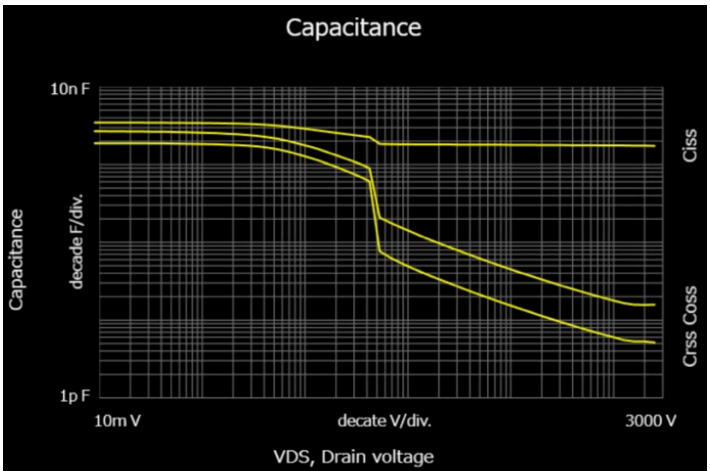

24-11. C_{ISS}, C_{OSS}, and C_{RSS} vs. drain voltage presented on a Keysight B1506A.

curately evaluate Q_G for both low voltage and high voltage power devices.

Besides driving loss, the designer may want to calculate conduc¬tion loss and switching loss. The Q_G curve can also be interpreted as a representation of the non-linearity of a power device's stray capacitances. This makes it possible to calculate switching parameters and switching loss using known equations that combine the gate resistance, the resistance in series to the gate, and the switching frequency. The test instrument should have the ability to accurately measure on-resistance, $R_{DS(ON)}$, and peak current, and also calculate conduction loss. These calculations should be performed automatically by the test instrument for a given frequency.

Understanding the input, output, and reverse return capacitances of three terminal devices (such as MOSFETs or IGBTs) is important, because these parameters dictate the switching speed and the switching loss when operating at high frequency. However, accurately measuring these parameters is not easy or straightforward. To make an accurate measurement, the capacitance between two terminals of a three terminal device, the other terminal needs to be appropriately configured.

It would be helpful if the test instrument automatically and accurately measures FET capacitance values (C_{ISS}, C_{OSS}, C_{RSS}). This involves using all the resistors, capacitors, and protection circuits necessary to make high-voltage capacitance measurements. Fig. 24-11 shows a typical presentation of these capacitance values.

An applied dc voltage causes a power MOSFET's depletion region to modulate, which in turn causes the junction capacitance to vary with voltage. The drain or collector terminal of a power MOSFET is often exposed to high voltages when it is off, which determines the value of its junction capacitances at the moment it turns on. Therefore, understanding how device capacitance changes with applied voltage is very important for designers. Knowing the true value of device capacitance at a specific voltage and the calculated voltage the device will experi¬ence in a circuit allows selection of a power MOSFET with the lowest loss. To produce reliable capacitance measurements, the power MOSFET capacitance measurement needs to be performed at relatively high frequencies.

Gate resistance is an important parameter for circuit designers because it influences device operation speed and switching loss. The tester should be able to measure the device gate resis-tance (R_G) when it performs a capacitance measurement, which eliminates the need for additional complicated data analysis.

Circuit simulators such as SPICE are an essential tool for designers. Accurately simulating the performance of a circuit can result in significant cost savings through reduced development cycles and prototyping. Therefore, it would be helpful if the test instrument can precisely model C_{RSS}, C_{ISS} and R_G. These device parameters are essential for accurate power circuit simulations.

Tektronix/Keithley's 2600-PCT-xB is intended for characterization of MOSFETS, IGBTs, diodes, and other high-power devices (Fig. 24-12). This instrument provides device-level characterization that includes breakdown voltage, on-state current, and capacitance measurements. This high-power Parametric Curve Trace supports the full spectrum of device types and test parameters. This Parametric Curve Trace configurations include everything necessary for the characterization engineer to develop a complete test system quickly. ACS Basic Edition software provides complete device characterization, including both real-time trace mode for quickly checking fundamental device parameters like

breakdown voltage and full parametric mode for extracting precise device parameters. ACS Basic Edition goes beyond traditional curve tracer interfaces by offering a broad array of sample libraries. Users have complete control of all test resources, allowing the creation of more advanced tests than previously possible on a curve tracer.

The measurement channels consist of Tektronix/Keithley's SourceMeter Source Measure Unit (SMU) Instruments and an optional Multi-frequency capacitance-voltage (C-V) meter. The dynamic range and accuracy of these instruments is orders of magnitude beyond what a traditional curve tracer could offer.

To achieve this performance, there is a complete set of precision cables to connect the instrumentation to either Tektronix/Keithley's Model 8010 High Power Device Test Fixture for package part testing, or the Model 8020 High Power Interface Panel for wafer-level testing. For the high-voltage channel, custom triax cables provide a guarded pathway that enables fast settling and very low currents, even at the full 3kV. For the high-current channel, special low-inductance cables provide fast rise-time pulses to minimize self-heating effects.

High-voltage capacitance-voltage (C-V) testing device capacitance versus dc voltage is becoming more and more important. For these tests, there is the Model PCT-CVU Multi-frequency capacitance-voltage meter. When combined with the optional 200V or 3kV bias tees, capacitance vs. voltage can be measured on two-, three-, or four-terminal devices. Capacitances from pF to 100nF can be measured, with test frequencies from 10kHz to 2MHz. ACS

Basic Edition software provides over 60 canned tests for C-V including MOSFET Ciss, Coss, Crss, Cgd, Cgs, Cds, and a full suite of other devices such as BJTs and diodes. Users have complete control to develop their own test algorithms in ACS Basic Edition.

24-12. Tektronix/Keithley's 2600-PCT-xB is intended for characterization of MOSFETS, IGBTs, diodes, and other high-power devices.

Testing Wide-Bandgap Devices

Among the new characterizing challenges for these new power devices is testing at both low and high current levels. It may be necessary to use special test cables to provide sufficient noise immunity at the low currents. In addition, the existing gallium nitride (GaN) and silicon carbide (SiC) semiconductors will require unique test fixtures because they are housed in different packages. Another complication is that some GaN are depletion-mode devices that are normally on so they include an integrated driver circuit to keep the device off. In contrast, EPC's GaN is enhancement mode that is normally off so it doesn't need an integrated driver. Cree's SiC devices would need an entirely different type of test fixture.

GaN and SiC power semiconductors need unique test equipment to accommodate them. SiC and GaN have higher power density, smaller size, better high-temperature performance, higher frequency response, and lower ON resistance than their silicon counterparts. Plus, these devices have lower leakage than silicon, so there is a need for sourcing higher test voltages, as well as appropriate low current-measurement sensitivity. For example, SiC leakages are more than two orders of magnitude lower than similarly rated silicon devices, so they require current measurements in the single microamps range.

Dynamic testing of devices switching kilowatts in microseconds requires advanced driver circuits and very well designed interconnect and layout of tester electronics as well as device-under-test sockets and contactors. Safe and reliable results requires tight design for creepage and clearances. Also, very fast, high power transition times requires attention to ground noise and EMI.

Voltage and current requirements for GaN and SiC devices require the handling of breakdown voltages up to 3000 V or even higher, more than 100 A, and junction capacitances for dc biases up to 3000 V. The tester must be able to withstand high SiC and GaN voltages and fast switching speeds. For best results, it is crucial to test these devices at their specified voltage, current and power rating.

One test equipment for use with GaN and SiC transistors is Tektronix/Keithley's Parametric Curve Tracer, specifically designed for high voltage and current characterization of high-power semiconductors. To meet the

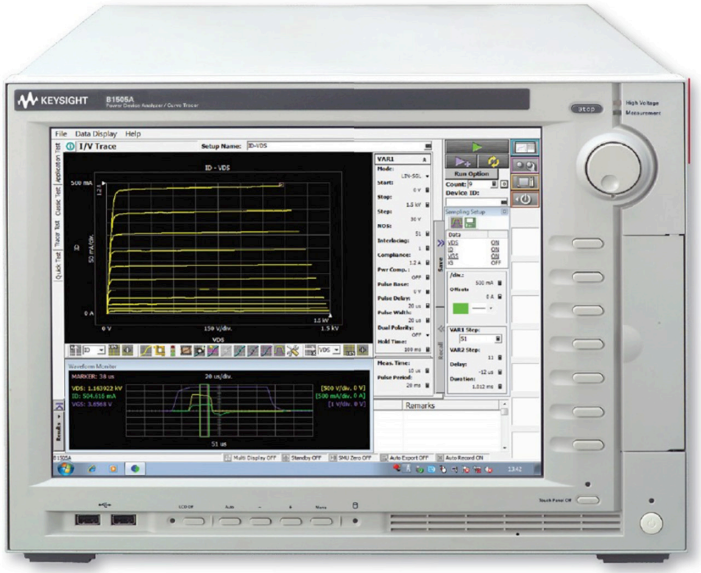

24-13. Keysight's' B1505A is a power-device analyzer/ curve tracer for high-power semiconductors.

requirements of the new generation of high-power semiconductors, Keysight has enhanced its B1505A Power Device Analyzer/Curve Tracer to significantly increase its voltage and current range, allowing it to test GaN and SiC transistors (Fig. 24-13).

The enhanced B1505A Power Device Analyzer/Curve Tracer can measure a device's characteristics from sub-pA up to 10 kV/1500 A, with a fast pulse down to 10 microseconds. Keysight also introduced the B1505AP, a preconfigured version of the B1505A that includes all modules, cables, and accessories necessary to ensure a quick startup. Both the enhanced B1505A and new B1505AP are intended for power-device researchers and manufacturers performing power-device characterization and failure analysis. These instruments can also be used for incoming device inspection and failure analysis.

Other features of the B1505A include:

- All-in-one solution for power-device characterization up to 1500 A & 10 kV
- Medium current measurement with high voltage bias (e.g., 500 mA at 1200 V)
- μΩ on-resistance measurement capability
- Accurate, sub-picoamp level, current measurement at high-voltage bias
- Capacitance measurement at up to ±3 kV DC bias
- 10μs high power-pulse measurement
- Temperature measurement capability
- High voltage/high current fast switch option for GaN current collapse effect characterization
- Automatically switch between high-voltage and high-current measurements without re-cabling
- Standard test fixtures with safety interlock for packaged power device testing
- Tested and supported high-power 200 A on-wafer testing
- MS Windows-based EasyEXPERT software simplifies data management and data analysis
- 10 module slots
- Support for high-power devices with up to six connection pins.

A curve tracer, such as the B1505A, produces I-V (current-voltage) curves that provide a good assessment of device behavior. Therefore, a curve tracer is the ideal instrument to determine the characteristics of these high-power, discrete semiconductors. Characterization of SiC and GaN devices requires an appropriate curve tracer with high breakdown voltage measurement capability as well as the ability to measure leakage currents at high voltage biases.

A GaN and SiC curve tracer needs a switch to automatically change the measurement resource between high voltage and high current. Otherwise, the operator must change measurement equipment connections to the device-under-test manually, which can cause trouble.

For best reliability results, I-V characteristics near the safe operating area (SOA) are an important measurement for GaN and SiC devices. When a high voltage is applied to a device, its impedance can change rapidly and apply medium to high current through the device. Using a narrow test pulse (less than 50μs) prevents device self-heating that could impact accurate characterization.

When originally introduced, curve tracers were analog instruments that employed a CRT (cathode ray tube) display. Today, curve tracers have become digitized and use flat-panel LCDs to present data. Digital techniques now provide the ability to store measurement data and retrieve it.

Older test equipment is not adequate for GaN and SiC because leakage current and breakdown voltage determine basic GaN and SiC behavior. Older test equipment, typically limited to the μA level, lacks sufficient resolution and accuracy for leakage characterization. And, if the breakdown voltage is more than 3kV, older instruments can't even measure it. Companies have had to design and build a custom test system to measure ultra-high voltage. However, these may have safety and traceability issues.

GaN and SiC on-resistance is now as low as a few milliohms and continues to decrease, which causes measurement accuracy problems. Accurate measurement of on-resistance requires precise constant current applied to the device using an accurate voltmeter with a full Kelvin connection. Older-generation curve tracers don't have current source capability, which makes it difficult to accurately perform characterization.

A current source mode can aid in accurately measuring GaN and SiC on-resistance. This requires continuous

monitoring and adjustments for the internal feedback circuit used by the current source. This way, set current flows regardless of contact resistance variations and you can measure on-resistance very accurately. In contrast, a voltage source mode for the on-resistance test involves immeasurable contact resistance that causes a voltage drop and degrades the measurement. Pulsed current testing can help control the effects of device self-heating.

Test instruments can make on-wafer measurements. On-wafer measurements require extension cables to connect the test equipment and prober. In this case, the drive voltage has to be high enough to overcome the IR voltage drop in the extension cable. The GaN or SiC drain or collector supply voltage must have enough margin even when IR voltage drop is high due to high current. To ensure sufficient drive-supply voltage requires a special extension cable with low residual resistance. High-voltage testing at the wafer level requires a properly designed safety system to prevent the user from exposure to the high voltage. Interlock mechanisms between the prober and the instruments must be used to protect the user.

24-14. Keysight's' B1506A is a power-device analyzer/curve tracer for high-power semiconductors.

A proper test-fixture solution is extremely important, both to insure safety (due to the high voltages and currents used) and to support the wide variety of power-device package types. Fig. 24-14 shows the Keysight B1506A with a test fixture for a device under test. A previous limitation of curve tracers was that some power devices could not be evaluated due to their size, or it was necessary to jury-rig an adapter in order to test the device. Therefore, you need a test fixture that can accept a wide variety of devices, regardless of their size or shape so the test-fixture adapter must be customizable. In addition, the test fixture should have a built-in interlock mechanism to ensure that high voltages and currents do not endanger the device-under-test or the test operator.

One complication is that the existing GaN and SiC semiconductors require unique test fixtures because they may be housed in different packages. Plus, some of the GaN devices are enhanced mode and others are depletion mode with integrated driver circuits. Existing SiC devices now use industry-standard packages, but as their portfolio grows, newer packages will certainly have to be optimized for high-speed, high-power switching.

Safety is a concern when configuring any high-voltage test system. Typically, the test systems require safety interlocks, double grounds, and other safety features to protect operators and sensitive system instrumentation. In Europe, it requires test and measurement equipment to demonstrate safety by complying with EN61010-1. Internationally it is IEC61010-1 and in the United States it is UL61010-1.

Making Low-Current Measurements in Electronic Systems

In the previous section we were concerned about high current and high voltage. We'll move to the extreme with an application note from Tektronix) that describes how to make accurate measurement of low currents using a Precision Measurement DC Power Supply. The application note is *Making Low Current Measurements with a Series 2280S Precision Measurement DC Power Supply.*

Minimizing the power consumption of integrated circuits and electronic sub-assemblies is a major focus for manufacturers of these components. This means minimizing the current drawn by all integrated circuits and electronic subassemblies.

In the past, power consumption could be measured with a standard digital multimeter (DMM). Today, devices can have operating currents as low as microamps or less and require more sophisticated measurement equipment.

One way to measure low current on a low-power device under test (DUT) is to use a power supply with a precision DMM in series with the DUT, as shown in Fig. 24-15. With a quality 6½-digit DMM, accurate current measurements can be made at microamp levels. Although this method can provide accurate measurement of current through the device, it can also introduce problems due to the loading of the DMM.

Even though the voltage at the output of the power supply may be at the programmed value, the voltage at the DUT is actually lower than the programmed value due to the loading of the DMM. Rather than the programmed voltage, the voltage seen at the DUT's terminals is equal to the programmed voltage minus the voltage across the DMM ($V_{DUT} = V_{SET} - V_{DMM}$). If this voltage drop is not accounted for and the user assumes the voltage at the device is equal to the programmed voltage, then power and resistance measure-

ments will have significant error because the voltage used to calculate them will be higher than the value at the DUT. This drop in voltage can also cause problems when testing the device at voltages near the minimum operating voltage. If the loading of the DMM is too great, the voltage seen at the device may be below the minimum operating voltage and the device will fail to operate correctly, resulting in incorrect measurements.

This drop in voltage could be compensated for by outputting a higher voltage at the power supply so the desired voltage appears at the DUT. However, the loading of the DMM varies with the amount of current flowing, so compensation is difficult. A second DMM could be used to measure the voltage at the device directly, but this not only adds cost and complexity to the test system by introducing yet another piece of equipment, it can also create a significant error source for low-current measurements. The DMM adds additional load to the test circuit, resulting in currents higher than those actually flowing through the device.

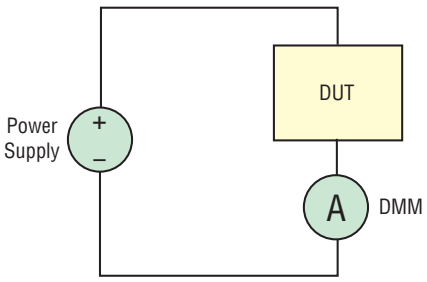

24-15. Measuring low current on a DUT using a power supply with a precision DMM in series with the DUT.

Using a Precision-Measurement Power Supply

A better way to measure the current is to use a precision-measurement power supply. The current through a device can be measured with the same precision as a high-quality 6½-digit DMM, but it can be done more simply and more accurately as well. Testing is simplified because only a single instrument is required to test the device.

With only a single instrument, testing can begin sooner because there is less equipment to set up. Automating the measurement is simpler as well with only one instrument to program. This eliminates the need to synchronize multiple instruments and allows the test engineer to focus on making the measurement.

Precision-measurement power supplies are capable of measuring both the current and voltage applied to the device. Current is measured internally, so it places no loading on the test circuit like a series DMM would. This results in the voltage at the device being equal to the programmed voltage.

For even greater accuracy, voltage can be sensed directly at the device using remote sense leads placed at the device terminals, allowing the precision-measurement power supply to compensate automatically for any voltage drops across the test leads that supply current to the device. These sense leads have very high input impedance, so they place virtually zero load on the test circuit. Using these features, precision-measurement power supplies are capable of performing very accurate characterization of devices at any current level. By containing all of this capability in one instrument, precision-measurement power supplies greatly decrease test system complexity as well as cost.

Precision-measurement power supplies reduce the amount of equipment necessary to make a current measurement on a device. In this example, the following equipment is used as illustrated in Fig 24-16 and 24-17. Test connections are extremely simple as only two test leads, HI and LO, are required for making connections to the DUT. Remote voltage sensing is not required for accurate voltage measurements because the currents are very low, so they won't produce significant voltage drop in the test leads. Shielded cabling is recommended to reduce noise. If the test circuit is grounded, grounding should be at a single point to avoid measurement error due to ground current loops.

You can configure a Series 2280S Precision Measurement DC Power Supply to measure the current consumption of a precision voltage reference when nothing is connected to the reference's output. This quiescent supply current of the voltage reference device being measured is specified in its datasheet at a typical current level of only 31µA and a 35µA maximum level. To make this measurement, the instrument will be configured for maximum precision and accuracy.

To make highly accurate current measurements in the low micro-amps range, the Series 2280S Precision Measurement DC Power Supply must be configured for maximum precision.

For accurate current measurements in the low micro-amps range, the Series 2280S Precision Measurement DC Power Supply should be configured for maximum precision.

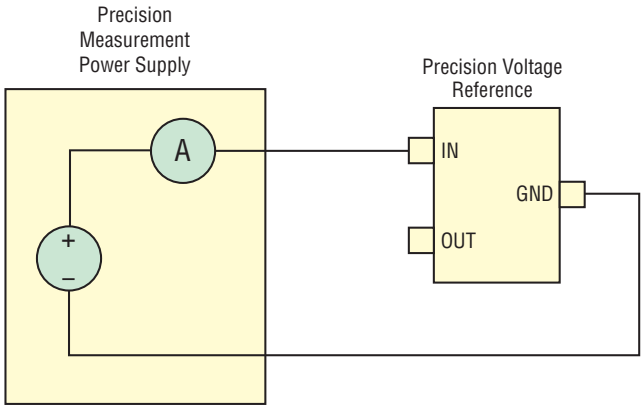

24-16. Precision-measurement power supplies reduce the amount of equipment necessary to make a low-current measurement on a device.

Use the front panel to configure the instrument from with the following steps:

- Set the instrument to 6½ digits of resolution.
- Turn Auto Zero On, which will automatically measure an internal reference to zero the instrument for each triggered measurement, resulting in measurements with greater accuracy.
- Set the NPLC value to 15 (12 for 50Hz power systems), the maximum measurement aperture time. This increases both measurement resolution and accuracy.
- Turn the averaging filter on, so the instrument will return readings that are the average of several measurements. Averaging measurements causes the readings to be more stable, enabling greater precision.
- Turn the Filter State on and set the filter count to 10. Filter count can be increased all the way up to 100 for even more stable readings.
- Set the Sample Count to 10 to match the filter count, which will fill the averaging filter with 10 back-to-back readings with very little time between readings.
- For low-current measurements, it is necessary to allow time for currents in the test system to settle to their final values before making measurements in order to obtain accurate results. By setting a source delay, measurements can be delayed long enough for the currents to settle.
- Set the Source Delay long enough to give the current time to settle. Although 10ms is adequate for most microamp level measurements, a longer source delay may be necessary if the DUT has a lot of input capacitance or there is an external filter capacitor on the fixture.

Related Articles

1. Steve Sandler, A New Technique for Testing Regulator Stability Non-Invasively, powerelectronics.com, September 2011.
2. Steve Sandler, Use A Signal Analyzer To Measure Power Supply, Regulator, and Reference Noise, powerelectronics.com, August 2012.
3. Steve Sandler, Making Accurate Ripple Measurements, powerelectronics.com, September 2012.
4. Faride Akretch, Power Analysis of PWM Motor Drives, powerelectronics.com, July 2013.
5. Sam Davis, Testing GaN and SiC Devices: FAQs, powerelectronics.com, October 2013.
6. Steve Sandler, Software Enables Accurate Stability Test, Improves Non-Invasive Phase Margin Measurement Accuracy, powerelectronics.com, April 2014.
7. Sam Davis, Comprehensive Power Semiconductor Testing Will Ensure Optimal Device Selection, powerelectronics.com, May 2014.
8. Sam Davis, Power Analyzer Optimizes Power Conversion System Designs, powerelectronics.com, February 2015.
9. Henry Santana, Electronic Load Achieves 0 Ohms, powerelectronics.com, April 2012.
10. Lee Stauffer, Test Equipment Must Keep Pace with New High Power Semiconductor Developments, powerelectronics.com, June 2012.
11. White Paper, The Fundamentals of Three-Phase Power Measurements, powerelectronics.com, April, 2014.

☞ **BACK TO TABLE OF CONTENTS**

CHAPTER 25:

DATA-CENTER POWER MANAGEMENT

Bob Conner
CEO and Co-Founder, Sarda Technologies
www.sardatech.com

Why More-Than-Moore Power Management Is Required to Keep Up With Exponential Growth in ICT Data Consumption

Significant gains in energy efficiency are required to keep up with the exponential growth in the data consumption of Information and Communications Technology (ICT) systems: end-user devices, networks, and data centers. Moore's Law scaling (monolithic integration in silicon) is the historical technology driver, but it no longer achieves the required gains. Fortunately, a new power-management technology has emerged. It achieves More-than-Moore scaling by integrating different components and materials to increase functional diversity and parallelism. This technology can improve voltage regulator power density, response time and granularity by an order-of-magnitude to reduce the ICT system energy consumption by 30% or more. This paper explains why a Heterogeneously Integrated Power Stage (HIPS) enables power management scaling to keep up with the rising demands on data centers and network systems.

Exponential Growth in Data Consumption

The digital universe—the data we create and copy annually—will grow 10x, from 4.4 zettabytes to 44ZB, from 2013 to 2020. The forecast for 2020 compared to 2014 expects many more Internet users (3.9 billion versus 2.8 billion), more connected devices (24.4 billion versus 14.2 billion), faster average broadband speeds (42.5Mbps versus 20.3Mbps) and more video streaming (80% versus 67% of traffic). Most people will use a tablet or smartphone for all online activities by 2018. Mobile data traffic is increasing 10x from 3.3 exabytes per month in 2014 to 30.5EB/month in 2020. Many websites (e.g., Facebook) require an order of magnitude more power to build a web page than to deliver it.

ICT Energy Consumption

According to one study, ICT systems in 2012 consumed 920 terawatt-hours of power, which is 4.7% of global electricity consumption. That power requires the equivalent of 300 coal plants and emits 2 trillion pounds of CO2-equivalent greenhouse-gas emissions.

A second study forecasts that improvements in energy efficiency will slow the growth in ICT electricity consumption from the historical 6.7% per year to 3.8% per year due to the following:

- Each new generation of ICT systems and components is more energy[efficient. For example, improvements in optical components enable an order-of-magnitude increase in data rates of optical modules within roughly the same power envelope.
- Usage is shifting from energy-intensive TVs and conventional desktop PCs to energy-efficient smartphones, ultrathin notebooks, tablets, and fanless all-in-one desktop PCs. In 2011, the average annual electricity consumption was just 5.5 kilowatt-hours for smartphones and 16kWh for tablets, compared to 219kWh for PCs.
- Increasingly, networks and data centers will be optimized for energy efficiency rather than capacity. One example of an industry initiative is Greentouch, whose mission is to deliver the architecture, specifications, and roadmap to increase network energy efficiency by 1,000x compared to 2010 levels.

However, a third study estimates that ICT systems' percentage of global electricity consumption was 9.3% in 2012 and will grow in 2017 to 9.2%, 11.7%, or 15.6% according to three different growth scenarios, as Fig. 25-1 shows. Data-center operating costs (OPEX) are beginning to exceed capital expenditures (CAPEX) in the total cost of ownership. As applications and data move into the cloud, energy consumption is shifting from client devices to networks and data-center infrastructure. This shift highlights the need to increase the energy efficiency of data centers and networks.

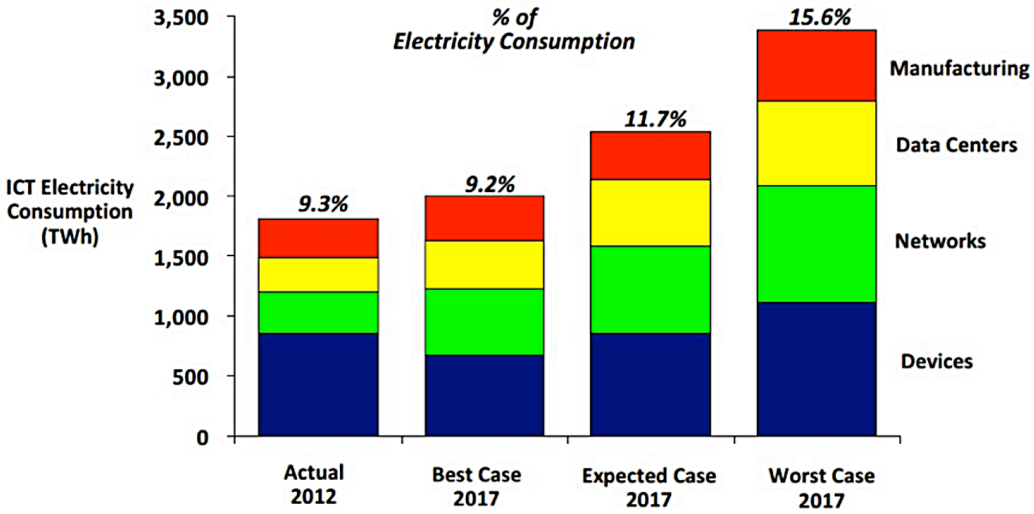

25-1. ICT Electricity Consumption Forecasts.

Moore's Law Scaling

Moore's Law (as revised by Gordon Moore in 1975) predicts that the number of transistors per chip can double every 24 months. Although the industry is now slipping behind this rapid pace, each new process-technology generation still provides significant gains. State-of-the-art processors used 22–28nm CMOS in 2013 and are advancing to 10–14nm in 2018 and 7–10nm in 2020. The increases in transistor density and processor shipments indicate that the number of processor transistors is scaling pretty well with data consumption. Processors continue to innovate, significantly increasing their compute density, data rates, and performance per watt. For example, 97% of mobile processors will use 64-bit cores in 2018, versus 15% in 2014. In addition, 93% will use 4-8 cores in 2018, versus 43% in 2014. A growing number of these processors support UltraHD (4K) video.

However, Moore's Law has hit some painful limits. Costs keep rising, with new fabs costing upwards of $10 billion. Designing a new high-performance processor using the latest technology costs more than $100 million. In the past, designers lowered the operating voltage to keep power consumption constant while doubling the transistor density (described as Dennard scaling). But this practice no longer works, because physical laws prevent designers from lowering the operating voltage much further below 1V. A direct result of this is that the amount of "dark silicon" —the processor cores that must be powered down at any given time to meet the chip's power budget—is rising with transistor density.

Energy efficiency is the new fundamental limiter of processor performance. Increasing it requires:

- Large-scale parallelism with discrete dynamic voltage and frequency scaling (DVFS)
- Near-threshold voltage operation
- Proactive fine-grain power and energy management.

DVFS significantly reduces power consumption (up to 100x) by dynamically adjusting the operating voltage to its optimal level, which varies according to the software workload and operating temperature. It gets more effective by increasing the response time of the voltage regulator (VR) and the number of voltage levels. To keep up with greater transistor densities, VRs require significant improvements in the following:

- **Response time:** To quickly change the processor's operating voltage, which typically varies from 1.0–1.5V for peak performance to 0.3–0.6V for low-power idling from a 12V supply used in data-center and network systems. (Low-power idling is preferred over power gating to minimize latency issues.) Fast response is required to provide energy proportionality—power consumption that scales with workloads. Fast response also realizes the benefits of the new adaptive voltage scaling (AVS) standard and software-defined power architecture.
- **Power density:** To decrease size, because supplying higher current requires additional VRs (Voltage Regulator). The processor's operating voltage is no longer scaling with transistor density, so the VR-supplied current is increasing. Today, each system board needs 10 to 100 or more VRs to supply 100A to 1,000A or more (e.g., up to 20,000A for a high-end server card). Each rack in a data center or network system has many system boards (Fig. 25-2).
- **Granularity:** To support the massive parallelism of many small energy-efficient elements (e.g., many heterogeneous processor cores, micro-server cards, small-cell base stations, etc.). Benefits include more integration and

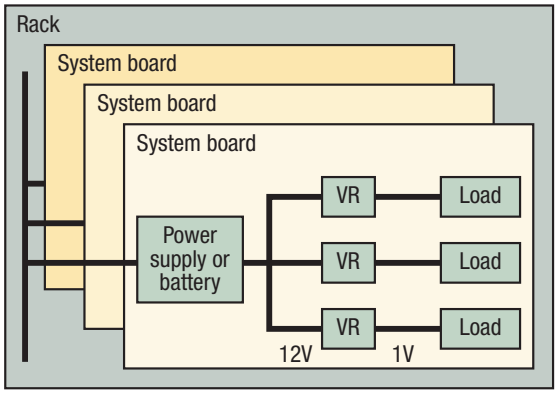

25-2. Many Voltage Regulators (POLs) per System.

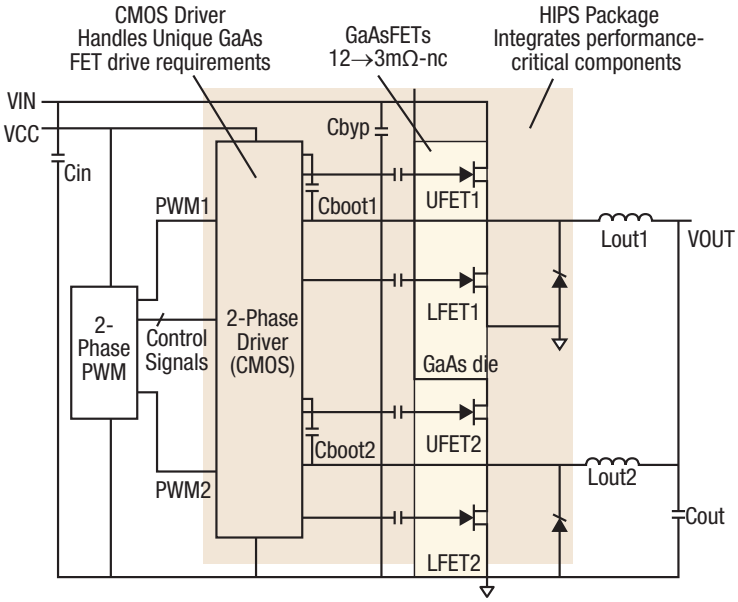

25-3. HIPS Module has two independent outputs or a two-phase input.

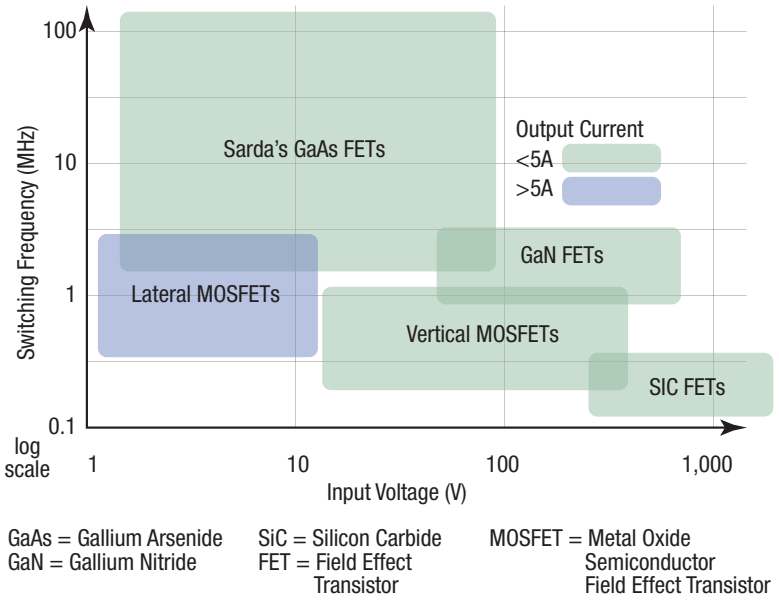

25-5. Comparison of the switching characteristics of GaAs, GaN, SiC, and Silicon MOSFETs

specialization, reduced thermal loads, and better dynamic resource allocation, thereby providing high efficiency at low to medium loads. Many ICT systems will increasingly spend a large percentage of their time operating in low-power standby modes.

Moore's Law scaling does not help the incumbent VR technologies, because they use many discrete components, such as controllers, MOSFETs, inductors, and capacitors. Due to MOSFETs' high switching-power losses, today's 12V, 10–30A VRs operate at a low (1.0MHz or less) switching frequency. This requires bulky inductors and capacitors, and they consume a large percentage of board space (~40%). They also suffer from a slow response time. MOSFETs are an aging 35-year-old technology and are hitting a performance asymptote. Moore's Law scaling does not help MOSFETs, either, because they must withstand high voltage on the drain (e.g., 18–20V for 12V input). There are a finite number of well-known techniques for improving MOSFET performance, most of which have already been exercised.

More-than-Moore Scaling

More-than-Moore scaling requires heterogeneous Integration, the integration of separately manufactured components into a higher level assembly that in the aggregate provides enhanced functionality and improved operating characteristics. An example is the Heterogeneously Integrated Power Stage (HIPS) shown in Fig. 25-3. Its cross-section is in Fig. 25-4.

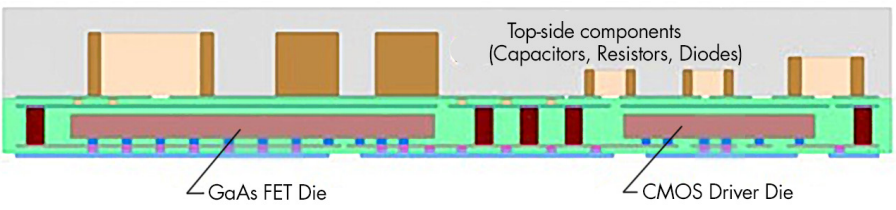

25-4. Cross-section of the HIPS module.

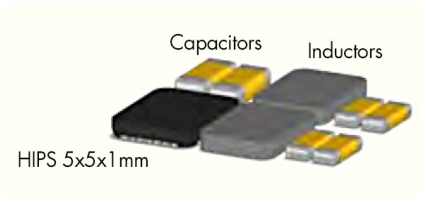

25-6. HIPS package contains passive and active components.

One of the important design decisions for the HIPS was selection of the optimum technology for the regulator's power switch. This determination was aided by a comparison of the characteristics of GaAs, GaN, SiC, and silicon MOSFETs power switches, as shown in Fig. 25-5. This figure shows that GaAs FETs offer benefits over the other switches for voltage regulators operating with up to a 100V DC supply. Table 25-1 compiles the characteristics of GaAs, GaN, silicon MOSFET power switches.

The HIPS module uses the optimum technology for each function:

- Gallium arsenide (GaAs) for the field-effect transistors (FETs).
- CMOS for drivers, protection, and control, handling the GaAs FETs' unique requirements.
- 3D packaging using embedded die-in-substrate technology to integrate in a 5mm x 5mm x 1mm QFN package the GaAs die, CMOS driver die, and passive components

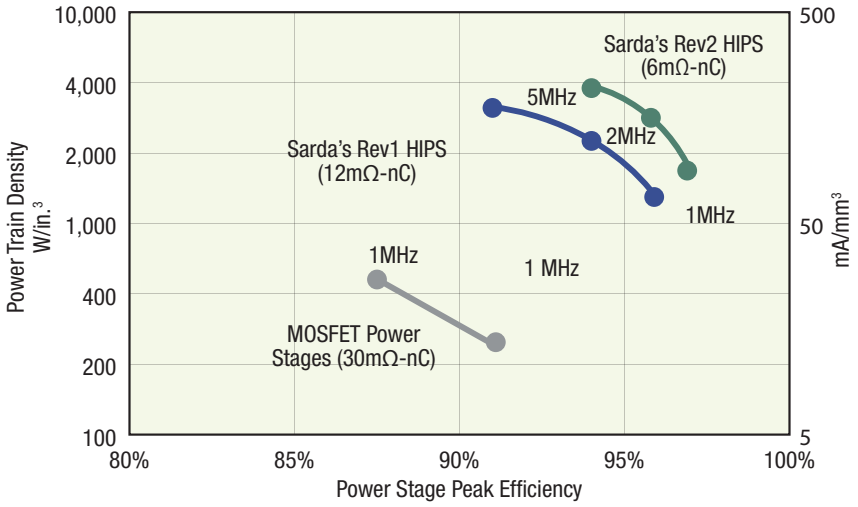

25-7. Comparison of the performance of a typical MOSFET output stage and the HIPS, Rev1 and Rev2. The Figure of Merit for Rev2 HIPS is 6mΩ-nC vs. 30mΩ-nC for a typical MOSFET output stage. These results are for a 12Vin and 1.2Vout power stage.

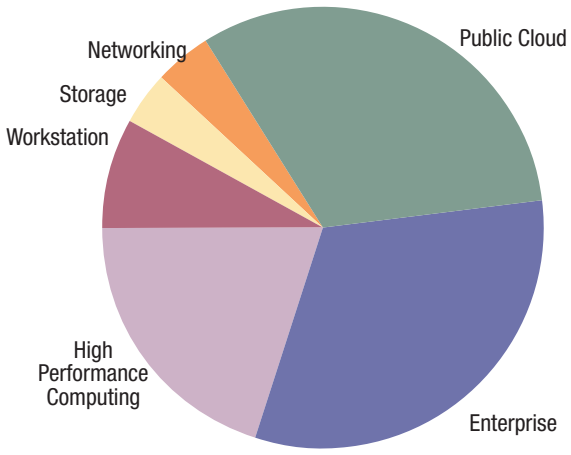

25-8. $10.3 Billion Market for Processors Used in Data Centers in 2018 (Source: The Linley Group)

required to minimize parasitics for the high switching frequency (Fig. 25-6).

An HIPS module is an evolutionary leap over the Driver-MOSFET (DrMOS) integrated power stage module. It replaces the MOSFET dies with a GaAs die, reducing packaging parasitics and integrating performance-critical components in a very small package. GaAs FETs have much lower switching-power loss than MOSFETs due to their superior intrinsic material properties: 5x higher electron mobility (8,500 versus 1,400 cm2/Vs), 5x lower on-resistance x gate charge (FOM), and no body diode (which eliminates reverse recovery loss). GaAs FETs also are more reliable, because they have no gate oxide, higher activation energy, higher bandgap, and the primary failure mechanism (sinking gates) is self-limiting.

The HIPS module can increase the voltage regulator switching frequency by 10x or more. Its switching frequency range of 2 to 5MHz reduces the size of the output capacitors and inductors while reducing the transient response time. An HIPS can readily be used in industry-standard synchronous buck converters with complementary components (PWM controllers and inductors) from third-party suppliers. No new architectures, materials, or components are required. A typical use for the HIPS is in point-of-load (POL) converters.

HIPS also increases the power density and granularity (providing more than one output) for board-mounted voltage regulators. The HIPS uniquely enables Package-Integrated Voltage Regulators (PIVRs) that integrate many fast, small VRs in the processor package as close as possible to the processor die without increasing its cost or heat dissipation.

HIPS modules enable many fast, small VRs that can reduce the energy consumption of ICT systems by 30% or more through fine-grain power management of multi-core processors, energy

TABLE 25-1. DETAILED CHARACTERISTICS OF POTENTIAL POWER SWITCHES FOR THE HIPS MODULE

Parameter	Units	GaAs FETs	GaN-on Si FETs	Vertical MOSFETs	GaAs Benefits
Electron Mobility	cm2/Vs	8,500	1,800	1,400	Faster switching
$R_{DS(ON)}$ x Q_G FOM	mΩ-nC	12→3	20-30	20-60	Lower switching loss
FET Switch Speed	nS	<1	1-2	2-5	
Body Diode		No	No	Yes	
Loop Inductance	nH	~0.2	~0.4	1-2	
FET Structure		Lateral	Lateral	Vertical	UFET/LFET monolithic integration • Reduced parasitics • Multiple phases
Bandgap	eV	1.4	3.4	1.1	Higher junction temperature
Activation Energy	eV	2.5	1.1-2.5	0.3-1.2	Higher reliability
Gate Oxide?		No	No	Yes	
2014 Market Size		$6B	$0.015B	$13B	Leverages proven manufacturing

proportionality and reduced cooling requirements. Fig. 25-7 compares the characteristics of a typical power MOSFET output stage with the first and second versions of the HIPS.

Samples of the HIPS were available in 2016 with full production scheduled for 2017.

Since VR-supplied current scales roughly with processor performance and price, we can check the processor market to estimate the HIPS market size. The market for processors, application-specific standard products (ASSPs), and FPGAs in data centers and network systems, the initial target markets for HIPS, is forecast to grow to $21.9 billion in 2018:

- $10.3 billion for server processors, most of which are used in data centers (Fig. 25-8). Captive processors, such as IBM's Power and Oracle's SPARC, are excluded.
- $11.6 billion for processors, ASSPs, and FPGAs used in voice and data networks (Fig. 25-9). Communications semiconductors include components for Ethernet, broadband infrastructure, customer premise equipment, home/access networking, network processors (NPUs), transport (Sonet/SDH, OTN), PCI Express, RapidIO, and network search engines.

Assuming it's approximately 5% of the processor content, the HIPS content for these systems is approximately $1.1 billion. HIPS modules also improve energy efficiency and, hence, the performance of ultrathin, fanless all-in-one desktop PCs, notebooks, tablets, and smartphones within a very challenging thermal envelope—a small, thin case that must remain cool enough to touch.

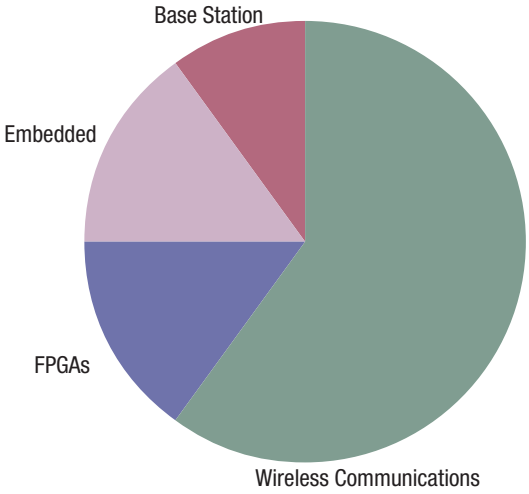

25-9. $11.6 Billion Market for Processors, ASSPs, and FPGAs Used in Voice and Data Networks in 2018 (Source: The Linley Group)

The GaAs industry today makes products for RF and microwave communications. In 2013, the industry produced 29.3 million square inches of GaAs, which is equivalent to 100,000 GaAs 150mm wafers per month. GaAs industry revenue exceeded $6 billion revenue in 2014. Hence, the GaAs industry has ample well-proven, high-volume manufacturing capacity for producing HIPS modules.

Related Articles

1. Brian Griffith, PMBusTakes Command of Data Center Power Issues, powerelectronics.com, April 2008.
2. Sam Davis, 380V DC Input Supplies Enable Data Centers to Use HVDC Power Distribution, powerelectronics.com, February 2014.
3. Sam Davis, 400VDC Power Distribution for Data Centers Emerges, powerelectronics.com, October 2014.
4. EET, Energy-Management Chip Suits Servers and Data Centers, EET, March 2011.
5. Technologies Under Development to Reduce Datacenters' Energy Consumption, powerelectronics.com, October 2015.

BACK TO TABLE OF CONTENTS